Università di Foggia
Dip.to di Scienze Agrarie, degli Alimenti

HR EXCELLENCE IN RESEARCH

CIHEAM

Università degli Studi di Foggia

in convenzione con CIHEAM- Istituto Agronomico Mediterraneo di Bari

Corso di Dottorato di Ricerca in

Gestione dell'Innovazione nei Sistemi Agro-Alimentari della Regione Mediterranea - XXXI Ciclo

TITOLO TESI DI DOTTORATO DI RICERCA

Study of the ribosomal DNA intergenic spacer (IGS) region as a molecular tool for identification of vascular fungi associated with Olive Quick Decline Syndrome in Southern Italy: *Phaeoacremonium italicum* as a study model

(s.s.d. AGR/12)

Tesi di dottorato di:

Dott. MERIEM LAIDANI

Coordinatore del corso

Prof. GIANCARLO COLELLI

Firma .....

Tutors

Dott. ANTONIA CARLUCCI

Firma .....

Dott. THAER YASEEN

Firma .....

Co-Tutor

Dott. MARIA LUISA RAIMONDO

Firma .....

A.A. 2018/19

Study of the ribosomal DNA intergenic spacer (IGS) region as a molecular tool for identification of vascular fungi associated with Olive Quick Decline Syndrome in Southern Italy: *Phaeoacremonium italicum* as a study model

MERIEM LAIDANI

Thesis submitted to the Università degli Studi di Foggia,
Department of the Sciences of Agriculture, Food and Environment
for the degree of Doctor of Philosophy

June 2019

This is dedicated to

To my wonderful Mother
You have successfully made me the person I am becoming

To the memory of my beloved Father

To my lovely Sisters Imene, Sihem, Yasmine and Sara

Acknowledgments

First and foremost, all praises to God Almighty for giving me the strength, ability, and patience to complete my dissertation, after all the challenges and difficulties.

Undertaking this PhD has been a life-changing experience for me and it would not have been possible to do without the support and guidance of so many people.

I would first like to express my sincere thanks to the Mediterranean Agronomic Institute of Bari (MAIB), along with the Università degli Studi di Foggia for giving me the opportunity to carry out my doctoral research and for their scientific and financial contributions.

I would like to express my sincere appreciation to the head of Integrated Pest Management Division; Dr. Anna Maria D'Onghia, to Dr. Toufic Elbeaino and all the staff of the IPM department.

My sincere thanks goes to the PhD coordinator Prof. Giancarlo Colelli and to Dr. Maria Luisa Amodio for their availability and kind help.

I heartily thank my supervisors Dr. Antonia Carlucci and Dr. Thaer Yaseen for their valuable guidance, support and kind advice throughout my PhD research study.

Special thanks to my adviser Dr. Maria Luisa Raimondo for her help and constructive suggestions which were determinant for the accomplishment of the work presented in this thesis.

I would particularly like to express my gratitude and appreciation to Dr. Josep Armengol and Dr. David Gramaje for giving me the opportunity to join their teams as intern in Spain, and who gave access to their respective laboratories and research facilities. Many thanks goes to Dr. Mónica Berbegal for her kind help and constructive remarks.

My most sincere thanks to my close friends I met during this path, to Robert, Saleh and Mokhtar, who believed in my potential during all those years. I am also truly thankful to my colleagues of the plant pathology and diagnosis Laboratory (Department SAFE-Foggia) for their prompt help whenever I needed.

Last but not least, I owe my success to my great Mother and my sisters who supported me and helped me throughout my life. I do not know how to thank you enough for your unconditional support, encouragement and love, and without which I would not have come this far.

LAIDANI Meriem

June 2019

Summary

This research concerns the first study of the ribosomal DNA intergenic spacer (IGS) region as a molecular target for detection and phylogenetic analyses of *Phaeoacremonium* spp. found associated with olive quick decline syndrome in southern Italy. The study follows a survey carried out during a period of three years (2015-2018), in different olive orchards of Salento (Apulia). Disease symptoms of wilt and dieback, browning and streaking under the bark and wood discoloration were observed. Three *Phaeoacremonium* species were isolated more frequently than other fungi. These *Phaeoacremonium* spp. were identified based on their morphological characteristics and by analyses of the β-tubulin and actin genes, namely *Phaeoacremonium italicum*, *Phaeoacremonium scolyti* and *Phaeoacremonium minimum*. *Pm. italicum* was the predominant *Phaeoacremonium* species isolated from olive wood discoloration and was used as a study model to explore originally, the ribosomal DNA intergenic spacer (IGS) region in these fungi. *Pm. italicum* isolates were subjected to PCR amplification of the intergenic spacer (IGS) region followed by cloning and sequencing. A structural analysis of the IGS sequences of *Pm. italicum* was performed but also for *Pm. scolyti* and *Pm. minimum*. The IGS region showed polymorphisms among *Pm. italicum* isolates and four categories of repeat elements of 12-15 nucleotides, organized in distinct patterns, were detected within a variable IGS region. A PCR-based assay, to provide a specific detection of *Pm. italicum* group was developed by designing a specific PCR primer on the basis of the nucleotide sequence variability of the rDNA intergenic spacer among *Phaeoacremonium* species. The primer pair specificity was checked and confirmed using 10 isolates of *Pm. italicum* isolates and other 14 non-target *Phaeoacremonium* spp. The PCR detection limit was up to 1 pg/μL. To understand whether the intergenic spacer (IGS) region could be used to improve phylogenetic resolution, within and among *Phaeoacremonium* species, this region was amplified from a collection of *Phaeoacremonium* spp. isolates, including the representative *Pm. italicum*, *Pm. scolyti* and *Pm. minimum* isolates collected from the field. Maximum parsimony analyses were performed on IGS, β-tubulin and actin gene dataset separately as β-tubulin and actin gene are considered as targeted markers for this genus. Multigenic analyses combining IGS-β-tubulin-actin sequences was also performed. The IGS region was informative and produced a phylogeny with essentialy the same topology of β-tubulin, actin and combined β-tubulin-actin trees in terms of species-level clades, however, they revealed conflicts related to

Summary

the grouping of isolates within *Pm. italicum, Pm scolyti* and *Pm. minimum* clades. Specifically, IGS tree showed a clear division of *Pm. italicum* group into distinct subclades. Combined IGS-β-tubulin-actin phylogeny showed similar results as those obtained in the single IGS phylogeny, and the latter was actually consistent with the IGS structural organization of representative *Pm. italicum* isolates. The present study indicates that analysis of IGS sequences revealed inter- and intraspecific variation and proved a suitable molecular tool for detection and phylogenetic analyses, within and among *Phaeoacremonium* species.

Key words: OQDS, *Phaeoacremonium* spp; intergenic spacer, *Pm. italicum;* IGS structure; genetic marker; primers design; phylogenetic studies.

Table of Contents

Table of Contents

Table of Contents

Table of Contents

List of figures

List of figures

List of figures

List of tables

I. LITERATURE REVIEW AND THESIS OBJECTIVES

I.1 Introduction

The cultivated olive, *Olea europaea* (L.) considered as an emblematic plant of the Mediterranean basin, can be attacked by a large number of fungal pathogens affecting roots, wood, leaves, flowers and fruits. Inventory studies conducted by Chliyeh *et al.* (2014) listed 124 olive fungal pathogens, that can represent a threat to the world olive cultivation. Among these diseases, decline, dieback and canker diseases on olives have acquired great importance worldwide. In fact, a severe decline of olive trees named Olive Quick Decline Syndrome (OQDS) has occurred some years ago in Italian olive groves (Southern Italy). Thorough studies revealed that the disease outbreak in Europe is caused by the quarantine bacterium *Xylella fastidiosa*. OQDS-affected trees were characterized by leaf scorching and dieback of twigs and branches, but also a variously extended browning of the sapwood of branches and trunks which have been associated with the presence of wood-inhabiting fungi, such as *Phaeoacremonium* spp., *Pleurostoma richardsiae*, *Pseudophaeomoniella* spp., and various species belonging to *Botryosphaeriaceae* family whose penetration is favored by the leopard moth *'Zeuzera pyrina'.* Subsequently, these fungi were considered as aggravators of OQDS, which now is posing serious threat to olive trees in the Mediterranean region (Carlucci *et al.* 2013b; Nigro *et al.* 2013; Nigro *et al.* 2014; Saponari *et al.* 2013; Saponari *et al.* 2017).

This chapter provides background on the study, giving an overview of the fungal pathogens associated with olive quick decline syndrome in Southern Italy. The chapter includes the importance and production of olive culture worldwide and in Italy; data on the distribution, host range of *Phaeoacremonium* spp. and *Pleurostoma richardsiae*, and their pathogenesis. The detection methods, and the recent molecular techniques used to detect and identify these fungal species are emphasized throughout the study. The chapter concludes with a summary of the objectives of the thesis.

I.2 Olive importance and production

I.2.1 History, worldwide importance and production of olive

Olive (*Olea europaea* L.*),* a member of the *Oleaceae* family, is among the oldest known cultivated plant species in the world. It was cultivated about 8000 years ago in Anatolia from where it spread very early to the Middle East, North Africa and Southern Europe and later in many other areas of the American continent suited to its cultivation (Efe *et al*. 2011). In more recent times, olive growing has also been introduced in other countries without an earlier tradition of olive oil production or consumption. As a result, nowadays it is found in South Africa, along the coast of Australia as well as in New Zealand and China (Figure I.1). (Cimato and Attilio, 2011).

In fact, the origin of domestication area of this millenary tree, from wild olive (*Olea europaea* var. sylvestris) (Moazzo *et al.* 1994; Diaz, 1988) was uncertain and controversial. While some authors affirmed that cultivated olive originated from the Eastern Mediterranean Basin (Zohary and Spiegel, 1975; Angiolillo *et al.* 1999), this assumption being supported by archeological evidence, others suggested that domestication took place in the Western Mediterranean area (Magdelaine and Ottaviani, 1984; Terral and Arnold-Simard, 1996; Terral, 1997). Later on, molecular studies proposed that cultivar selection was multilocal, taking place in different areas of the Mediterranean region (Besnard *et al.* 2001). More recently however, Besnard *et al.* (2013) examined the DNA of 1,797 wild and cultivated trees from the Mediterranean basin and, by analyzing the genomes, were able to create the genealogy of the trees and determine how the olive tree dissemination progressed. Three basic ancestral ‘gene pools’ of the olive tree were identified, namely the Near East, the area of the Aegean Sea and the Strait of Gibraltar. These ancestral wild gene pools have provided the essential foundations for cultivated olive breeding.

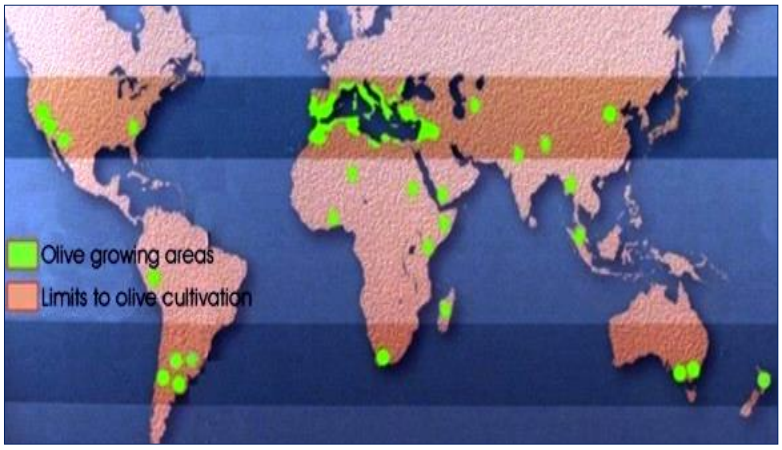

Figure I.1. Geographical distribution of olive growing areas

The edible olive has a huge economic and social importance in olive-producing countries worldwide. It is widely cultivated for the production of both table olives and oil and very significant because of its commercial value. Olives and olive oil, as traditional food products with thousands of years of history, are the essential components of the Mediterranean diet and are largely consumed in the world. Beside of their economical contribution to national economy, these are an important food in terms of their nutritional value (Uylaşer and Yildiz, 2014). The great commercial value of the olive and the recognition of olive oil dietetic properties have led to an increase in its production and consumption worldwide (Veloso *et al.* 2018).

In terms of areas harvested and production, the olive production area has increased worldwide, due to the introduction of innovations in the farming systems (Russo *et al.* 2016). Nowadays, over 10 million hectares are cultivated with olive groves globally, of which 95% are located in the Mediterranean basin (IOC, 2016). The world production of olives was about 20.8 million tonnes in 2017. Of the total production, the countries of the Mediterranean region produced about 2.33 million tonnes of olive oils in the 2016/17 season, accounting for more than 90% of total global output, with Spain, Italy, Greece, Turkey and Morocco as the top producing countries (IOC, 2018).

I.2.2 Olive culture in Italy

Italy is the second largest olive producing country covering approximately 1.325.451 ha with a production of 2.576.891 tonnes in 2017 (FAOSTAT, 2018). Indeed, olive growing is an important agricultural activity in Italy, generating 3 151 million euros in the olive oil sector, and accounting for 2.4% of the value of agri-food production. The most important olive growing areas are in the Apulia region, which accounts for 45% of the total olive growing area; Calabria (19%); Sicily (10%); Campania (7%), Lazio (5%), Tuscany and Sardinia (3% respectively), Basilicata and Umbria (2% respectively); with the rest of the surface area found in Molise, Liguria, Marche and Veneto. These areas have relatively warm temperatures, suitable for olive cultivation. In Italy, there are over 500 varieties of olive trees and more than 90% of oil production is obtained from some 45 varieties. Eighty per cent of the production of olive oil in Italy is centred around three regions: Apulia, Calabria and Sicily (IOC, 2017).

Over the last decade, the production of olive has followed a slight downward trend, before entering a sharp decline down in 2014, but then increased up to 2.732.894t in 2015/16. Subsequently, the output in 2016/17 had dropped by 24% compared to the previous crop year. Adverse weather conditions and olive tree diseases have led to a fall in production. In 2017/18 the output increased up again reaching 2.576.891t as illustrated in Figure I.2 (FAOSTAT, 2018).

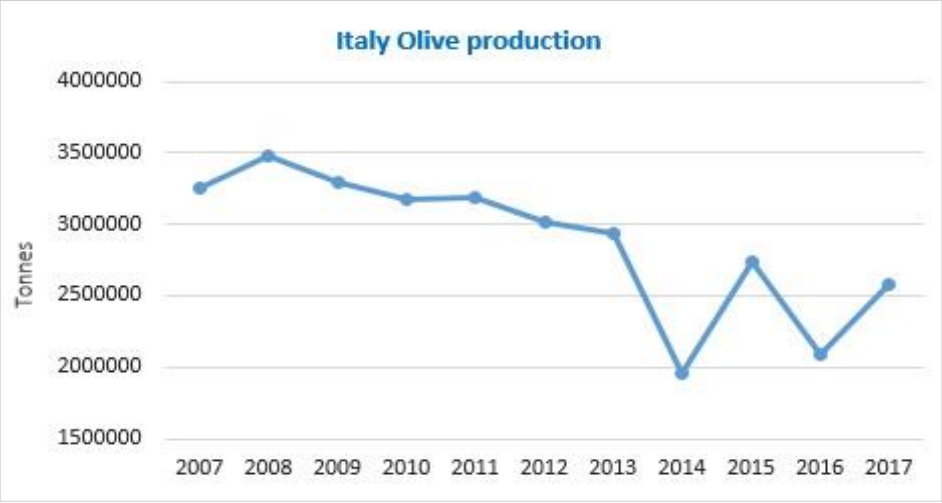

Figure I.2. Development of Italian Olive production
Source: (FAOSTAT, 2018)

I.3 Fungal pathogens associated with olive wilt and decline

Olive tree is susceptible to a variety of pathogens, that can affect its health, yield and quality of the extracted oil (Sanei and Razavi, 2012). Indeed, several fungal pathogens have been reported to be associated with olive tree branch wilting and dieback. Notable among them, Verticillium wilt caused by *Verticillium dahliae* Kleb., which is considered the main fungal soilborne pathogen threatening olive production worldwide (Jiménez-Díaz *et al*. 2012). Many soilborne root rot fungi were also reported, such as *Armillaria* spp., *Phytophthora* spp., *Rosellinia necatrix*, *Macrophomina phaseolina*, *Sclerotium rolfsii*, and *Cylindrocarpon destructans* (Rumbos, 1993; Sanchez-Hernández *et al*. 1996; Sanchez-Hernández *et al*. 1998; Nigro *et al*. 2018).

Moreover, olive cankers and branch dieback have been associated with *Phoma incompta, Cytospora oleina* and *Eutypa lata* (Malathrakis *et al*., 1979; Rumbos, 1988; Rumbos, 1993; Tosi and Zazzerini, 1994). *Phoma incompta* was also associated with olive dieback by Ivic *et al*. (2010) in Croatia and by Rhouma *et al.* (2010) in Tunisia.

Several *Botryosphariaceae* species have been associated with such symptoms on olive. The species *Diplodia mutila, D. seriata, Dothiorella iberica, Lasiodiplodia theobromae*, *Botryosphaeria ribis*, *Neofusicoccum mediterraneum*, *Neofusicoccum luteum*, *N. parvum* and *N. vitifusiforme* were reported to cause branch dieback and blight, and eventual death of shoots in different olive-growing areas (Taylor *et al.* 2001; Romero *et al.* 2005; Lazzizera *et al.*, 2008; Moral *et al.* 2010; Kaliterna *et al.* 2012; Urbez-Torres *et al.* 2013; Carlucci *et al.* 2013b).

In addition, Urbes-Torres *et al.* (2013), have reported 18 different fungal species from symptomatic olive trees affected by stem canker, twig and branch dieback in California. These species included *Diaporthe viticola*, *Diatrype oregonensis*, *Diatrype stigma*, *Diplodia mutila*, *Dothiorella iberica*, *Lasiodiplodia theobromae*, *Phaeomoniella chlamydospora*, *Phomopsis* sp. group 1, *Phomopsis* sp. group 2, and *Schizophyllum commune*, which were reported for the first time in olive trees; in addition to *Eutypa lata*, *Neofusicoccum luteum*, *Neofusicoccum vitifusiforme*, *Phaeoacremonium aleophilum*, *Botryosphaeria dothidea*, *Diplodia seriata*, *Neofusicoccum mediterraneum*, and *Trametes versicolor.*

Recently, Moral *et al.* (2017) have elucidated the etiology of olive branch dieback in Spain, that six fungal species were identified on olive plants, including *Cytospora pruinosa, Neofusicoccum mediterraneum, Nothophoma quercina, Comoclathris incompta,* and *Diaporthe* sp. They stated that only *N. mediterraneum and C. incompta* were able to induce the typical dieback symptoms and cankers, where *N. mediterraneum* was the most virulent among the evaluated species. In addition, *Colletotrichum* spp., the causal agents of olive anthracnose, have also been implicated earlier as responsible for leaf wilting and branch dieback symptoms (Moral *et al.* 2014).

In southern Italy, several fungi including *Pleurostoma richardsiae, Neofusicoccum parvum*, six species belonging to genus *Phaeoacremonium*, *Pseudophaeomoniella oleicola* and *Ps. oleae* were isolated from olive tree showing wilting and branch dieback (Carlucci *et al.* 2013b, 2015b; Crous *et al.* 2015). Similarly, Nigro *et al.* (2013) reported the presence of *Phaeoacremonium parasiticum, P. rubrigenun, P. aleophilum, P. alvesi* and of fungi belonging to the genus *Phaeomoniella* on olive trees in the outbreak area of the Olive quick decline syndrome in Lecce.

I.4 Fungi associated with the olive quick decline syndrome in southern Italy

In autumn 2013, a severe and rapidly spreading decline of olive trees has occurred in a large part of the Salento peninsula (Apulia, southern Italy), the main olive-producing region of Italy. The disease, named "Complesso del Disseccamento Rapido dell'Olivo, CoDiRo" (Saponari *et al.* 2013) or "Olive Quick Decline Syndrome, OQDS" (Cariddi *et al.* 2014) appeared mainly in olive trees aged from 60–70 years or older growing in Lecce province (Carlucci *et al.* 2013a).

Following the appearance of Olive Quick Decline Syndrome (OQDS) in Apulian olive groves, it has been found that several factors are involved in its emergence, including the bacterium *X. fastidiosa* considered as the primary causal agent, which invades, multiplies and occludes the treachery elements of olive (Saponari *et al.* 2013), but also the leopard moth *Zeuzera pyrina*, responsible of numerous galleries and necrosis which open the way to an extensive fungal colonization of the sapwood. Indeed, the olive trees affected by OQDS were

seen to be massively infested by *Zeuzera pyrina*, while the wood contained various vascular fungi belonging to different genera (Carlucci *et al.* 2017).

The disease is characterized by the presence of leaf scorching and desiccation of twigs and small branches which, in the early stages of the infection, prevail on the upper part of the canopy, then become severe and extend to the rest of the crown, which acquires a burned look (Martelli *et al.* 2016). Leaf tips and margins turn brown, tissue discoloration then spreads inward, causing necrosis of the blade. A rapid dieback of shoots, twigs and branches, eventually leading to death of the tree. Symptoms progress in severity from the older to the younger leaves. Dried leaves and mummified fruits remain attached to shoots and branches. Trunks, branches and twigs show discolorations of the vascular system. Sapwood and vascular cambium show intense dark streaking or light brown tissue discoloration (Figure I.3) (Nigro *et al.* 2014).

In fact, researchers have mobilized to study the association of fungi with the severe olive decline in the outbreak area of Lecce. Isolations from discolored sapwood samples, made on different media allowed the identification of several fungi species primarily, *Phaeoacremonium* spp. *Pm. parasiticum* was the most frequent species, followed by *Pm. rubrigenun*, *Pm. minimum*, *Pm. alvesi* and of fungi of the genus *Phaemoniella* (Nigro *et al.* 2013).

Figure I.3. Symptoms of quick decline observed in Apulia (IT) on olive trees
Source: (EPPO, 2013)

Simultaneously, a survey of olive groves in the Canosa di Puglia, Cerignola and Foggia areas, revealed the association of olive decline and the fungi *Pleurostoma richardsiae, Phaeoacremonium minimum* and *Neofusicoccum parvum*. The symptoms comprised a leaf browning and leaf drop, wilting of apical shoots, twig and branch dieback, subcortical brown wood streaking and formation of cankers on the bark. *Pleurostoma richardsiae* was the most aggressive and it was often the only fungus isolated from diseased younger trees (Carlucci *et al.* 2013b). The authors pointed out that it was the first report of *Pl. richardsiae* as a pathogen of olive trees in Italy and worldwide.

In southern Italy, various fungi including *Pleurostoma richardsiae, Neofusicoccum parvum,* seven species belonging to genus *Phaeoacremonium, Pseudophaeomoniella oleicola* and *Pseudophaeomoniella oleae* are known to affect olive trees showing OQDS (Carlucci *et al.* 2013b, 2015b; Crous *et al.* 2015).

I.5 Background on *Phaeoacremonium* spp.

I.5.1 Taxonomy and classification

Phaeoacremonium spp. are ascomycete fungi that belong to the class *Sordariomycetes*, order *Togniniales* and family *Togniniaceae* (Réblová *et al.* 2015). The genus *Phaeoacremonium* was originally described by Crous *et al.* (1996). In fact, the genus *Phaeoacremonium*, with *Pm. parasiticum* as type, is morphologically intermediate between *Acremonium* and *Phialophora* Medlar. It was reported that *Phialophora parasitica* and morphologically similar strains were examined by Crous *et al.* (1996) who established the genus *Phaeoacremonium* for these strains that originated from humans and various woody hosts.

In fact, the genus *Togninia* previously has been linked to *phaeoacremonium*-like anamorphs, in culture and via DNA phylogeny and mating studies by (Mostert *et al.* 2003). This finding was also confirmed by Pascoe *et al.* (2004) and Rooney-Latham *et al.* (2005). The genus was shown to represent an undescribed family, *Togniniaceae* (Réblová *et al.* 2004). Further work demonstrated that the *Togniniaceae* do not cluster in the *Diaporthales*, but from the order *Togniniales* (Réblová *et al.* 2015). Detailed taxonomic practice including phylogenetic analyses of this genus over the last decade, allowed its expansion, bringing the number of species described to a total of 65 *Phaeoacremonium* spp. (Huang *et al.* 2018; Marin-Felix *et al.* 2018; Spies *et al.* 2018).

I.5.2 Distribution, host range and Pathogenesis

Phaeoacremonium species are well-known vascular plant pathogens causing wilt and dieback of various woody plants. They have a global distribution, with species being reported from Europe, Africa, South, Central and North America, Scandinavia, Ukraine, the Middle East and Oceania (Gramaje *et al.* 2015). Indeed, numerous *Phaeoacremonium* species have been isolated from a wide range of hosts such as woody plants, larvae of bark beetles, soil and humans. Eleven *Phaeoacremonium* species have been confirmed as human pathogens causing mycoses in patients in various countries (Mostert *et al.* 2005; Gramaje *et al.* 2015).

The most known plant diseases in which *Phaeoacremonium* species are involved are Petri disease and Esca, which occur on grapevines and are caused by a complex of fungi, including

multiple species of *Phaeoacremonium* (Mostert *et al*. 2006b). Indeed, most *Phaeoacremonium* species described, have been associated with decline and dieback diseases or Esca in vineyards worldwide (Gramaje *et al.* 2015). *Phaeoacremonium minimum* seems to be the most common species on grapevines (Crous *et al*., 1996; Mostert *et al.* 2006a), followed by *Pm. parasiticum* (Mostert *et al.* 2006a).

It has been reported by Damm *et al.* (2008), that fourteen (14) *Phaeoacremonium* species were isolated from necrotic woody tissue of *Prunus* spp. (plum, peach, nectarine and apricot) from different stone fruit growing areas in South Africa. *Phaeoacremonium* scolyti was most frequently isolated, and present on all *Prunus* species sampled, followed by *Togninia minima* (anamorph: *Pm. minimum*) and *Pm. australiense.* Almost all taxa isolated represent new records. Moreover, *Phaeoacremonium scolyti* was reported for the first time, associated with other *Phaeoacremonium spp.*, during surveys in Turkish vineyards (Ankara) (Özben *et al.* 2012) and Spanish grapevine nursery (Valencia) (Gramaje *et al.* 2008), causing Esca and Petri disease. Its involvement in the disease was confirmed by pathogenicity assays in the two mentioned studies.

A study carried out in Italy by Essakhi *et al.* (2008) on a big collection of *Phaeoacremonium* isolates from grapevines, revealed the presence of 13 species of *Phaeoacremonium* isolated from Esca diseased grapevines. *Phaeoacremonium minimum* was the most frequently isolated species associated with foliar symptoms. Four distinct species of *Phaeoacremonium,* namely *Pm. croatiense, Pm. hungaricum, Pm. sicilianum* (Sicily) and *Pm. tuscanum* (Tuscany) were newly described from grapevine in the mentioned study.

During surveys in pome fruit orchards in Iran (2011-2013), six species of *Phaeoacremonium* namely, *Pm. minimum, Pm. parasiticum, Pm. rubrigenum, Pm. scolyti, Pm. mortoniae* and *Pm. iranianum* were isolated from wood samples (branches) of apple, pear, quince and hawthorn trees showing yellowing, wilting, dieback, cankers and various internal wood discoloration (Sami *et al.* 2014). In this study, *Phaeoacremonium* spp. were reported for the first time in the world, on quince and hawthorn. Also, the authors mentioned that it was the first report of isolation of *Pm. parasiticum, Pm. iranianum* and *Pm. mortoniae* from apple wood, while *Pm. minimum, Pm. rubrigenum, Pm. scolyti* and *Pm. parasiticum* were newly reported from pear trees.

In Italian olive groves, several *Phaeoacremonium* species were isolated and characterized by Nigro *et al.* (2013) following the appearance of the severe quick decline of Apulia in 2013, namely, *Phaeoacremonium minimum, Pm. alvesii, Pm. rubrigenun,* and *Pm. parasiticum* which was the most frequent species isolated. Furthermore, the fungus *Phaeoacremonium minimum* was also identified by Carlucci *et al.* (2013b) in diseased olive trunks and branches by OQDS, although isolated at low frequencies.

During a survey carried out in Italian vineyards (Foggia Province), three known *Phaeoacremonium* spp. were found associated with Esca symptoms such as foliage discoloration, defoliation, wilt, vascular brown streaking and central brown necrosis of grapevine. The species were namely *Pm. minimum, Pm. parasiticum and Pm. scolyti.* In addition, one new species named *Phaeoacremonium italicum,* was isolated and described for the first time in Apulia (southern Italy) (Raimondo *et al.* 2014). In this study, *Phaeoacremonium* fungi were isolated in combination with other fungal species, namely *Phaeomoniella chlamydospora, Fomitiporia mediterranea* and *Botryosphaeriaceae* spp.

In Western Australia, Gramaje *et al.* (2014) reported five *Phaeoacremonium* spp. within pruning wounds of tropical sandalwood, namely *Phaeoacremonium alvesii, Pm. parasiticum, Pm. venezuelense* and two new species described for the first time: *Pm. luteum* and *Pm. santali*.

More recently, Carlucci *et al.* (2015b) identified six *Phaeoacremonium* species associated with declining olive plants in Apulia (southern Italy), they were isolated from symptomatic wood of olive trees that showed crown wilt and twig and branch dieback. The species are *Pm. minimum, Pm. alvesii, Pm. parasiticum, Pm. italicum, Pm. sicilianum* and *Pm. scolyti*. The last three species were associated for the first time with wilt, decline and dieback of olive groves in Italy and worldwide.

Da Silva *et al.* (2017) have investigated the distribution of *Phaeoacremonium* species associated with Petri disease of table grapes in three regions in the Northeastern Brazil. Three species were identified: *Pm. minimum, Pm. nordesticola* and *Pm. parasiticum,* where *Phaeoacremonium minimum* was the most prevalent species.

Recently, Spies *et al.* (2018) have investigated the species diversity and host-range of *Phaeoacremonium* in the Western Cape (South-Africa) and reported a total of 35 *Phaeoacremonium* species from different woody hosts, including 13 new species described: *Pm. album, Pm. aureum, Pm. bibendum, Pm. gamsii, Pm. geminum, Pm. junior, Pm. longicollarum, Pm. meliae, Pm. oleae, Pm. paululum, Pm. proliferatum, Pm. rosicola* and *Pm. spadicum*.

Pathogenicity of *Phaeoacremonium* species have been demonstrated experimentally in many studies with the inoculation of many various woody hosts such as olive, grapevine, apricot, peach, plum and quince (Rumbos, 1986; Damm *et al.* 2008; Urbez-Torres *et al.* 2013; Mohammadi and Sharifi, 2016).

Phaeoacremonium parasiticum, identified as *Phialophora parasitica,* was inoculated onto shoots of young apricot, cherry, peach, and olive trees. The tests showed that the pathogen was capable to induce disease symptoms presented by vascular discoloration on all these fruit trees (Rumbos, 1986). As well, Two-year-old potted kiwifruit vines of the cultivar Hayward were inoculated with strains of *Phaeoacremonium parasiticum* and *Phaeoacremonium minimum*. Six months after inoculation, wood discolouration was clearly observed in all plants inoculated with *Phaeoacrernonium* species (Di Marco *et al.* 2004). Gramaje *et al.* (2015) reported that many inoculation studies have demonstrated that *Pm. minimum* can cause brown wood streaking (Adalat *et al*. 2000; Sparapano *et al.* 2000; Feliciano *et al*. 2004; Halleen *et al*. 2007; Gramaje *et al.* 2010), esca symptoms on leaves and berries (Graniti *et al.* 2001; Feliciano *et al.* 2004) and reduced shoot growth (Zanzotto *et al.* 2008; Gramaje *et al.* 2010).

Pathogenicity studies were conducted by Halleen *et al.* (2007) in glasshouse experiments where grapevine rootstocks were artificially inoculated, as well as in the field with mycelial plugs and spore suspensions of *Pm. minimum, Pm. krajdenii, Pm. subulatum, Pm. venezuelense,* and *Pm. viticola*. All the *Phaeoacremonium* spp. were able to infect, colonise and produce lesions statistically different to those caused by the water control and the non-pathogen.

Damm *et al.* (2008) conducted pathogenicity tests on detached apricot and plum shoots, with 14 *Phaeoacremonium* strains obtained from discoloured wood of different *Prunus* species in South Africa. They observed that most species were shown to be potentially pathogenic to plum, while only a few species were shown to be potentially pathogenic to apricot.

Aroca & Raposo (2009) studied the pathogenicity of nine *Phaeoacremonium* species on grapevine seedlings and cuttings: *Phaeoacremonium minimum, Pm. angustius, Pm. inflatipes, Pm. krajdenii, Pm. mortoniae, Pm. parasiticum, Pm. scolyti, Pm. venezuelense* and *Pm. viticola*. All the inoculated grapevine seedlings of *Vitis vinifera* cv. Malvar and cv. Airen showed typical symptoms of a vascular disease two months after inoculation. Grapevine cuttings of *Vitis vinifera* cv. Monastrell were vacuum inoculated and individually planted and the plants rated after five months showed that all *Phaeoacremonium* species caused a significant vascular discoloration, while only *Phaoeacremonium mortoniae* and *Pm. minimum* caused a significant root weight reduction compared with a non-inoculated control. *Phaoeacremonium parasiticum, Pm. angustius, Pm. inflatipes* and *Pm. venezuelense* caused significant foliar symptoms that included interveinal chlorosis and stunted leaves.

Pathogenicity studies conducted by Urbez-Torres *et al.* (2014) on dormant Chardonnay and rootstock 3309C with five *Phaeoacremonium* species, namely *Pm iranianum, Togninia fraxinopennsylvanica, Togninia minima, Pm. canadense* and *Pm. roseum,* showed all fungi to cause vascular symptoms similar to those observed in esca and Petri disease infected vines in British Columbia (BC). Additionally, the "tiger-stripes" foliar symptom of esca disease was successfully reproduced when healthy potted vines were inoculated with the same BC species.

Mohammadi and Sharifi (2016) reported for the first time the occurrence and pathogenicity of *Pm. viticola* and *Pm. alvesii* on detached shoots of quince, that have been inoculated with different *Phaeoacremonium* isolates obtained from discoloured woody tissues, borer holes, larvae of the beetles associated with insect-damaged shoots of quince trees in Iran.

I.5.3 Conventional and Molecular Identification

An accurate identification and characterization of plant pathogens require an understanding of the disease, and are crucial in disease management. Indeed, a range of diagnostic techniques has been described for the detection and identification of *Phaeoacremonium* spp. in infected plants. Traditionally, the identification of these fungi was based on conventional and culturing approaches, such as visual symptoms, fungal isolation and subsequent description of growth morphology and colony characteristics.

Generic descriptions of *Phaeoacremonium* species have been published by Crous *et al.* (1996) and Mostert *et al.* (2005). Numerous *Phaeoacremonium* spp. were identified by reference to the keys description including; conidiophore morphology, phialide type, size and shape, size of hyphal warts, conidial size and shape, and on culture characteristics, such as color of colonies, and cardinal growth temperatures (Crous *et al.* 1996; Mostert *et al.* 2005; Mostert *et al.* 2006a; Essakhi *et al.* 2008). However, a difficulty of differentiating between species has been proven resulted in some misidentifications. Additionally, *Phaeoacremonium* spp. are slow-growing fungi, which usually take up to 20 days to grow on a given medium. *Phaeoacremonium* is frequently overgrown by other microorganisms; then subculturing is required, which makes the identification process longer (Aroca and Raposo, 2007).

Since traditional methods of identification based on morphological characteristics are difficult, time-consuming, require specialist training and can lead to some misidentifications, the molecular techniques have been widely developed to detect and identify *Phaeoacremonium* species based on the DNA sequence data provided from Mostert *et al.* (2006a).

Indeed, several molecular methods were developed to detect and identify *Phaeoacremonium* species. Restriction Fragment Length Polymorphisms (RFLP) markers of the ITS region were used to distinguish *Phaeoacremonium minimum, Phaeoacremonium inflatipes,* and *Phaeoacremonium rubrigenum* (Tegli *et al.* 2000). Also, Dupont *et al.* (2002) used PCR-RFLP markers from the ITS regions and the partial b-tubulin gene to distinguish five species of *Phaeoacremonium*, namely *Pm. minimum, Pm. inflatipes, Pm. parasiticum, Pm. rubrigenum,* and *Pm viticola*.

DNA phylogenies based on the sequences of the ITS ribosomal DNA (rDNA), and partial fragments of the β–tubulin, actin and calmodulin gene regions have been used in various studies, to help in the determination of new species of *Phaeoacremonium* (Dupont *et al.* 2000; Mostert *et al.* 2006b; Essakhi *et al.* 2008; Gramaje *et al*. 2009, 2014). Moreover, Urbez-Torres *et al.* (2014) used the translation elongation factor 1-a with other DNA markers to describe two new species of *Phaeoacremonium*, namely *Phaeoacremonium canadense*, and *Phaeoacremonium roseum.*

Other PCR assays have been performed targeting even a partial β-tubulin region (TUB) for *Phaeoacremonium* isolates using the primers T1 (O'Donnell and Cigelnik, 1997) and Bt2b (Glass and Donaldson, 1995), and the actin gene (ACT) that was amplified using primers ACT-512F and ACT-783R (Carbone and Kohn, 1999). (White *et al.* 2011; Carlucci *et al.* 2013b; Carlucci *et al*. 2015b).

Several PCR primer sets have been developed to facilitate rapid *Phaeoacremonium* species identification and detection. Overton *et al*. (2004) designed genus-specific primers (Pac1f + Pac2r) from the ITS1 and ITS2 regions, for their use in real-time PCR with SYBR" Green. These primers have been used to detect *Pm. minimum* in naturally infected grapevines (Overton *et al.* 2005b).

A nested PCR approach was developed by Aroca and Raposo, (2007) to detect *Phaeoacremonium* spp. at genus level directly in grapevine wood, although the nested PCR has a risk of contamination with amplification products. This nested PCR method uses universal primers ITS1 and ITS4 in the primary reaction and specific primers (Pm1 and Pm2) designed on the ITS regions ITS1 and ITS2 of some *Phaeoacremonium* spp. Later on, a TaqMan qPCR was developed by Aroca *et al*. (2008) by using new designed degenerate primers (F2bt–R1bt) for the detection of *Phaeoacremonium* spp. in naturally infected grapevine cuttings.

A TaqMan rtPCR was successfully developped by Martın *et al.* (2012) by designing species-specific primers from the β -tubulin gene (palFI1 and palRI1) to identify *Pm. minimum* purified DNA from isolated fungi and from spore suspensions without DNA purification. Moreover, Pouzoulet *et al.* (2013) developed a multiplex real-time PCR method targeting the β-tubulin gene (primers PalQF and PalQR) of the pathogens and the actin gene of plant material, to detect

and quantify *Pm. minimum* in inoculated grapevine-wood samples and in young vines from nurseries.

A DNA macroarray based on reverse dot-blot hybridization containing 102 oligonucleotides complementary to portions of the β-tubulin region was developed for detection of young vine decline fungi (Urbez-Torres *et al.* 2015). The probes selected for the final array to detect and identify species in the genus *Phaeacremonium* allowed the discrimination of 29 *Phaeoacremonium* species.

I.6 Background on *Pleurostoma richardsiae*

I.6.1 Taxonomy and classification

Pleurostoma richardsiae is an ascomycete fungus that belongs to the class *Sordariomycetes*, order *Calosphaeriales* and family *Pleurostomataceae* (Réblová *et al.* 2015). It is a rare dematiaceous (darkly pigmented or black) fungus that was previously known as *Phialophora richardsiae* but has been renamed by Vijaykrishna *et al.* (2004) to accommodate the phialophora-like anamorphs of *Pleurostoma* species. Up to now, four species have been described within *Pleurostoma*, namely *Pl. richardsiae*, *Pl. repens*, *Pl. ootheca* (Vijaykrishna *et al.*, 2004) and *Pl. ochracea* (Mhmoud *et al.* 2012).

I.6.2 Distribution, host range and Pathogenesis

This fungus is found in soil, decaying wood and vegetation (Levenstadt *et al.* 2012). According to Schol-Schwarz, (1970), It has been isolated from wood, ground wood pulp, sewage and soil in North America, Europe, Africa and Asia. *Pleurostoma richardsiae* can also cause subcutaneous cysts in humans, usually through traumatic implantation (Pitrak *et al.*, 1988). It has also been reported recently causing perilacrimal mass in the lacrimal sac region in humans (Alam *et al.* 2017).

The fungus is a lesser known vascular grapevine fungal pathogen involved in Petri and esca disease complex. It was reported as a pathogen of grapevines by Eskalen *et al.* (2004), Rolshausen *et al.* (2010) in California, and Halleen *et al.* (2007) in South Africa. It has been isolated from wood tissue of grapevines that show Petri and Esca disease symptoms in California (USA) and South Africa. Pathogenicity testing showed that *Pl. richardsiae* could

infect pruning wounds of grapevine, although other fungi such as *Botryosphaeriaceae* species and *Phaeomoniella chlamydospora* were more aggressive.

In Italian olive groves, *Pleurostoma richardsiae* was associated with wilt of apical foliage, brown streaking under the bark, and cankers of trunks and branches of olive. According to Carlucci *et al.* (2013b), the fungus was isolated from symptomatic wood tissues, and it was often isolated from younger (18–22 old years) diseased olive trees. Pathogenicity tests carried out on young shoots showed that *Pl. richardsiae* was pathogenic and capable of causing brown wood streaking on olive.

During an assessment in vineyards of Apulia (southern Italy), *Pleurostoma richardsiae* was isolated from wood showing brown subcortical patches and streaking of trunks of grapevine cultivars that showed decline and dieback symptoms. The fungus was always isolated in association with *Botryosphaeria, Diplodia, Dothiorella, Lasiodiplodia* or *Neofusicoccum* species, and sometimes with *Phaeoacremonium* spp. and *Fomitiporia mediterranea*. Pathogenicity tests of *Pl. richardsiae*, conducted on young grapevine plants of two cultivars, demonstrated the production of brown streaking in both cultivars. The fungus is considered as pathogen of grapevine and was reisolated from discolored tissue of all inoculated shoots, fulfilling Koch's postulates (Carlucci *et al*. 2015a).

Olmo *et al.* (2015) have isolated *Pleurostoma richardsiae* in association with other fungi, from wood samples with internal necroses and brown to black vascular streaking of almond trees showing symptoms of decline in Spain. Pathogencity tests on almond trees with this fungal species in greenhouse showed that it was pathogenic and produced lesions statistically different from the control, being the most aggressive. It was reported by the authors that it should be considered as a trunk pathogen of almond trees.

Pintos *et al.* (2016) reported *Pleurostoma richardsiae* as a grapevine pathogen in Spain. The fungus was isolated in association with *Neofusicocum parvum*, *Botryosphaeria dothidea*, and *Phaeomoniella chlamydospora* from 2-year-old plants of grapevine showing decline symptoms, brown vascular streaking of the internal wood, and dark brown to black spots around the pith on the trunk. Results of pathogenicity tests revealed that *Pl. richardsiae* could produce

vascular necroses on inoculated plants, and it was reisolated of the lesions completing Koch's postulates.

Recently, Ivic *et al.* (2018) carried out a survey for olive diseases in Istria (Croatia) where the fungus *Pleurostoma richardsiae* was isolated in many orchards, from declining trees showing necrotic areas beneath the bark of root collars and lower part of the trunk, as well as from cankers and purple-brown streaking on olive twigs and branches. Pathogenicity tests performed on 2-year-old potted plants of local olive cultivar Buza revealed that the fungus was pathogen and was reisolated from the necrotic areas under the bark. The authors stated that it was the first report of *Pl. richardsiae* associated with dieback and collar rot of olive in Croatia and that the presence of this fungus in Croatia indicates that this olive pathogen might be more broadly distributed in European olive-growing regions than previously reported.

I.6.3 Conventional and Molecular Identification

Some reports have described the approach to be adopted for *Pleurostoma richardsiae* identification based on its micromorphology and cultural characters (Schol-Schwarz, 1970; Vijaykrishna *et al.* 2004; Carlucci *et al*. 2013b).

Vijaykrishna *et al.* (2004) characterized three *Pleurostoma* species, previously known as *Phialophora* spp., among them the fungus *Pleurostoma richardsiae.* Sequence analysis of the 5.8S nuclear ribosomal RNA gene and the flanking internal transcribed spacers (ITS1 and ITS2) that were amplified using primers ITS1 and ITS4 (White *et al.* 1990), and molecular data from partial 18S small subunit (SSU) permitted the new classification of the fungus.

Recent studies were carried out by Carlucci and her colleagues to characterize the *Pleurostoma* isolates initially on the basis of their microsatellite primed polymerase chain reaction (MSP-PCR) profiles, as described by (Santos and Phillips, 2009) using the primer M13 (Meyer *et al.,* 1993). The PCR assays have been developed targeting the 5.8S rDNA gene and flanking internal transcribed spacers 1 and 2 (ITS) of many representative *Pleurostoma* strains, that were amplified with primers ITS1 and ITS4 (Carlucci *et al.* 2013b; Carlucci *et al.* 2015a).

I.7 Scope of the thesis

Several fungal species have been associated with the olive quick decline syndrome, and are involved in producing complex symptoms on wood. Among those fungi, *Phaeoacremonium* species have been frequently isolated from declining olive trees, in addition to the fungus *Pleurostoma richardsiae*. As discussed previously, molecular techniques including phylogenetic analyses of the genus *Phaeoacremonium* over the last decade, based on partial fragments of the β–tubulin, and actin gene sequences, provided a good foundation for the identification of species within the genus. However, the increasing number of *Phaeoacremonium* species and the reports of new species of the genus associated with many other woody host plants, could lead to misidentifications. Additional genetic markers are therefore needed to provide more specific detection, and mainly to improve phylogenetic studies among *Phaeoacremonium* species. In this context and in order to establish a more robust resolution in the *Phaeoacremonium* phylogeny, and to identify new specific-species genetic markers, the aim of the research described in this thesis was to assess whether the ribosomal DNA intergenic spacer (IGS) region could be used to improve molecular discrimination and phylogenetic studies, among *Phaeoacremonium* spp., a DNA region that has not previously been studied in these fungal species.

In the introductory **Chapter 1**, we gave some background on fungal pathogens associated with olive quick decline by discussing their distribution, host range and pathogenesis. This was followed by short descriptions of detection methods and molecular techniques that have been used to detect and identify these fungal species.

Chapter 2 deals with survey of fungal species associated with olive quick decline syndrome in different orchards located in Salento. Morphological and cultural features were used to identify fungal genera and species obtained during the survey. This chapter describes also the use of molecular tools by amplifying portions of the β-tubulin (TUB2) and actin (ACT) genes to identify and confirm *Phaeoacremonium* spp. that were commonly isolated from declined olive trees.

Chapter 3, the central theme of the study, focuses on the amplification and structural analysis of the ribosomal DNA intergenic spacer (IGS) region of *Phaeoacremonium italicum,*

specifically selected here, being the most frequent *Phaeoacremonium* species that has been isolated from declined olive trees in Salento, as a study model. The IGS structure and organization of *Phaeoacremonium scolyti* and *Phaeoacremonium minimum* is also explored.

Chapter 4, the possibility to set up a PCR-based approach targeting the intergenic spacer (IGS) region of *Phaeoacremonium italicum* group, that could provide a specific detection of the fungus is explored. This assay could be used and optimized for detection of *Pm. italicum* in olive but also in other host plants.

Chapter 5 deals with the individual and combined phylogenetic analysis of the rDNA intergenic spacer (IGS), β-tubulin (TUB2) and actin (ACT) genes sequences of *Phaeoacremonium* spp. To this end, the IGS region; β-tubulin and actin genes are amplified from a collection of *Phaeoacremonium* spp. isolates, sequenced and phylogenetically analyzed. The objective of this study is to assess whether the intergenic spacer (IGS) region can be used as an integrative molecular tool to improve phylogenetic resolution of *Phaeoacremonium* spp.

1.8 Literature cited

Adalat, K., Whiting, C., Rooney, S., & Gubler, W. D. (2000). Pathogenicity of three species of *Phaeoacremonium* spp. on grapevine in California. *Phytopathologia Mediterranea*, 39(1),92-99.

Alam, M., Vaidehi, D., Therese, K. L., & Ali, M. J. (2017). Rare *Pleurostomophora richardsiae* Mass Causing Transient Nasolacrimal Duct Obstruction. *Ophthalmic plastic and reconstructive surgery*, 33(6), e154-e156.

Angiolillo, A., Mencuccini, M., & Baldoni, L. (1999). Olive genetic diversity assessed using amplified fragment length polymorphisms. *Theoretical and Applied Genetics*, 98(3-4), 411-421.

Aroca A. and Raposo R. (2007). PCR-based strategy to detect and identify species of *Phaeoacremonium* causing grapevine diseases. *Applied and Environmental Microbiology*, 73(9),2911-2918.

Aroca, A., Raposo, R., & Lunello, P. (2008). A biomarker for the identification of four *Phaeoacremonium* species using the β-tubulin gene as the target sequence. *Applied microbiology and biotechnology*, 80(6),1131-1140.

Besnard, G., Baradat, P., & Bervillé, A. (2001). Genetic relationships in the olive (*Olea europaea* L.) reflect multilocal selection of cultivars. *Theoretical and Applied Genetics*, 102(2-3), 251-258.

Besnard, G., Khadari, B., Navascués, M., Fernández-Mazuecos, M., El Bakkali, A., Arrigo, N., ... & Savolainen, V. (2013). The complex history of the olive tree: from Late Quaternary diversification of Mediterranean lineages to primary domestication in the northern Levant. *Proc. R. Soc. B*, 280(1756), 20122833.

Carbone, I., & Kohn, L. M. (1999). A method for designing primer sets for speciation studies in filamentous ascomycetes. *Mycologia*, 553-556.

Cariddi, C., Saponari, M., Boscia, D., De Stradis, A., Loconsole, G., Nigro, F., ... & Martelli, G. P. (2014). Isolation of a *Xylella fastidiosa* strain infecting olive and oleander in Apulia, Italy. *Journal of Plant Pathology*, 96(2),425-429.

Carlucci A., Cibelli F., Francesco L., Phillips A. J., Ciccarone C. and Raimondo M. L. (2015a). *Pleurostomophora richardsiae* associated with trunk diseases of grapevines in southern Italy. *Phytopathologia Mediterranea*, 54(1),109-123.

Carlucci A., Francesco L., Marchi G., Mugnai L. and Surico G. (2013a). Has *Xylella fastidiosa* "chosen" olive trees to establish in the Mediterranean basin? *Phytopathologia Mediterranea*, 52(3),541-544.

Carlucci A., Ingrosso F., Lops F. Sustainable strategies to contain the Olive Quick Decline Syndrome in south east Italy. In ,D 'Onghia A.M. (ed.), Brunel S. (ed.), Valentini F. (ed.). *Xylella fastidiosa* & the Olive Quick Decline Syndrome (OQDS). A serious worldwide challenge for the safeguar of olive trees. Bari, CIHEAM, 2017. p. 81-82 (*Options Méditerranéennes, Série A. Séminaires Méditerranéens; n . 121).*

Carlucci, A., Lops, F., Cibelli, F., & Raimondo, M. L. (2015b). *Phaeoacremonium* species associated with olive wilt and decline in southern Italy. *European Journal of Plant Pathology*, 141(4),717-729.

Carlucci A., Raimondo M. L., Cibelli F., Phillips A. J. and Francesco L. (2013b). *Pleurostomophora richardsiae, Neofusicoccum parvum* and *Phaeoacremonium aleophilum* associated with a decline of olives in southern Italy. *Phytopathologia Mediterranea*, 52(3),517-527.

Chliyeh, M., Touati, J., Selmaoui, K., Touhami, A. O., Filali-Maltouf, A., El Modafar, C., & Douira, A. (2014). Bibliographic inventory of the olive tree (*Olea europaea* L.) fungal diseases in the world. *Int J Pure Appl Biosci*, 2, 46-79.

Cimato, A., and Attilio, C. (2011). Worldwide diffusion and relevance of olive culture. In, Schena L. A. G. E., Cacciola S.O. (ed). Olive Diseases and Disorders. *Transworld Research NetWork*, 1-21.

Crous P. W., Gams W., Wingfield M. J. and Van Wyk P. (1996). *Phaeoacremonium* gen. nov. associated with wilt and decline diseases of woody hosts and human infections. *Mycologia*,786-796.

Crous, P. W., Wingfield, M. J., Guarro, J., Hernández-Restrepo, M., Sutton, D. A., Acharya, K., ... & Dutta, A. K. (2015). Fungal Planet description sheets,320–370. *Persoonia,Molecular Phylogeny and Evolution of Fungi*, 34, 167.

Da Silva, M. A., Correia, K. C., Barbosa, M. A. G., Câmara, M. P. S., Gramaje, D., & Michereff, S. J. (2017). Characterization of *Phaeoacremonium* isolates associated with Petri disease of table grape in Northeastern Brazil, with description of *Phaeoacremonium nordesticola* sp. nov. European *Journal of Plant Pathology*, 149(3),695-709.

Damm U., Mostert L., Crous P. and Fourie P. (2008). Novel *Phaeoacremonium* species associated with necrotic wood of Prunus trees. *Persoonia-Molecular Phylogeny and Evolution of Fungi*, 20(1),87-102.

Diaz, J. (1988). Teofrasto, historia de las plantas. Gredos, Madrid.

Dupont, J., Magnin, S., Cesari, C., & Gatica, M. (2002). ITS and β-tubulin markers help delineate *Phaeoacremonium* species, and the occurrence of *P. parasiticum* in grapevine disease in Argentina. *Mycological Research*, 106(10),1143-1150.

Dupont, J., Laloui, W., Magnin, S., Larignon, P., & Roquebert, M. F. (2000). *Phaeoacremonium viticola*, a new species associated with Esca disease of grapevine in France. *Mycologia*,499-504.

Efe, R., Soykan, A., Cürebal, I., Sönmez, S., Efe, R., Öztürk, M., and Ghazanfar, S. (2011). Olive and olive oil culture in the Mediterranean Basin. *Environment and Ecology in the Mediterranean Region. Cambridge, UK,Cambridge Scholars Publishing*, 51-62.

EPPO (2013). First reports of *Xylella fastidiosa* in the EPPO region. https://www.eppo.int/QUARANTINE/special_topics/Xylella_fastidiosa/Xylella_fastidiosa.htm.

Eskalen, A., Latham, S. R., & Gubler, W. D. (2004, June). Pathogenicity of *Phialophora* sp on grapevines in California. *In Phytopathology* (Vol. 94, No. 6, pp. S151-S151). 3340 PILOT KNOB ROAD, ST PAUL, MN 55121 USA,AMER PHYTOPATHOLOGICAL SOC.

Essakhi S., Mugnai L., Crous P., Groenewald J. and Surico G. (2008). Molecular and phenotypic characterisation of novel *Phaeoacremonium* species isolated from esca diseased grapevines. *Persoonia-Molecular Phylogeny and Evolution of Fungi*, 21(1),119-134.

FAOSTAT (2018). Food and Agriculture Organization of the United Nations, FAOSTAT database. http://www.fao.org/faostat/en/. (accessed on 08 december 2018).

Feliciano, A. J., Eskalen, A., & Gubler, W. D. (2004). Differential susceptibility of three grapevine cultivars to P*haeoacremonium aleophilum* and *Phaeomoniella chlamydospora* in California. *Phytopathologia Mediterranea*, 43(1),66-69.

Glass, N. L., & Donaldson, G. C. (1995). Development of primer sets designed for use with the PCR to amplify conserved genes from filamentous ascomycetes. *Applied and Environmental Microbiology*, 61(4),1323-1330.

Gramaje, D., Armengol, J., Mohammadi, H., Banihashemi, Z., & Mostert, L. (2009). Novel *Phaeoacremonium* species associated with Petri disease and esca of grapevine in Iran and Spain. *Mycologia,* 101(6),920-929.

Gramaje D., Alaniz S., Pérez-Sierra A., Abad-Campos P., García-Jiménez J. and Armengol J. (2008). First report of *Phaeoacremonium scolyti* causing Petri disease of grapevine in Spain. *Plant Disease,* 92(5),836-836.

Gramaje, D., García-Jiménez, J., & Armengol, J. (2010). Grapevine rootstock susceptibility to fungi associated with Petri disease and esca under field conditions. *Phytopathologia Mediterranea,* 49(1),128.

Gramaje, D., León, M., Pérez-Sierra, A., Burgess, T., & Armengol, J. (2014). New *Phaeoacremonium* species isolated from sandalwood trees in Western Australia. *IMA fungus,* 5(1),67-77.

Gramaje, D., Mostert, L., Groenewald, J. Z., & Crous, P. W. (2015). *Phaeoacremonium*,from esca disease to phaeohyphomycosis. *Fungal biology,* 119(9),759-783.

Graniti, A., Bruno, G., & Sparapano, L. (2001). Three-year observation of grapevines cross-inoculated with esca-associated fungi. *Phytopathologia Mediterranea, 40*(3),376-386.

Halleen, F., Mostert, L., & Crous, P. W. (2007). Pathogenicity testing of lesser-known vascular fungi of grapevines. *Australasian Plant Pathology*, 36(3),277-285.

Huang, S. K., Jeewon, R., Hyde, K. D., Bhat, D. J., Chomnunti, P., & Wen, T. C. (2018). Beta-tubulin and Actin gene phylogeny supports *Phaeoacremonium ovale as* a new species from freshwater habitats in China. *MycoKeys,* (41), 1.

IOC (2016). International Olive Council. Available online,http://www.internationaloliveoil.org/. (accessed on 18 April 2016).

IOC (2017). International Olive Council. MARKET NEWSLETTER No 115 –April 2017. Available online,http://www.internationaloliveoil.org/. (accessed on 09 mai 2017).

IOC (2018). International Olive Council. World Olive Oil Figures. Available online: http://www.internationaloliveoil. org/estaticos/view/131-world-olive-oil-figures (accessed on 2 February 2018).

Ivic, D., Ivanovic, A., Milicevic, T., & Cvjetkovic, B. (2010). Shoot necrosis of olive caused by *Phoma incompta*, a new disease of olive in Croatia. *Phytopathologia Mediterranea,* 49, 414–416.

Ivic, D., Tomic, Z., & Godena, S. (2018). First report of *Pleurostomophora richardsiae* causing branch dieback and collar rot of olive in Istria, Croatia. *Plant Disease*, (ja).

Jiménez-Díaz, R. M., Cirulli, M., Bubici, G., del Mar Jiménez-Gasco, M., Antoniou, P. P., & Tjamos, E. C. (2012). Verticillium wilt, a major threat to olive production,current status and future prospects for its management. *Plant Disease,* 96(3),304-329.

Kaliterna, J., Milicevic, T., Ivic, D., Bencic, D., & Mesic, A. (2012). First report of *Diplodia seriata* as causal agent of olive dieback in Croatia. *Plant disease,* 96(2),290-290.

Lazzizera, C., Frisullo, S., Alves, A., Lopes, J., & Phillips, A. J. L. (2008). Phylogeny and morphology of *Diplodia* species on olives in southern Italy and description of *Diplodia olivarum* sp. nov. *Fungal Divers,* 31, 63-71.

Levenstadt, J. S., Poutanen, S. M., Mohan, S., Zhang, S., & Silverman, M. (2012). *Pleurostomophora richardsiae*–an insidious fungus presenting in a man 44 years after initial inoculation,A case report and review of the literature. *Canadian Journal of Infectious Diseases and Medical Microbiology*, 23(3),110-113.

Magdeleine, J., & Ottaviani, J. C. (1984). L'occupation pré et proto historique de l'abri de Scaffa Piana près de Saint Florent. *Bull. Soc. Sci. Hist. Nat. Corse*, 647, 39-48.

Malathrakis, N.E. (1979). Studies on a disease of olive due to fungus *Phoma incompta* Sacc. & Mart. *Ph.D. diss.* University of Athens, Greece.

Marin-Felix, Y., Hernández-Restrepo, M., Wingfield, MJ., Akulov, A., Carnegie, AJ., Cheewangkoon, R., Gramaje, D., Groenewald, JZ., Guarnaccia, V., Halleen, F., Lombard, L., Luangsaard, J., Marincowitz, S., Moslemi, A., Mostert, L., Quaedvlieg, W., Schumacher, R. K., Spies, CFJ., Thangavel, R., Taylor, PWJ., Wilson, AM., Wingfield, BD., Wood, AR., Crous, P.W. (2018). Genera of phytopathogenic fungi: GOPHY 2. Studies in Mycology. https://doi.org/10.1016/j.simyco.2018.04.002

Martelli G., Boscia D., Porcelli F. and Saponari M. (2016). The olive quick decline syndrome in south-east Italy,a threatening phytosanitary emergency. *European Journal of Plant Pathology*, 144(2),235-243.

Martín, M. T., Cobos, R., Martín, L., & López-Enríquez, L. (2012). Real-time PCR detection of *Phaeomoniella chlamydospora* and *Phaeoacremonium aleophilum*. *Applied and environmental microbiology*, AEM-07360.

Meyer, W., Mitchell, T. G., Freedman, E. Z., & Vilgalys, R. (1993). Hybridization probes for conventional DNA fingerprinting used as single primers in the polymerase chain reaction to distinguish strains of Cryptococcus neoformans. *Journal of Clinical Microbiology*, 31(9),2274-2280.

Mhmoud, N. A., Ahmed, S. A., Fahal, A. H., de Hoog, G. S., van den Ende, A. G., & van de Sande, W. W. (2012). *Pleurostomophora ochracea*, a novel agent of human eumycetoma with yellow grains. *Journal of clinical microbiology*, JCM-01470.

Moazzo, G. P. (1983). plantes d'Homere et de quelques autres poetes de l'antiquite. I. Avant-propos. Safran (Krokos). In Annales Musei Goulandris.

Mohammadi, H., & Sharifi, S. (2016). Association of Botryosphaeriaceae and Phaeoacremonium species with insect-damaged quince shoots. *Journal of Plant Pathology*, 35-42.

Mohammadi, H., Sarcheshmehpour, M., & Mafi, E. (2015). Fungal trunk pathogens associated with wood decay of pistachio trees in Iran. *Spanish journal of agricultural research*, (2), 6.

Mostert L., Groenewald J. Z., Summerbell R. C., Gams W. and Crous P. W. (2006a). Taxonomy and pathology of *Togninia* (Diaporthales) and its *Phaeoacremonium* anamorphs. *Studies in Mycology*, 54,1-113.

Mostert L., Groenewald J. Z., Summerbell R. C., Robert V., Sutton D. A., Padhye A. A. and Crous P. W. (2005). Species of *Phaeoacremonium* associated with inf-ections in humans and environmental reservoirs in infected woody plants. *Journal of clinical microbiology*, 43(4),1752-1767.

Mostert L., Halleen F., Fourie P. and Crous P. W. (2006b). A review of *Phaeoacremonium* species involved in Petri disease and esca of grapevines. *Phytopathologia Mediterranea*, 45(4),12-29.

Moral, J., Agustí-Brisach, C., Pérez-Rodríguez, M., Xaviér, C., Raya, M. C., Rhouma, A., & Trapero, A. (2017). Identification of fungal species associated with branch dieback of olive and resistance of table cultivars to *Neofusicoccum mediterraneum* and *Botryosphaeria dothidea*. *Plant disease*, 101(2),306-316.

Moral, J., Muñoz-Díez, C., González, N., Trapero, A., & Michailides, T. J. (2010). Characterization and pathogenicity of *Botryosphaeriaceae* species collected from olive and other hosts in Spain and California. *Phytopathology*, 100(12),1340-1351.

Moral, J., Xavier, J. C., Roca, L. F., Moreda, W., & Trapero, A. (2014). La Antracnosis del olivo y su efecto en la calidad del aceite.

Mostert, L., Crous, P. W., Groenewald, J. Z., Gams, W., & Summerbell, R. C. (2003). *Togninia* (Calosphaeriales) is confirmed as teleomorph of *Phaeoacremonium* by means of morphology, sexual compatibility and DNA phylogeny. *Mycologia*, 95(4),646-659.

Nigro F., Antelmi I. and Ippolito A. (2014). Identification and characterization of fungal species associated with the quick decline of olive.In, (eds). *Prooceedings "International Symposium on the European Outbreak of Xylella fastidiosa in Olive"*, Gallipoli–Locorotondo, Italy. 29.

Nigro, F., Antelmi, I., Sion, V., Parente, P., & Pacifico, A. (2018). First Report of Dactylonectria torresensis Causing Foot and Root Rot of Olive Trees. *Plant Disease*, (ja).

Nigro, F., Boscia, D., Antelmi, I., & Ippolito, A. (2013). Fungal species associated with a severe decline of olive in southern Italy. *Journal of plant pathology*, 95(3).

O'Donnell, K., & Cigelnik, E. (1997). Two divergent intragenomic rDNA ITS2 types within a monophyletic lineage of the fungusfusariumare nonorthologous. *Molecular phylogenetics and evolution*, 7(1),103-116.

Olmo, D., Armengol, J., León, M., & Gramaje, D. (2015). Pathogenicity testing of lesser-known fungal trunk pathogens associated with wood decay of almond trees. *European journal of plant pathology*, 143(3),607-611.

Overton, B. E., Stewart, E. L., Qu, X., Wenner, N. G., & Christ, B. J. (2004). Qualitative real-time PCR SYBR® Green detection of Petri disease fungi. *Phytopathologia Mediterranea*, 43(3),403-410.

Overton, B. E., Stewart, E. L., & Wenner, N. G. (2005). Molecular phylogenetics of grapevine decline fungi from Pennsylvania and New York. *Phytopathologia Mediterranea*, 44,90-91.

Özben S., Degirmenci K., Demirci F. and Uzunok S. (2012). First report of *Phaeoacremonium scolyti* associated with esca and petri diseases of grapevine in Turkey. *Plant Disease, 96*(5),766-766.

Pascoe, I. G., Edwards, J., Cunnington, J. H., & Cottral, E. H. (2004). Detection of the Togninia teleomorph of *Phaeoacremonium aleophilum* in Australia. *Phytopathologia Mediterranea*, 43(1),51-58.

Pouzoulet, J., Mailhac, N., Couderc, C., Besson, X., Daydé, J., Lummerzheim, M., & Jacques, A. (2013). A method to detect and quantify *Phaeomoniella chlamydospora* and *Phaeoacremonium* aleophilum DNA in grapevine-wood samples. *Applied microbiology and biotechnology*, 97(23),10163-10175.

Pintos Varela, C., Redondo Fernandez, V., Aguin Casal, O., Ferreiroa Martinez, V., & Mansilla Vazquez, J. P. (2016). First report of *Pleurostoma richardsiae* causing grapevine trunk disease in Spain. *Plant Disease*, 100(10),2168-2168.

Pitrak, D. L., Koneman, E. W., Estupinan, R. C., & Jackson, J. (1988). *Phialophora richardsiae* infection in humans. *Clinical Infectious Diseases*, 10(6), 1195-1203.

Raimondo M. L., Lops F. and Carlucci A. (2014). *Phaeoacremonium italicum* sp. nov., associated with esca of grapevine in southern Italy. *Mycologia,* 106(6),1119-1126.

Réblová, M., Jaklitsch, W. M., Réblová, K., & Štěpánek, V. (2015). Phylogenetic Reconstruction of the Calosphaeriales and Togniniales Using Five Genes and Predicted RNA Secondary Structures of ITS, and *Flabellascus tenuirostris* gen. et sp. nov. *PloS one, 10*(12), e0144616.

Réblová, M., Mostert, L., Gams, W., & Crous, P. W. (2004). New genera in the Calosphaeriales,Togniniella and its anamorph *Phaeocrella,* and *Calosphaeriophora* as anamorph of *Calosphaeria. Studies in Mycology,* 50(2),533-550.

Rhouma, A., Triki, M. A., Krid, S., & Masallem, M. (2010). First report of a Branch dieback of olive trees in Tunisia caused by a *Phoma* sp. *Plant Disease,* 94, 636.

Rolshausen, P. E., Úrbez-Torres, J. R., Rooney-Latham, S., Eskalen, A., Smith, R. J., & Gubler, W. D. (2010). Evaluation of pruning wound susceptibility and protection against fungi associated with grapevine trunk diseases. *American Journal of Enology and Viticulture,* 61(1),113-119.

Romero, M. A., Sánchez, M. E., & Trapero, A. (2005). First report of *Botryosphaeria ribis* as a branch dieback pathogen of olive trees in Spain. *Plant Disease,* 89(2),208-208.

Rooney-Latham, S., Eskalen, A., & Gubler, W. D. (2005). Teleomorph formation of *Phaeoacremonium aleophilum*, cause of esca and grapevine decline in California. *Plant Disease,* 89(2),177-184.

Rumbos, I. C. (1986). *Phialophora parasitica*, causal agent of cherry dieback. *Journal of Phytopathology*, 117(3),283-287.

Rumbos, I. C. (1988). *Cytospora oleina* causing canker and dieback of olive in Greece. *Plant Pathology,* 37,441-444.

Rumbos, I. C. (1993). Dieback symptoms on olive trees caused by the fungus *Eutypa lata* 1. *EPPO Bulletin,* 23(3),441-445.

Russo, C., Cappelletti, G. M., Nicoletti, G. M., Di Noia, A. E., & Michalopoulos, G. (2016). Comparison of European olive production systems. *Sustainability*, 8(8), 825.

Sami S., Mohammadi H. and Heydarnejad J. (2014). *Phaeoacremonium* species associated with necrotic wood of pome fruit trees in Iran. *J Plant Pathol,* 96,19-27.

Sanchez-Hernandez, M. E., Pérez, D. A., Blanco, L., & Trapero-Casas, A. (1996). Vascular wilt of young olive trees. Agricultura, *Revista Agropecuaria,* 65(772),928-932.

Sanchez-Hernández, M.E., Ruiz-Davila, A., Pérez de Algaba, A., Blanco-Lopez, M.A., & Trapero-Casas, A. (1998). Occurrence and etiology of death of young olive trees in southern Spain. *European Journal of Plant Pathology,* 104(4),347-357.

Sanei, S. J., & Razavi, S. E. (2012). Survey of olive fungal disease in north of Iran. *Annu Rev & Res Biol,* 2,27-36.

Santos, J. M., & Phillips, A. J. L. (2009). Resolving the complex of Diaporthe (*Phomopsis*) species occurring on *Foeniculum vulgare* in Portugal. *Fungal Diversity,* 34(11),111-125.

Saponari, M., Boscia, D., Nigro, F., & Martelli, G. P. (2013). Identification of DNA sequences related to *Xylella fastidiosa* in oleander, almond and olive trees exhibiting leaf scorch symptoms in Apulia (Southern Italy). *Journal of Plant Pathology,* 95(3),659-668.

Saponari, M., Boscia, D., Altamura, G., Loconsole, G., Zicca, S., D'Attoma, G., ... & Savino, V. N. (2017). Isolation and pathogenicity of Xylella fastidiosa associated to the olive quick decline syndrome in southern Italy. *Scientific reports*, *7*(1), 17723.

Schol-Schwarz M. B. (1970). Revision of the genus *Phialophora* (Moniliales). *Persoonia-Molecular Phylogeny and Evolution of Fungi*, 6(1),59-94.

Sparapano, L., Bruno, G., Ciccarone, C., & Graniti, A. (2000). Infection of grapevines by some fungi associated with esca. II. Interaction among *Phaeoacremonium chlamydosporum, P. aleophilum* and *Fomitiporia punctata*. *Phytopathologia Mediterranea*, 39,53-58.

Spies, C. F. J., Moyo, P., Halleen, F., & Mostert, L. (2018). *Phaeoacremonium* species diversity on woody hosts in the Western Cape Province of South Africa. *Persoonia*, 40,26-62.

Taylor, R. K., Hale, C. N., & Hartill, W. F. T. (2001). A stem canker disease of olive (*Olea europaea*) in New Zealand. *New Zealand Journal of Crop and Horticultural Science*, 29(3),219-228.

Tegli, S., Bertelli, E., & Surico, G. (2000). Sequence analysis of ITS ribosomal DNA in five *Phaeoacremonium* species and development of a PCR-based assay for the detection of P. chlamydosporum and P. aleophilum in grapevine tissue. *Phytopathologia mediterranea*, 39(1),134-149.

Terral, J. F. (1997). Débuts de la domestication de l'olivier (Olea europaea L.) en Méditerranée nord-occidentale, mise en évidence par l'analyse morphométrique appliquée à du matériel anthracologique. *Comptes rendus de l'Académie des sciences. Série 2. Sciences de la terre et des planètes*, 324(5), 417-425.

Terral, J. F., & Arnold-Simard, G. (1996). Beginnings of olive cultivation in eastern Spain in relation to Holocene bioclimatic changes. *Quaternary Research*, 46(2), 176-185.

Tosi, L., & Zazzerini, A. (1994). *Phoma incompta* a new olive parasite in Italy. *Petria*, 4(2),161-169.

Úrbez-Torres, J. R., Haag, P., Bowen, P., & O'Gorman, D. T. (2014). Grapevine trunk diseases in British Columbia,incidence and characterization of the fungal pathogens associated with esca and Petri diseases of grapevine. *Plant Disease*, 98(4),469-482.

Úrbez-Torres, J. R., Haag, P., Bowen, P., Lowery, T., & O'Gorman, D. T. (2015). Development of a DNA macroarray for the detection and identification of fungal pathogens causing decline of young grapevines. *Phytopathology*, 105(10),1373-1388.

Úrbez-Torres, J. R., Peduto, F., Vossen, P. M., Krueger, W. H., & Gubler, W. D. (2013). Olive twig and branch dieback,etiology, incidence, and distribution in California. *Plant Disease*, 97(2),231-244.

Uylaşer, V., and Yildiz, G. (2014). The historical development and nutritional importance of olive and olive oil constituted an important part of the Mediterranean diet. *Critical reviews* in *food science and nutrition*, 54(8),1092-1101.

Veloso, M. M., Simões-Costa, M. C., Carneiro, L. C., Guimarães, J. B., Mateus, C., Fevereiro, P., & Pinto-Ricardo, C. (2018). Olive tree (Olea europaea L.) diversity in traditional small farms of Ficalho, Portugal. *Diversity*, *10*(1), 5.

Vijaykrishna, D., Mostert, L., Jeewon, R., Gams, W., Hyde, K. D., & Crous, P. W. (2004). *Pleurostomophora*, an anamorph of *Pleurostoma* (Calosphaeriales), a new anamorph genus morphologically similar to *Phialophora*. *Studies in Mycology*, 50,387-395.

White, T. J., Bruns, T., Lee, S. J. W. T., & Taylor, J. L. (1990). Amplification and direct sequencing of fungal ribosomal RNA genes for phylogenetics. *PCR protocols, a guide to methods and applications*, 18(1),315-322.

White, C. L., Halleen, F., Fischer, M., & Mostert, L. (2011). Characterisation of the fungi associated with esca diseased grapevines in South Africa. *Phytopathologia Mediterranea*, 50(4),204-223.

Zanzotto, A., Gardiman, M., & Lovat, L. (2008). Effect of *Phaeomoniella chlamydospora* and *Phaeoacremonium sp.* on in vitro grapevine plants. *Scientia horticulturae*, 116(4),404-408.

Zohary, D., & Spiegel-Roy, P. (1975). Beginnings of fruit growing in the Old World. *Science*, 187(4174), 319-327.

II. SURVEY OF FUNGAL SPECIES ASSOCIATED WITH OLIVE QUICK DECLINE IN SOUTHERN ITALY

II.1 Introduction

The evergreen tree *Olea europaea* is one of the most widely grown tree-crop species in the Mediterranean basin, which has always been the authentic place for its cultivation and olive oil production since ancient times. It has been cultivated in Mediterranean basin around 4000 BC, where olive trees have played an important role in the rural and economic development of the Mediterranean's areas over the centuries (Loumou and Giourga, 2003).

Unfortunately, olive tree is subjected to be attacked by various pathogens, which affect its health, yield and its oil quality. In Italy, Olive quick decline syndrome (OQDS) causes severe damages to the olive trees in Salento (Apulia, Italy) and poses a severe threat for the agriculture of Mediterranean countries. The bacterium *Xylella fastidiosa* was confirmed to be the causal agent of OQDS in Salento olive crops (Saponari *et al.* 2013), however a number of fungi have been reported to be involved in the olive quick decline (Carlucci *et al.* 2013; 2015b; Nigro *et al.* 2013). The aim of the present study was to identify the different fungi associated with the decline syndrome of olive trees in Apulia.

II.2 Materials and methods

II.2.1 Survey location and sampling

A survey was undertaken during a period of three years (2015-2018), piloted by the research team of the laboratory of 'Patologia vegetale' (Dept. SAFE-Univ Foggia), across different olive orchards of Salento in Apulia, to assess the occurrence of the fungal species associated to olive quick decline syndrome. The samples were collected from the base of the trunk, the trunks and branches, from 150 symptomatic olive plants, exhibiting external and internal symptoms on the olive trunks, branches and stems; manifested by wilting and dieback of entire and/or part of the crown, with browning areas and brown streaking under the bark of the trunk and branches; as well, extended necrotic areas with brown discolouration (in cross section) (Figure II.1).

Figure II.1. Disease symptoms observed on olive trees. (a) and (b) Wilt and Dieback. (c) and (d) Browning and streaking under the bark and discoloration of wood.

II.2.2 Fungal isolations

The samples were transported to the laboratory for analysis and were washed in running tap water before surface sterilization was performed according to Fisher *et al.* (1992). Then the tissues were cut into small pieces (2–5 mm) from discoloured wood of xylematic areas of the base of the trunk, the trunk and the branches, and were placed on malt extract agar (MEA; 2% malt extract and 2% agar Oxoid Ltd.), amended with 300 mg/l streptomycin sulphate (Sigma-Aldrich, USA). The isolation plates were incubated at 23 °C (±2 °C) in the dark. To

obtain purified cultures, conidia were separated by dilution plating onto agar plates. After 24 to 36 h of incubation, single germinating conidia were collected under a light microscope and transferred to plates of potato dextrose agar (PDA; 3.9 % potatodextrose agar; Oxoid Ltd., UK) and incubated at 25°C in the dark, with observation after 7 to 21 days.

II.2.3 Morphological characterization of the isolated fungi

Fungi isolated from symptomatic olive tissues were identified to genus and species level, based on the morphological and culture characteristics. Genera and species in the Botryosphaeriaceae were identified by reference to the keys, and descriptions provided in Phillips *et al.* (2013). *Phaeoacremonium* spp. were morphologically identified based on the conidiophore morphology, phialide type and shape, size of hyphal warts and conidial size and shape (Mostert et *al.* 2006a; Essakhi *et al*. 2008; Raimondo *et al.* 2014). Representative isolates from each group of *Phaeoacremonium* spp. were selected for molecular studies.

Pleurostomophora species was identified referring to Carlucci *et al.* (2013). Other fungi were identified according to descriptions provided by De Hoog *et al.* (2000), Crous *et al.* (2015), Valenzuela-Lopez *et al*. (2018). All reference isolates were deposited in the culture collection of Department of Science of Agricultural, Food and Environment (SAFE), University of Foggia, Italy.

II.2.4 Isolation frequency and principal component analysis

The fungal isolation frequency (IF %) per olive plant was calculated as the number of tissue portions infected by a given fungus, divided by the overall number of tissue portions incubated.

$$IF\ (\%) = \text{Number of isolates of a fungus} \times 100 / \text{Total number of isolates.}$$

To determine which fungus was correlated to which plant organ (i.e., trunk, base of trunk, branches), principal component analysis (PCA) was performed using XLStat 2018.3 (Addinsoft SARL, France).

II.2.5 DNA extraction of *Phaeoacremonium* spp., amplification and sequencing

Genomic DNA of all fungal isolates identified morphologically as *Phaeoacremonium* spp. was extracted from fresh fungal mycelia grown on PDA plates in the dark for 2 to 3 weeks, according to a protocol provided by Carlucci *et al.* (2013).

Portions of the β-tubulin (TUB2) and actin (ACT) genes of *Phaeoacremonium* spp. were amplified using primer sets T1 (O'Donnell and Cigelnik, 1997) and Bt-2b (Glass and Donaldson, 1995), and ACT-512F and ACT-783R (Carbone and Kohn 1999), respectively (Table II.1). Each 50 µl PCR mixture included, 30 ng of DNA template, 1x PCR buffer, 2 mM $MgCl_2$, 200 mM deoxynucleotide triphosphates, 2.5 pmol each primer and 0.5 U Taq polymerase. PCR reactions were carried out in a C-1000 Touch™ Thermal Cycler (Bio Rad, USA). The cycling parameters consisted of an initial denaturation step at 96 °C for 5 min, followed by 36 cycles of denaturation at 94 °C for 30 s, 52 °C for 30 s, 72 °C for 80 s and final cycle at 72 °C for 7 min. The cycling parameters for TUB2 gene were initiated at 96 °C for 5 min followed by 36 cycles at 94 °C for 30 s, annealing (58 °C for TUB, 52 °C for ACT) for 30 s, 72 °C for 80 s and final extension cycle at 72 °C for 7 min (Raimondo *et al.* 2014). Negative control reactions were used to detect contamination in the samples.

The PCR amplification products were separated by electrophoresis at 100 V for 30 min, in 1.5% agarose gels in 1.0× Tris-acetate acid EDTA (TAE) buffer and were visualized under UV light after staining with ethidium bromide in a Gel Doc™ EZ System (Biorad). The DNA Ladder 100-1000pb (Canvax™) was used as a molecular size marker. PCR products were purified using the NucleoSpin® Plasmid kit (NoLid) (Machery-Nagel, Düren, Germany) following the manufacturer instructions and sequenced in both directions by Eurofins Genomics (Ebersbeg, Germany).

Table II.1 Primers used for PCR amplification

Name	Sequence (5′->3′)	Direction	Locus	Reference
T1	5`- AACATGCGTGAGATTGTAAGT-3`	Forward	Partial beta-tubulin gene (Tub2)	O'Donnell & Cigelnik (1997)
Bt-2b	5`- ACCCTCAGTGTAGTGACCCTTGGC-3`	Reverse		Glass & Donaldson (1995)
ACT-512F	5`- ATGTGCAAGGCCGGTTTCGC-3`	Forward	Partial actin gene (ACT)	Carbone & Kohn (1999)
ACT-783R	5`- TACGAGTCCTTCTGGCCCAT -3`	Reverse		

Forward and reverse sequences obtained were assembled using the BioEdit v7.2.6 (Hall, 1999). To identify the isolates and verify the preliminary morphological identification, sequence homology searches were performed with Basic Local Alignment Search Tool (BLAST 2.7.1+; Altschul *et al.* 1997).

II.3 Results

II.3.1 Isolations and identification of fungi

The survey revealed that the mycoflora isolated from 150 symptomatic olive plants sampled was variable. Different fungi isolated from olive tissues are presented in Table (II.2). *Phaeoacremonium* spp., Botryosphaeriaceae, *Acremonium* spp., *Pleurostoma richardsiae*, *Alternaria alternata* and *Aspergillus* spp. were isolated more frequently than other fungi, although *Acremonium* spp, *Alternaria alternata* and *Aspergillus* spp. are considered to be saprophytic.

Table II.2 Isolation frequencies of the fungi isolated from internal symptoms of discoloured wood and brown streaking of olive trees

	% fungal isolation frequency (number)			
Fungi isolated	**Base of trunk**	**Trunk**	**Branches**	**Total**
Acremonium spp.	2.4 (55)	3.4 (76)	4.5 (102)	10.4 (233)
Aereobasidium pullulans	0.4 (8)	0.2 (4)	0.7 (16)	1.2 (28)
Alternaria alternata	2.4 (55)	1.4 (32)	3.0 (67)	6.8 (154)
Aspergillus spp.	3.2 (71)	0.4 (10)	0.8 (17)	4.4 (98)
Botryosphaeriaceae	5.6 (127)	8.4 (188)	5.9 (132)	19.9 (447)
Caeniochaeta spp.	0.6 (13)	0.7 (16)	0.9 (21)	2.2 (50)
Cylindrocarpon destructans	0.6 (14)	0.2 (4)	0.0 (0)	0.8 (18)
Cytospora oleina	0.0 (0)	0.3 (6)	0.7 (16)	1.0 (22)
Diaporthe spp.	0.0 (0)	0.7 (16)	1.9 (43)	2.6 (59)
Epicoccum nigrum	0.9 (21)	0.4 (8)	0.7 (15)	2.0 (44)
Lecythophora lignicola	0.3 (6)	1.2 (26)	0.3 (7)	1.7 (39)
Lewia spp.	0.2 (5)	0.0 (0)	0.8 (17)	1.0 (22)
Microsphaeropsis olivacea	0.2 (5)	0.6 (13)	0.0 (0)	0.8 (18)
Paracucurbitaria spp.	0.0 (0)	0.0 (0)	0.5 (11)	0.5 (11)
Penicillium spp.	1.2 (27)	0.0 (0)	0.1 (3)	1.3 (30)
Phaeoacremonium italicum	4.3 (98)	5.5 (123)	2.3 (51)	12.1 (272)
Phaeoacremonium minimum	2.1 (49)	3.2 (71)	1.6 (35)	6.9 (155)
Phaeoacremonium scolyti	0.8 (20)	0.8 (18)	0.6 (12)	2.2 (50)
***Phaeoacremonium* spp. (subtotal)**	**7.4 (167)**	**9.4 (212)**	**4.4 (98)**	**21.2 (477)**
Phaeomoniella spp.	1.6 (37)	2.0 (44)	0.6 (13)	4.2 (94)
Phoma incompta	1.2 (27)	1.4 (31)	0.5 (11)	3.1 (69)
Pleurostoma richardsiae	2.5 (56)	3.5 (78)	1.3 (29)	7.2 (163)
Sarocladium kiliense	0.3 (7)	0.0 (0)	0.6 (13)	0.9 (20)
Verticillium spp.	0.1 (3)	0.0 (0)	0.0 (0)	0.1 (3)
Micelia sterilia	1.2 (26)	0.3 (7)	1.1 (24)	2.5 (57)
No fungi or bacteria	2.0 (46)	0.7 (15)	1.5 (33)	4.2 (94)
N. of tissue portions used	750	750	750	2250
Number of plants analysed		150		
N. infected plants from *Phaeoacremonium* spp.		149		

Phaeoacremonium species were the most predominant fungi isolated from olive trees. A total of 477 isolates (21.2 %) of *Phaeoacremonium* spp. were isolated, mostly of all of the olive plants sampled, from internal symptoms that consisted of discoloured wood of the base of the trunk (7.4 %), the trunk (9.4 %) and the branches (4.4 %) (Table II.2). All *Phaeoacremonium* species showed morphological features typical of the genus *Phaeoacremonium* described by Mostert *et al.* (2006a) specifically, presence of different types of phialides observed in the aerial mycelium, and either discrete or integrated in conidiophores, and conidia hyaline and aseptate. *Phaeoacremonium italicum* was the predominant species isolated (12.1 % of total isolates) from wood discolouration of the base of the trunk, trunk and branches of affected olive trees, followed by *Pm. minimum* (6.9 %) and *Pm. scolyti* (2.2 %).

PCR amplifications of the β-tubulin (TUB) and actin (ACT) genes regions of *Phaeoacremonium* spp. isolates gave products of approximately 0.6, and 0.3 kb, respectively. The TUB and the ACT sequences were generated and identities of all *Phaeoacremonium* species was confirmed by BLAST searches in GenBank. All sequences showed 99 to 100% homology with the corresponding sequences of the type strain: *Pm. italicum* isolates (GenBank accession no. for β-tubulin KJ534074, ACT KJ534046, Raimondo *et al*. 2014); *Pm. minimum* (GenBank accession no. AF246806/AY735498, Mostert *et al.* 2005) and *Pm. scolyti* (GenBank accession no. AF246800//AY579224, Mostert *et al*. 2005).

Fungi belonging to Botryosphaeriaceae were the second most prevalent fungi isolated from the base of the trunk (5.6 %), the trunk (8.4 %) and the branches (5.9 %) and were frequently collected in association with *Phaeoacremonium* isolates. *Pleurostoma richardsiae* was commonly isolated from the wood tissues of base of the trunk (2.5 %), from the trunk (3.5%) and from the branches (1.3%) (Table II.2).

Other fungi were isolated with lower frequencies, such as *Phaeomoniella* spp., *Phoma incompta*, *Diaporthe* spp., *Cylindrocarpon destructans*, *Epicoccum nigrum*, *Lecythophora lignicola*, *Penicillium* spp., *Aureobasidium pullulans*, *Cytospora oleina*, *Microsphaeropsis olivacea and Verticillium* spp. These fungi were isolated from 0.1 to 4.2% of the branches, trunk and base of the trunk (Table II.2), however, the occurrence of each genus/species was

variable. Among them, *Phaeomoniella* spp. and *Phoma incompta* were the most prevalent. These fungi were identified to genus or species level based on morphological characteristics.

According to PCA (Figure II.1), the three variables related to the plant organs (i.e., Var1-3: Branches, trunk, base of trunk) of the olive plants were reduced to two factors, (factor 1, 87.58%; factor 2, 8.67%). The projection of the variables and cases (i.e., biplot analysis; Figure II.1) showed that from trunk and base of trunk (i.e., Var2, Var3), the species of *Phaeoacremonium* spp. with greater IFs were mainly associated, in addition to *Pleurostoma richardsiae*, *Phaeomoniella* spp. and *Aspergillus*. From branches (Var1), species of Botryosphaeriaceae, *Acremonium* spp. and *Alternaria alternata* were associated, each with IFs of 5.9%, 4.9% and 3% respectively (Figure II.1, Table II.2).

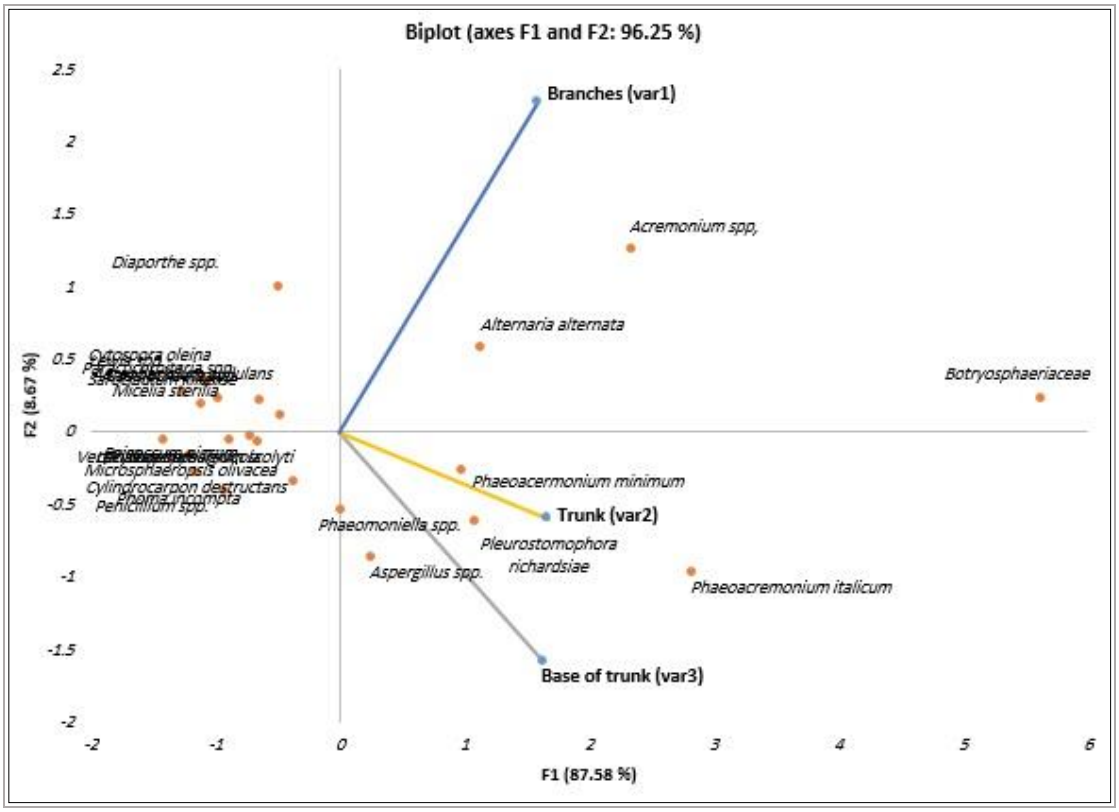

Figure II.1 Principal component analysis based on isolation frequencies (IFs)

II.4 Discussion

A range of fungi belonging to different genera were isolated from symptomatic wood of olive trees affected by OQDS in Apulia and identified by means of morphological characters and also analyses of partial sequences of actin and β-tubulin genes, namely for *Phaeoacremonium* spp.

The dominant fungal species on olive trees were *Phaeoacremonium* species. These latter included *Pm. italicum, Pm. minimum* and *Pm. scolyti* which were isolated from all different organs sampled. The colony characteristics and conidiophores, phialides and conidia dimensions of the *Phaeoacremonium* species obtained were similar to those previously described in the literature (Mostert *et al.* 2006a; Raimondo *et al*. 2014).

In the literature, *Phaeoacremonium italicum* was reported by Raimondo *et al.* (2014), as a new *Phaeoacremonium* species from grapevine in Italy and later on from olive trees showing decline in Apulia (Carlucci *et al*. 2015b). Similarly, the presence of *Phaeoacremonium minimum* in olives was confirmed by Carlucci *et al.* (2013) and Nigro *et al.* (2013) in diseased olive trunks and branches by OQDS in southern Italy, although isolated at low frequencies. While, *Pm. scolyti* was reported for the first time from olive trees in Italy and worldwide by Carlucci *et al.* (2015b). The present study confirms the presence of these *Phaeoacremonium* species already known from olive trees showing decline, and all of these have been previously reported associated with esca diseases of grapevine.

Indeed, *Pm. italicum* has been isolated for the first time in Apulia (southern Italy), from grapevine that had esca symptoms such as foliage discoloration, defoliation, wilt, vascular brown streaking and central brown necrosis (Raimondo *et al.* 2014) and Petri disease (Carlucci *et al.* 2017). *Phaeoacremonium minimum* is also known as one of the causal organisms of Petri disease and esca, being recognized as the most common species on grapevines worldwide (Groenewald *et al*. 2001; Mostert *et al.* 2006b; Essakhi *et al.* 2008; Martín et *al*. 2014; Raimondo *et al.* 2014; Úrbez-Torres *et al.* 2013; Carlucci *et al.* 2017). Likewise, *Phaeoacremonium scolyti* has previously been found on *V. vinifera* in South Africa, Turkey and Italy (Mostert *et al*. 2006b; Özben *et al.* 2012; Raimondo *et al.* 2014; Carlucci *et al*. 2017).

Phaeoacremonium minimum has been isolated from other host plants than grapevine, including *Actinidia chinensis* (Crous and Gams, 2000); *Cydonia oblonga* (Sami *et al.* 2014); *Diospyros kaki* (Moyo *et al.* 2016); *Malus domestica, Pyrus communis* (Cloete *et al.* 2011); *Phoenix dactylifera* (Mohammadi, 2014); *Prunus armeniaca, Prunus persica, Prunus salicina* (Damm *et al.* 2008); *Prunus pennsylvanica* (Hausner *et al.* 1992) and *Salix* sp. (Hausner et *al.* 1992). The other fungus *Phaeoacremonium scolyti* isolated at lower frequency (2.2 %) in this study, was also found on other hosts, on *Prunus* in South Africa (Damm *et al.* 2008) and was associated with necrotic wood of various pome trees in Iran (Sami *et al.* 2014).

Among the fungal taxa isolated from symptomatic wood of olive trees in this study, species of Botryosphaeriaceae were the second most prevalent. These species are primarily known to cause olive fruit rot (Chattaoui *et al.* 2011; Lazzizera *et al*. 2008; Moral *et al.* 2008; Moral *et al.* 2008; Phillips *et al.* 2005). However, some have not only been associated with olive branch dieback in New Zealand (Taylor *et al*. 2001), in Spain (Moral *et al*. 2010; Romero *et al*. 2005), in Croatia (Kaliterna *et al*. 2012), in California (Moral *et al*. 2010; Úrbez-Torres *et al*. 2013), but also associated with decline of olive trees in southern Italy (Carlucci *et al*. 2013). The family Botryosphaeriaceae involve several pathogens responsible for cankers and dieback in a wide range of hosts, including olive, grapevine, almond, pistachio, apricot, peach, oak and bay laurel (Michailides *et al.* 1991; Alves *et al*. 2004; Damn *et al*. 2007; Burruano *et al*. 2011; Inderbitzin *et al*. 2011; Úrbez-Torres *et al*. 2011; Lawrence *et al*. 2017).

The dematiaceous fungus *Pleurostoma richardsiae* was the third most prevalent fungus isolated during this study from symptomatic olive wood. The fungus has been reported by Carlucci *et al.* (2013) in association with brown streaking under the bark, and cankers of trunks and branches of olive in southern Italy. The current study corroborates the presence of this latter species in southern Italian olive groves.

Pleurostoma richardsiae is also known to be a vascular grapevine pathogen in California (Eskalen *et al.* 2004; Rolshausen *et al.* 2010), in South Africa (Halleen *et al.* 2007), in Italy (Carlucci *et al.* 2015a) and Spain (Pintos *et al.* 2016). It has been reported to cause branch dieback and collar rot of olive in Istria-Croatia (Ivic *et al.* 2018), and has also been associated

with necroses and vascular streaking of almond trees showing decline in Spain (Olmo *et al.* 2015).

Although less prevalent, other fungi such as *Phaeomoniella* spp., *Phoma incompta*, *Diaporthe* spp., *Cylindrocarpon destructans*, *Cytospora oleina* and *Microsphaeropsis olivacea*, were isolated at low frequencies from symptomatic wood of olive trees, these fungi have been previously reported to occur in olive trees in Italy (Carlucci *et al.* 2015b).

II.5 References

Alves, A., Correia, A., Luque, J., & Phillips, A. (2004). Botryosphaeria corticola, sp. nov. on Quercus species, with notes and description of Botryosphaeria stevensii and its anamorph, Diplodia mutila. *Mycologia*, *96*(3), 598-613.

Altschul, S. F., Madden, T. L., Schäffer, A. A., Zhang, J., Zhang, Z., Miller, W., & Lipman, D. J. (1997). Gapped BLAST and PSI-BLAST: a new generation of protein database search programs. *Nucleic acids research*, *25*(17), 3389-3402.

Burruano, S., Mondello, V., Conigliaro, G., Alfonzo, A., Spagnolo, A., & Mugnai, L. (2008). Grapevine decline in Italy caused by Lasiodiplodia theobromae. *Phytopathologia Mediterranea*, *47*(2), 132-136.

Carbone, I., & Kohn, L. M. (1999). A method for designing primer sets for speciation studies in filamentous ascomycetes. *Mycologia*, 553-556.

Carlucci, A., Cibelli, F., Francesco, L. O. P. S., Phillips, A. J., Ciccarone, C., & Raimondo, M. L. (2015a). Pleurostomophora richardsiae associated with trunk diseases of grapevines in southern Italy. *Phytopathologia mediterranea*, *54*(1), 109-123.

Carlucci, A., Francesco, L. O. P. S., Mostert, L., Halleen, F., & Raimondo, M. L. (2017). Occurrence fungi causing black foot on young grapevines and nursery rootstock plants in Italy. *Phytopathologia Mediterranea*, *56*(1), 10-39.

Carlucci, A., Lops, F., Cibelli, F., & Raimondo, M. L. (2015b). *Phaeoacremonium* species associated with olive wilt and decline in southern Italy. *European Journal of Plant Pathology*, 141(4),717-729.

Carlucci, A., Raimondo, M. L., Cibelli, F., Phillips, A. J. and Francesco, L. (2013). *Pleurostomophora richardsiae*, *Neofusicoccum parvum* and *Phaeoacremonium aleophilum* associated with a decline of olives in southern Italy. *Phytopathologia Mediterranea*, 52(3),517-527.

Chattaoui, M., Rhouma, A., Krid, S., Triki, M. A., Moral, J., Msallem, M., & Trapero, A. (2011). First report of fruit rot of olives caused by Botryosphaeria dothidea in Tunisia. *Plant Disease*, *95*(6), 770-770.

Cloete, M., Fourie, P. H., Ulrike, D. A. M. M., Crous, P. W., & Mostert, L. (2011). Fungi associated with die-back symptoms of apple and pear trees, a possible inoculum source of grapevine trunk disease pathogens. *Phytopathologia Mediterranea*, *50*(4), 176-190.

Crous, P. W., & Gams, W. (2000). Phaeomoniella chlamydospora gen. et comb. nov., a causal organism of Petri grapevine decline and esca. *Phytopathologia Mediterranea*, *39*(1), 112-118.

Crous, P. W., Wingfield, M. J., Guarro, J., Hernández-Restrepo, M., Sutton, D. A., Acharya, K., ... & Dutta, A. K. (2015). Fungal Planet description sheets: 320–370. *Persoonia: Molecular Phylogeny and Evolution of Fungi*, *34*, 167.

Damm, U., Crous, P. W., & Fourie, P. H. (2007). Botryosphaeriaceae as potential pathogens of Prunus species in South Africa, with descriptions of Diplodia africana and Lasiodiplodia plurivora sp. nov. Mycologia, 99(5), 664-680.

Damm, U., Mostert, L., Crous, P. W., & Fourie, P. H. (2008). Novel Phaeoacremonium species associated with necrotic wood of Prunus trees. *Persoonia: Molecular Phylogeny and Evolution of Fungi*, *20*, 87.

De Hoog, G. S., Guarro, J., Gene, J., & Figueras, M. J. (2000). Atlas of clinical fungi, Centraalbureau voor Schimmelcultures. *Utrecht, The Netherlands*, 276-282.

Eskalen, A., Latham, S. R., & Gubler, W. D. (2004, June). Pathogenicity of Phialophora sp on grapevines in California. In *Phytopathology* (Vol. 94, No. 6, pp. S151-S151). 3340 PILOT KNOB ROAD, ST PAUL, MN 55121 USA: AMER PHYTOPATHOLOGICAL SOC.

Essakhi, S., Mugnai, L., Crous, P. W., Groenewald, J. Z., & Surico, G. (2008). Molecular and phenotypic characterisation of novel *Phaeoacremonium* species isolated from esca diseased grapevines. *Persoonia: Molecular Phylogeny and Evolution of Fungi*, *21*, 119.

Fisher, P. J., Petrini, O., Petrini, L. E., & Descals, E. (1992). A preliminary study of fungi inhabiting xylem and whole stems of *Olea europaea*. *Sydowia*, *44*(2), 117-121.

Glass, N. L., & Donaldson, G. C. (1995). Development of primer sets designed for use with the PCR to amplify conserved genes from filamentous ascomycetes. *Applied and Environmental Microbiology*, *61*(4), 1323-1330.

Groenewald, M., Ji-Chuan, K. A. N. G., Crous, P. W., & Walter, G. A. M. S. (2001). ITS and β-tubulin phylogeny of *Phaeoacremonium* and *Phaeomoniella* species. Mycological Research, 105(6), 651-657.

Hall, T. A. (1999). BioEdit: a user-friendly biological sequence alignment editor and analysis program for Windows 95/98/NT. In *Nucleic acids symposium series*, 41, 95-98.

Halleen, F., Mostert, L., & Crous, P. W. (2007). Pathogenicity testing of lesser-known vascular fungi of grapevines. *Australasian Plant Pathology*, *36*(3), 277-285.

Hausner, G., Eyjólfsdóttir, G. G., Reid, J., & Klassen, G. R. (1992). Two additional species of the genus Togninia. *Canadian Journal of Botany*, *70*(4), 724-734.

Inderbitzin, P., Bostock, R. M., Trouillas, F. P., & Michailides, T. J. (2010). A six locus phylogeny reveals high species diversity in Botryosphaeriaceae from California almond. *Mycologia*, *102*(6), 1350-1368.

Ivic, D., Tomic, Z., & Godena, S. (2018). First report of *Pleurostomophora richardsiae* causing branch dieback and collar rot of olive in Istria, Croatia. *Plant Disease*, (ja).

Kaliterna, J., Milicevic, T., Ivic, D., Bencic, D., & Mesic, A. (2012). First report of Diplodia seriata as causal agent of olive dieback in Croatia. *Plant disease*, *96*(2), 290-290.

Lawrence, D. P., Hand, F. P., Gubler, W. D., & Trouillas, F. P. (2017). Botryosphaeriaceae species associated with dieback and canker disease of bay laurel in northern California with the description of Dothiorella californica sp. nov. *Fungal biology*, *121*(4), 347-360.

Lazzizera, C., Frisullo, S., Alves, A., & Phillips, A. J. L. (2008). Morphology, phylogeny and pathogenicity of Botryosphaeria and Neofusicoccum species associated with drupe rot of olives in southern Italy. *Plant Pathology*, *57*(5), 948-956.

Loumou, A., & Giourga, C. (2003). Olive groves: ``The life and identity of the Mediterranean". *Agriculture and Human Values*, *20*(1), 87-95.

Martín, L., de Miera, L. E. S., & Martín, M. T. (2014). AFLP and RAPD characterization of Phaeoacremonium aleophilum associated with Vitis vinifera decline in Spain. *Journal of Phytopathology*, *162*(4), 245-257.

Michailides, T. J. (1991). Pathogenicity, distribution, sources of inoculum, and infection courts of Botryosphaeria dothidea on pistachio. *Phytopathology*, *81*(5), 566-573.

Mohammadi, H. (2014). Phaeoacremonium spp. and Botryosphaeriaceae spp. Associated with Date Palm (P hoenix dactylifera L.) Decline in I ran. *Journal of Phytopathology*, *162*(9), 575-581.

Moral, J., Luque, F., & Trapero, A. (2008). First report of Diplodia seriata, the anamorph of "Botryosphaeria" obtusa, causing fruit rot of olive in Spain. *Plant Disease*, *92*(2), 311-311.

Moral, J., Muñoz-Díez, C., González, N., Trapero, A., & Michailides, T. J. (2010). Characterization and pathogenicity of Botryosphaeriaceae species collected from olive and other hosts in Spain and California. *Phytopathology*, *100*(12), 1340-1351.

Mostert, L., Groenewald, J. Z., Summerbell, R. C., Robert, V., Sutton, D. A., Padhye, A. A., & Crous, P. W. (2005). Species of *Phaeoacremonium* associated with infections in humans and environmental reservoirs in infected woody plants. *Journal of Clinical Microbiology*, *43*(4), 1752-1767.

Mostert, L., Groenewald, J. Z., Summerbell, R. C., Gams, W., & Crous, P. W. (2006a). Taxonomy and pathology of Togninia (Diaporthales) and its Phaeoacremonium anamorphs. *Studies in Mycology*, *54*, 1-113.

Mostert, L., Halleen, F., Fourie, P., & Crous, P. W. (2006b). A review of Phaeoacremonium species involved in Petri disease and esca of grapevines. *Phytopathologia Mediterranea*, *45*, S12-S29.

Moyo, P., Mostert, L., Bester, M., & Halleen, F. (2016). Trunk disease fungi associated with Diospyros kaki in South Africa. *Plant disease*, *100*(12), 2383-2393.

Nigro F, Boscia D, Antelmi I and Ippolito A, 2013. Fungal species associated with a severe decline of olive in Southern Italy. Disease note. Journal of Plant Pathology, 95, 668.

O'Donnell, K., & Cigelnik, E. (1997). Two divergent intragenomic rDNA ITS2 types within a monophyletic lineage of the fungus fusarium are nonorthologous. *Molecular phylogenetics and evolution*, *7*(1), 103-116.

Özben, S., Değirmenci, K., Demirci, F., & Uzunok, S. (2012). First report of Phaeoacremonium scolyti associated with esca and petri diseases of grapevine in Turkey. *Plant disease*, *96*(5), 766-766.

Phillips, A. J. L., Alves, A., Abdollahzadeh, J., Slippers, B., Wingfield, M. J., Groenewald, J. Z., & Crous, P. W. (2013). The Botryosphaeriaceae: genera and species known from culture. *Studies in mycology*, *76*, 51-167.

Phillips, A. J. L., Rumbos, I. C., Alves, A., & Correia, A. (2005). Morphology and phylogeny of Botryosphaeria dothidea causing fruit rot of olives. *Mycopathologia*, *159*(3), 433-439.

Raimondo, M. L., Lops, F., & Carlucci, A. (2014). *Phaeoacremonium italicum* sp. nov., associated with esca of grapevine in southern Italy. *Mycologia*, *106*(6), 1119-1126.

Rolshausen, P. E., Úrbez-Torres, J. R., Rooney-Latham, S., Eskalen, A., Smith, R. J., & Gubler, W. D. (2010). Evaluation of pruning wound susceptibility and protection against fungi associated with grapevine trunk diseases. *American Journal of Enology and Viticulture*, *61*(1), 113-119.

Romero, M. A., Sánchez, M. E., & Trapero, A. (2005). First report of Botryosphaeria ribis as a branch dieback pathogen of olive trees in Spain. *Plant Disease*, *89*(2), 208-208.

Sami, S., Mohammadi, H., & Heydarnejad, J. (2014). Phaeoacremonium species associated with necrotic wood of pome fruit trees in Iran. *Journal of plant pathology*, *96*(3), 487-495.

Taylor, R. K., Hale, C. N., & Hartill, W. F. T. (2001). A stem canker disease of olive (Olea europaea) in New Zealand. *New Zealand Journal of Crop and Horticultural Science*, *29*(3), 219-228.

Thompson, J. D., Gibson, T. J., Plewniak, F., Jeanmougin, F., & Higgins, D. G. (1997). The CLUSTAL_X windows interface: flexible strategies for multiple sequence alignment aided by quality analysis tools. *Nucleic acids research*, *25*(24), 4876-4882.

Urbez-Torres, J. R. (2011). The status of Botryosphaeriaceae species infecting grapevines. *Phytopathologia Mediterranea*, *50*(4), 5-45.

Úrbez-Torres, J. R., Peduto, F., Vossen, P. M., Krueger, W. H., & Gubler, W. D. (2013). Olive twig and branch dieback: etiology, incidence, and distribution in California. *Plant Disease*, *97*(2), 231-244.

Valenzuela-Lopez, N., Cano-Lira, J. F., Guarro, J., Sutton, D. A., Wiederhold, N., Crous, P. W., & Stchigel, A. M. (2018). Coelomycetous Dothideomycetes with emphasis on the families Cucurbitariaceae and Didymellaceae. *Studies in Mycology*, *90*, 1-69.

III. AMPLIFICATION AND STRUCTURAL ANALYSIS OF THE RIBOSOMAL DNA INTERGENIC SPACER (IGS) REGION OF *PHAEOACREMONIUM ITALICUM* - A STUDY MODEL

III.1 Introduction

A wide range of fungal diseases impact on olive production. Among them, olive diseases such as wilt, dieback and decline associated with fungal species have acquired great importance worldwide. In recent years, various *Phaeoacremonium* species have been associated with the olive quick decline syndrome in Southern Italy, and studies have reported their importance in causing brown wood streaking of *Olea europea* (Nigro *et al.* 2013; Carlucci *et al.* 2015). Indeed, the genus *Phaeoacremonium* has a global distribution and wide host range, including woody plants, insect larvae and humans, with species being reported from South, Central and North America, Europe, Scandinavia, Ukraine, the Middle East, Far East, Oceania and Africa (Gramaje *et al*. 2015). Detailed taxonomic studies including phylogenetic analyses of the genus *Phaeoacremonium* based on partial fragments of the β–tubulin, and actin gene sequences provided a good basis for the identification of species within the genus (Mostert *et al*. 2006). However, the taxonomic reassignment and the increasing recognition of novel *Phaeoacremonium* species associated with various wood host plants is to be considered (Gramaje *et al.* 2015; Spies *et al.* 2018).

In this sense, further studies in order to pick out additional phylogenetic markers are needed to improve phylogenetic resolution of species and prevent their misidentifications. The intergenic spacer (IGS) region of rDNA is commonly considered the most variable part of the rDNA unit, both in sequence and in length and various studies have indicated that, molecular phylogenetic analysis based on this region might be a suitable tool to investigate intra- and interspecific divergence and would provide significant molecular evidence for classification and evolutionary studies of various fungi (Pramateftaki *et al.* 2000; kim *et al.* 2001; Roose-Amsaleg *et al.* 2002; Papaioannou *et al.* 2013; Durkin *et al.* 2015).

In fact, we have been studying the occurrence of fungi associated with olive quick decline in some orchards of Salento (see Chapter II) and, in that study, we report the dominant fungal

species on olive trees, which were *Phaeoacremonium* species. These latter included first *Pm. italicum*, but also *Pm. scolyti* and *Pm. minimum* which were isolated from different wood organs sampled. Thus, the aim of the present study was to study for the first time the intergenic spacer (IGS) region of rDNA of *Phaeoacremonium italicum*, the most frequent *Phaeoacremonium* species that has been isolated from declined olive trees, as a study model, and to assess whether IGS sequences can be used for further molecular discrimination among *Phaeoacremonium* isolates. In addition, the IGS region of *Pm. scolyti* and *Pm. minimum* was also studied here. To this end, amplifications of the intergenic spacer of rDNA from a set of *Phaeoacremonium* isolates were performed and the entire IGS region was determined. This region was sequenced and structurally analyzed.

III.2 Materials and methods

III.2.1 Fungal isolates and culture conditions

Isolates of *Pm. italicum, Pm. scolyti and Pm. minimum* were obtained from symptomatic olive trees samples collected during a field survey carried out across olive orchards of Salento in southern Italy (see chapter II). *Phaeoacremonium* isolates from host species other than olive were also included in the study and were obtained from the culture collection of Department of Science of Agricultural, Food and Environment (SAFE), University of Foggia, Italy (Table III.1). To extract total genomic DNA, single-spore cultures of all isolates were grown on potato dextrose agar plates (PDA; 3.9 % potatodextrose agar; Oxoid Ltd., UK) for 2 to 3 weeks and incubated at 25°C for further DNA isolation.

III.2.2 DNA extraction from fungal cultures

Genomic DNA of all isolates was extracted from 300 mg fresh fungal mycelia, according to a protocol provided by Carlucci *et al.* (2013). The mycelium was scraped off the plates and ground in liquid nitrogen to a fine powder with a pestle and mortar. Then, 300 mg of the ground mycelium was collected in 2 mL microcentrifuge tubes, re-suspended in 600 µL DNA extraction buffer [200 mM Tris-HCl, pH 8.0, 200 mM EDTA, pH 8.0, 0.5% (w/v) SDS, pH 7.2, 1.2% (v/v) β-mercaptoethanol], supplemented with 5 µL proteinase K (stock, 20 mg L^{-1}; Oxoid Ltd.), and kept at 65°C for 1h. Then, 600 µL of Chloroform (Oxoid Ltd.) were added to each tube, vortexed for 15 to 20 seconds. The samples were centrifuged (10,000 rpm, 18°C,

15 min), and the aqueous phase was transferred to new 2 mL microcentrifuge tubes, with the addition of 3 µL RNAase (stock, 40 mg L^{-1}; Oxoid Ltd.). The samples were left at 37°C for 30 min, and then an equal volume of chloroform was added to each sample, vortexed for 15 s, followed by centrifugation (10,000 rpm, 18°C, 10 min). The supernatants were transferred into new 1.5 mL centrifuge tubes, with the addition of 0.5 vol. cold 7.5 M ammonium acetate (Oxoid Ltd.). Following gentle mixing, the samples were left on ice for 30 min, and then centrifuged (13,000 rpm, 2°C, 10 min). The aqueous phase was collected and transferred to 2.0 mL centrifuge tubes, with the addition of 0.7 vol. cold isopropanol (Oxoid Ltd.) and gentle mixing; these were then left at -25°C overnight. After, the samples were centrifuged (13,000 rpm, 2°C, 25 min), the supernatants discarded, and the pellets washed twice with 700 µL cold 70% ethanol, with centrifugation (13,000 rpm, 2°C, 15 min) and discarding of the supernatants. After the final centrifugation, the pellets were left to dry at room temperature with the tubes open, for 10–15 min. The pellets were then dissolved in 100µL hot (65°C) TE buffer (10 mM Tris, pH 8.0, 1 mM EDTA). DNA concentration was then determined by spectrophotometer (UV-1800, Shimadzu) at λ = 260-280nm. Thereafter, DNA was diluted to a final concentration of 30 ng/µl and stored at -20°C for further PCR assays.

Table III.1 *Phaeoacremonium* isolates used in this study for IGS-PCR amplification with code names, original hosts, and geographical origins.

Species	Isolate code	Subgroup	Host	Origin
Pm. italicum	Pm 1	A	Olive	Salento, Apulia, Italy
	Pm 2	A	Olive	Salento, Apulia, Italy
	Pm 6	F	Olive	Salento, Apulia, Italy
	Pm 15	E	Olive	Salento, Apulia, Italy
	Pm 17	E	Olive	Salento, Apulia, Italy
	Pm 18	F	Olive	Salento, Apulia, Italy
	Pm 19			San Severo, (Fg),
	CBS 137763	A	Grapevine	Apulia, Italy
	Pm 23	A	Grapevine	Cerignola (Fg), Apulia, Italy
	Pm 31M	B	Almond	San Giovanni Rotondo, (Fg), Apulia, Italy

Table III.1 Continued

Species	Isolate code	Subgroup	Host	Origin
Pm. italicum	Pm 34	A	Olive	Salento, Apulia, Italy
	Pm 35M	B	Olive	Salento, Apulia, Italy
	Pm 38	A	Olive	Salento, Apulia, Italy
	Pm 45	D	Olive	Salento, Apulia, Italy
	Pm 50M	C	Olive	Salento, Apulia, Italy
	Pm 59	F	Olive	Salento, Apulia, Italy
	Pm 60	D	Olive	Salento, Apulia, Italy
	Pm 77	F	Olive	Salento, Apulia, Italy
	Pm 105	D	Olive	Salento, Apulia, Italy
	Pm 180	E	Olive	Salento, Apulia, Italy
	Pm 196	E	Olive	Salento, Apulia, Italy
	Pm 210	E	Olive	Salento, Apulia, Italy
	Pm 235	E	Olive	Salento, Apulia, Italy
	Pm 250	E	Olive	Salento, Apulia, Italy
Pm. scolyti	Pm 1M	A1	Olive	Salento, Apulia, Italy
	Pm 5	C1	Cherry	Foggia, Apulia, Italy
	Pm 10M	A1	Olive	Salento, Apulia, Italy
	Pm 44M	B1	Olive	Salento, Apulia, Italy
	Pm 51M	A1	Olive	Salento, Apulia, Italy
	Pm 73M	B1	Olive	Salento, Apulia, Italy
	Pm 81M	B1	Olive	Salento, Apulia, Italy
	Pm 90	D1	Cherry	Foggia, Apulia, Italy
	Pm 92A	D1	Cherry	Foggia, Apulia, Italy
	Pm 155	C1	Olive	Foggia, Apulia, Italy
	Pm 233	D1	Cherry	Foggia, Apulia, Italy
Pm. minimum	Pm 7	A2	Grapevine	Cerignola, Apulia, Italy
	Pm 35	B2	Olive	Salento, Apulia, Italy
	Pm 39	B2	Olive	Salento, Apulia, Italy
	Pm 41	B2	Olive	Salento, Apulia, Italy
	Pm 67	A2	Olive	Cerignola, Apulia, Italy

Table III.1 Continued

Species	Isolate code	Subgroup	Host	Origin
Pm. minimum	Pm 68	D2	Grapevine	Barletta (Bat), Apulia, Italy
	Pm 90	A2	Grapevine	Barletta (Bat), Apulia, Italy
	Pm 109	C2	Olive	Salento, Apulia, Italy
	Pm 302	C2	Olive	Salento, Apulia, Italy
	Pm 351	D2	Grapevine	Barletta (Bat), Apulia, Italy
	Pm 369	D2	Grapevine	Barletta (Bat), Apulia, Italy
	Pm 400	C2	Olive	Salento, Apulia, Italy

III.2.3 PCR amplification for ribosomal intergenic spacer IGS region of the fungal isolates

The extracted DNA of all fungal isolates was tested for PCR amplification using two different pairs of universal primer (see Table III.2 for primer sequences and references). The primers used in our study were designed at terminal part of the large ribosomal subunit (28S) and at initial part of the small ribosomal subunit (18S) (Figure III.1) in order to amplify the complete intergenic spacer region (IGS) placed between these tandem repeat rDNA units, of many ascomycete and basidiomycete fungi.

Table III.2 Universal primers used for the amplification of IGS region within nuclear rDNA of *Phaeoacremonium* isolates.

Name	Sequence (5′->3′)	Direction	comments	Reference
LR12R	5`- GAACGCCTCTAAGTCAGAATCC-3`	Forward	located within the LSU RNA	Vilgalys laboratory, Duke University
invSR1R	5`- ACTGGCAGAATCAACCAGGTA -3`	Reverse	located within the SSU RNA	
IG11F	5`- CGTGAGCTGGGTTTAGACCGTCGT -3`	Forward	located within the LSU RNA	Yaseen *et al.* (unpublished data).
IG12R	5`- GATTGGGTAATTTGCGCGCCTGCT -3`	Reverse	located within the SSU RNA	

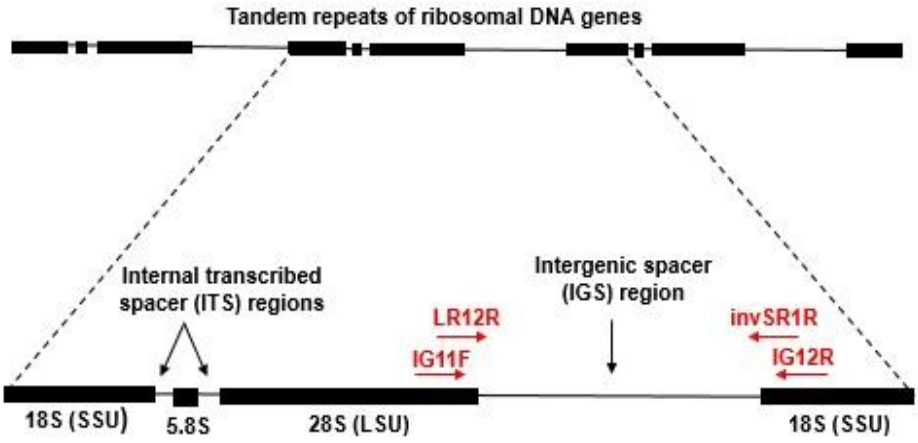

Figure III.1. Schematic representation of the ribosomal DNA and the location of the IGS universal primers used. Ribosomal genes (18S, 5.8S and 28S), included internal transcribed (ITS), and intergenic spacer non-coding regions (IGS).

The PCR assays using the primer pair LR12R/invSR1R were set up in a 25 µl mixture final volume with a C-1000 Touch™ Thermal Cycler (Bio Rad, USA). The PCR was standardized to amplify IGS region, in a reaction mixture containing 30 ng of genomic DNA, 1x PCR buffer (TaKaRa), 3 mM MgCl2 (TaKaRa), 200 µM deoxynucleoside triphosphates (TaKaRa), 0.2 µM forward and reverse primers and 1.25 unit of Taq DNA Polymerase (TaKaRa LA Taq®). The reaction involved initial denaturation at 95°C for 10 min, followed by 30 cycles in series of denaturation at 95°C for 1 min, annealing at 55°C for 1 min, and extension at 72°C for 150 s, with a final step of one cycle at 72°C for 10 min to final extension.

The PCR reactions using the primers pair IG11F/IG12R were performed in a 25 µl mixture final containing 30 ng of genomic DNA, 1x PCR buffer (TaKaRa), 2.5 mM MgCl2 (TaKaRa), 400 µM deoxynucleoside triphosphates (TaKaRa), 0.4 µM forward and reverse primers and 1.25 unit of Taq DNA Polymerase (TaKaRa LA Taq®). The thermal cycling conditions for IGS region were initial denaturation step at 94°C for 1 min, followed by 35 amplification cycles consisting of denaturation at 94°C for 10 seconds, and a 5 min 73°C primer annealing/extension step, with a final extension step at 72°C for 10 min. For both PCR protocols, a reaction mixture without sample DNA was used as a negative control to ensure that there was no contaminating DNA in the solution.

Amplicons were seperated by electrophoresis at 100 V, on 1.2 % agarose gels in 1x TAE buffer (40 mM Tris, 40 mM acetate, 2 mM EDTA, pH 8.0) (Sambrook *et al.*, 1989), stained with ethidium bromide and detected by UV fluorescence (Gel Doc™ EZ System - Biorad). The DNA Ladder 500pb -10kb (Canvax™) was used as a molecular size marker.

III.2.4 Cloning and Sequencing

III.2.4.1 Cloning into StrataClone™ PCR cloning vector pSC-A

The obtained PCR products of all fungal DNA were cloned using StrataClone™ PCR Cloning Kit (Agilent Technologies). The cloning reaction was set up in a sterile microcentrifuge tubes, including 3 µl of StrataClone™ Cloning Buffer, 2 µl of PCR products, and 1 µl of StrataClone™ Vector Mix to get a final volume of 6 µL for each reaction. The preparation was mixed gently by repeated pipetting and incubated for a minimum of 5 min to 15 minutes at room temperature (25°C). When the incubation was complete, the tubes were placed on ice.

III.2.4.2 Transformation of pSC-A StrataClone vector into *E. coli*

Once the ligation reaction was performed, 3 µl of each cloning reaction mixture was added to a tube of StrataClone SoloPack thawed competent cells, mixed gently and incubated on ice for 20 minutes. The tubes were then heat shocked at 42°C for 45 secs, and immediately incubated on ice 2 min, for transforming the recombinant plasmid inside the bacteria. Then, 250 µL pre-warmed LB medium was added and cells were incubated at 37°C for 1 hour shaking at 240 rpm to allow the recovery of the bacteria. During the outgrowth period, LB–ampicillin plates were prepared for blue-white color screening by spreading 40 µl of 2% X-gal on each plate. After plating 100 µl of the transformation mixture on 2% X-gal LB-ampicillin plates, incubation of plates overnight at 37°C was carried out. Then, white or light blue colonies were picked using sterile toothpicks and grown in 3 mL LB liquid medium containing ampicillin, and incubated overnight at 37°C on shaker at 480rpm for plasmid DNA analysis.

III.2.4.3 Extraction of DNA plasmid (Miniprep)

DNA plasmids were extracted from bacterial colonies likely containing the recombinant plasmids to check their successful insertion. The grown bacteria were pelleted by centrifugation at 13,000 rpm for 1min, re-suspended in 400 µL of STET and 20µL of lysozyme (20mg/ml),

the pellets were disrupted by vortex then incubated at 100 °C for 2min in a boiling water bath and chilled on ice for 5min. After centrifugation at 13,000rpm for 20min, the pellets were eliminated using sterile toothpicks, and then 3µl of RNase (10µg/µl) were added and incubated at 37°C for 30 min. After incubation, 300 µL of Phenol and 300 µL of chloroform were added into the eppendorfs, vortexed well, centrifuged at 10,000 rpm for 10min. After centrifugation, 300 µL of the supernatants were transferred into new tubes, with the addition of 300 µL Ammonium hydroxide (NH4OHC) and 1 mL of 100% cold (-20°C) Ethanol, followed by 5min incubation on ice and centrifugation at 13000rpm for 20min. The aqueous phase was eliminated, and the pellets were then washed with 500µl of 70% cold (-20°C) Ethanol, centrifuged at 13,000 for 10min. The supernatant was removed, and the pellets were dried at room temperature and finally re-suspended in 35µl sterile water.

III.2.4.4 Enzymatic digestion of plasmid

To confirm the presence of cloned inserts in the plasmids, a digestion with restriction enzyme EcoR1 (Promega®) was carried out; 4 µl of plasmid DNA were incubated with 1µl 10× buffer H (Promega®), 0.2µl 12U/µl EcoRI, 4.8µl sterile water (10µl final volume of digestion) at 37°C for 2h. The preparation was analyzed by electrophoresis in 1.2% agarose gel in 1× TAE buffer. The gel was loaded with 10µl of Plasmid DNA and 2µl of loading dye mixture. The DNA was visualized under UV fluorescence (UVP GelDoc-IT Imaging system), to examine the presence or absence of the amplicons.

III.2.4.5 Purification and sequencing

Based on the results of the previous step, the corresponding bacterial colonies in LB solid media were selected to be further cultured. The selected colonies were inoculated in 3 ml of liquid LB containing kanamycin/ampicillin and incubated overnight at 37°C, by shaking at 480rpm. The plasmids DNA were purified by using the NucleoSpin® Plasmid kit (NoLid) (Machery-Nagel, Düren, Germany) before used as templates for sequencing. The target DNA fragments were sequenced from both strands for all the fungal isolates, by Eurofins Genomics (Ebersbeg, Germany), starting from commercial T3–T7 primers. Based on these initial IGS sequences, internal sequencing primers for *Pm. italicum* (Ital_INT_R: 5`-ATATAATGTCGCAGGGTC-3); *Pm. scolyti* (Scol_INT_F: 5`-TGATATCCTTCGCGCTGG-3`) and *Pm. minimum*

(Minim_ INT_R1: 5`-GCCTCTTAGGTATCATAC-3` and Minim_INT_R2: 5`-GGCTATATCCTTATCCTACC-3`), were designed for further sequencing and assembly of the IGS. The complete IGS region was assembled for each isolate using BioEdit v7.2.6. (Hall, 1999). Final sequence submission to GenBank database (NCBI) is going on in order to obtain the accession numbers.

III.2.5 IGS Analysis

After assembly and trimming off the vector sequence ends. The DNA sequences obtained from each fungal isolate, using the primer pair LR12R/invSR1R were aligned along with those obtained using the pair IG11F/IG12R in order to confirm our IGS sequences. DNA similarity searches were performed with Basic Local Alignment Search Tool (BLAST 2.7.1+; Altschul *et al.*, 1997). Since the IGS region has not been studied so far for *Phaeoacremonium* spp., it was not possible to retrieve available sequences in the Genbank database. Alignment of the IGS sequences was prepared using ClustalX version 1.83 (Thompson *et al.*, 1997). The program GeneQuest of the software package Lasergene 6 (DNAstar, Madison, WI) was used for structural analysis of the IGS rDNA region. The IGS sequences from *Phaeoacremonium* isolates were compared using MegAlign v. 15 (DNAstar, Madison, WI) to obtain similarities scores.

III.3 Results

III.3.1 PCR amplification, cloning and sequencing of ribosomal intergenic spacer IGS region

The DNA samples of all fungal isolates gave positive results in all sets of reactions. Agarose gel electrophoresis of the PCR products of *Pm. italicum* using primers LR12R/invSR1R, showed that IGS fragments vary slightly in size among the isolates tested (Figure III.2).

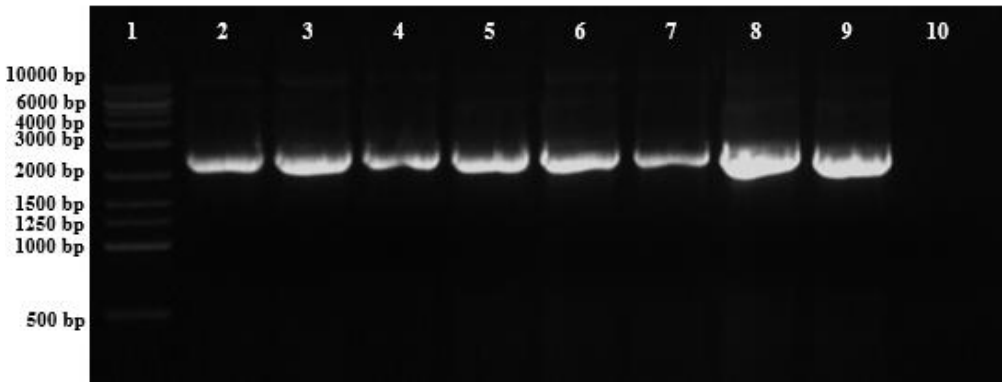

Figure III.2. Agarose gel electrophoresis of the IGS-PCR amplification products of representative *Pm. italicum* isolates. Lane 1: 10-kb DNA ladder; Lane 2: isolate 2; Lane 3: isolate 15; Lane 4: isolate 17; Lane 5: isolate 31M; Lane 6: isolate 35M; Lane 7: isolate 45; Lane 8: isolate 50M; Lane 9: isolate 59M; Lane 10: negative control.

Selected clones for *Pm. italicum* were sequenced in both the forward and reverse directions and the IGS fragments consisted of a partial region of LSU-rRNA gene followed by complete sequences of IGS and a partial region of SSU-rRNA gene, with fragments size ranging from 2194 to 2300 bp nucleotides long. Substantial fulllength sequences of the IGS region was obtained for the isolates of *Pm. italicum* and their submission to NCBI GenBank is going on in order to obtain the accession numbers.

Similarly, the DNA samples of *Pm. scolyti* and *Pm. minimum* isolates gave positive results in all PCR reactions (data not shown). Selected clones were sequenced in both the forward and reverse directions and substantial fulllength sequences of the IGS region was obtained for all isolates. IGS fragments vary slightly in size among the isolates tested ranging from 2172 to 2219 bp for *Pm. scolyti* and 2273 to 2314 bp for *Pm. minimum* isolates. Sequences submission to NCBI GenBank is going on in order to obtain the accession numbers.

III.3.2 Structural analysis of the IGS region of *Pm. italicum*

The sequencing results of the IGS region showed length variation among *Pm. italicum* isolates, as complete sequences ranged in size from 2194 to 2300 bp, thus representing intraspecific polymorphisms in the length of the IGS region.

Chapter III. Amplification and structural analysis of *Pm. italicum* IGS

Analysis of the DNA sequences showed that the 5S rDNA gene could not be amplified, thus IGS could include a single region. The IGS sequences of all *Phaeoacremonium* isolates listed in Table III.1 were aligned, then *Pm. italicum* isolates were structurally analyzed and grouped to subgroups based on their length heterogeneity and polymorphism at the intra-species level, hence, we chose six different isolates (Pm 2, Pm 45, Pm 17, Pm 31M, Pm 50M and Pm 59) representatives to outline the structural organization of the IGS region among isolates (Figure III.3). Based on the distribution of polymorphisms along the multiple sequence alignment, the spacer could be divided into three structural regions: a central, polymorphic region PR (nucleotide positions 236–2086), and two flanking conserved regions on both sides of the central area, CR1 (nucleotides 1–235) and CR2 (nucleotides 2087–2634), as shown in Figure III.3.a.

The CR1 region, adjacent to the 28S rRNA gene, exhibits sequence conservation ranging between 99% and 100% (pairwise identities). Region CR2, adjacent to the 18S rRNA gene, showed high conservation between 99.6% and 100% pairwise identity. Slight polymorphisms in these two conserved regions resulted from single-base substitutions (transitions and transversions) and few (1 to 2bp) insertions and deletions (indels). The polymorphic region (PR) was less conserved among isolates, with percentages of pairwise identities as low as 84.1% and was marked by indels of varying sizes in addition to point mutations.

The detailed analysis of the structure of IGS sequences of the six representative isolates revealed the presence of four short repeat elements organized in different patterns (Elements P, R, A, B). All of the isolates shared a common structural organization in CR1 and CR2 regions, while in the PR region, we found characteristic differences between the different IGS sequences mainly due to the number, the presence or absence of these repeat elements and their positions (Figure III.3.b and c).

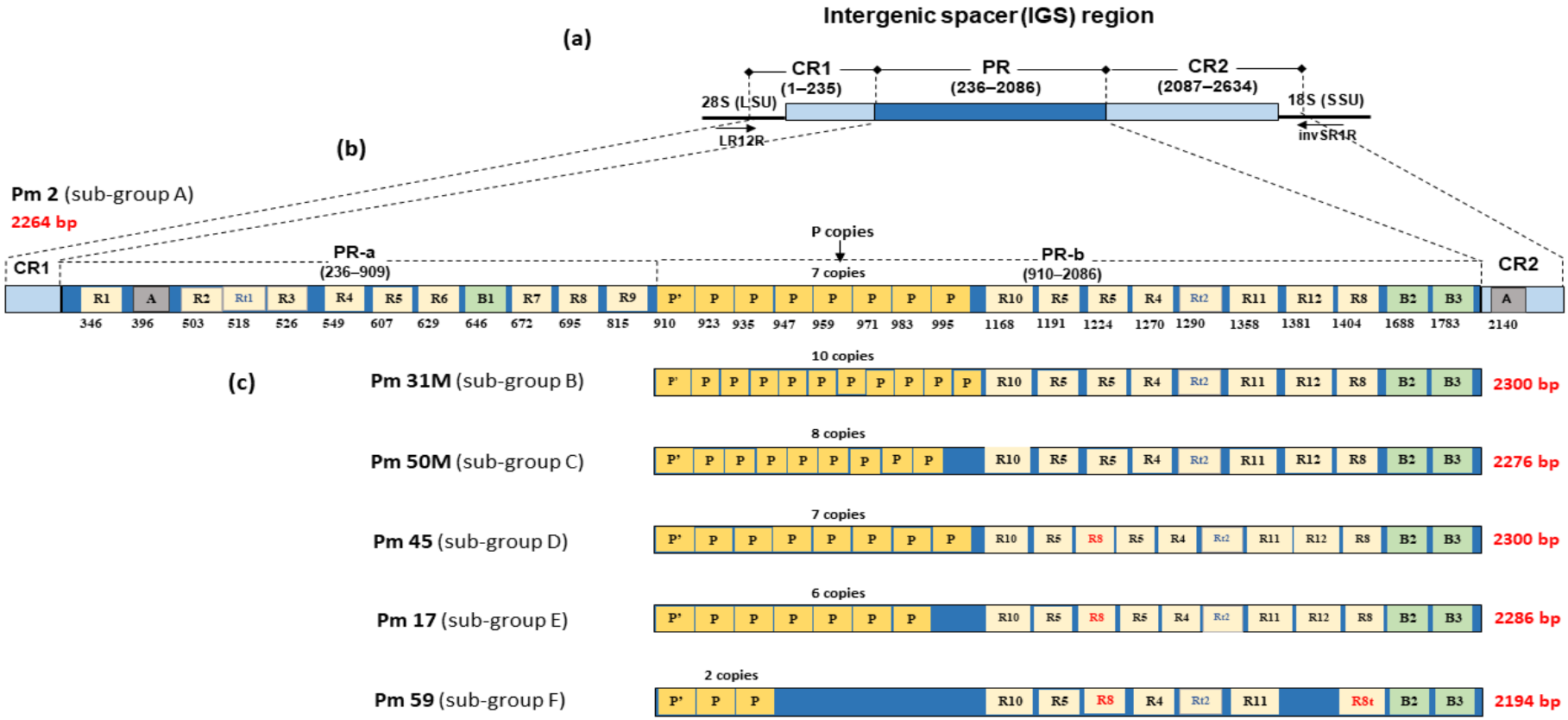

Figure III.3. (a) Organization of the nuclear rDNA IGS region of *Phaeoacremonium italicum* isolate Pm 2 divided into regions CR1, PR, and CR2, with corresponding nucleotide positions indicated in parentheses. The arrows below the bar indicate the annealing positions of PCR universal primers LR12R and invSR1R, within the extremities of the 28S and 18S rRNA genes. **(b)** Structural organization of repeat elements P, R, A and B in the IGS region of *Pm. italicum* Pm 2. The division of PR region into two areas (PR-a and PR-b) is shown above the bar. Nucleotide start positions of P, R, A, and B copies is provided below the bar. The number next to the designations of R, B and Rt elements indicates sequence variants of them; the corresponding sequences are shown in Figure.III.4. the numbers in red next to each bar indicate the sequence length. **(c)** Organization of region PR sequences of different representative *Pm. italicum* isolates. Areas CR1, PR-a and CR2 are not shown because they have the same structural organization in all isolates.

Based on the distribution of the short repeat elements, the central region PR could be subdivided in two sub-regions, PR-a (nucleotides 236–909) and PR-b (nucleotides 910–2086). The sub-region PR-a, which shared a common structural organization of these short repeats in all isolates, contains: one perfect repeat of -12bp long, named (A); nine copies of imperfect repeats of 15-bp long, named (R), showing one to nine base substitutions in addition to a truncated imperfect repeat named here (Rt1); and one imperfect repeat of 15-bp long, named (B1).

The sub-region PR-b, which has characteristic differences between the different IGS sequences, consisted of conserved and imperfect copies of repeated elements. In fact, the main feature of this sub-region is the presence of perfect consecutive repeats of 12-bp, here named as P elements, extending from position 923 to 1045, found in all sequences examined, in 2 to 10 copies as shown in Figure III.3. (b, c). All P modules were direct perfect repeats, except the first, imperfect inverted copy (P'), located at the beginning of the polymorphic sub-region PR-b (nucleotide 910) (See alignment in Figure III.5). In addition to the P repeats, imperfect elements were also identified, that we named previously (elements R) in the PR-a region. The 15 bp long R imperfect repeats (found in 5 to 7 copies) showed variants differing by 1 to 5 base substitutions in addition to a truncated imperfect repeat named here (Rt2); and two other imperfect repeats of 15-bp long, named (B2 and B3) (Figure III.3.b, c and Figure III.4).

Furthermore, the CR2 region contained only one perfect repeat (A) of 12 bp long, that we found previously in PR-a, encountered in all sequences. In contrast, no repeated element was found in the sub-region CR1, thus being the most conserved region within IGS sequences (see Figure III.3.b).

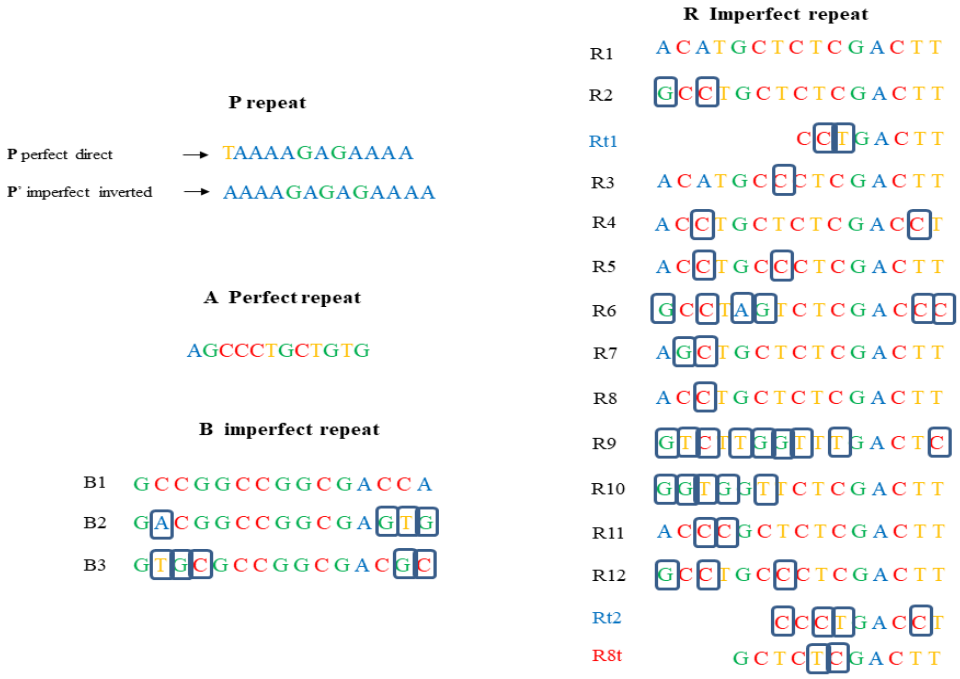

Figure III.4. DNA short repeat elements P, R, A, and B and the variants of the R and B elements present in *Pm. italicum* isolates. For each element, the sequences identified in the six representative isolates shown in Figure III.3 are provided. All polymorphic bases in the R and B elements are indicated with boxes.

Comparison results of the polymorphic region PR sequences of all isolates listed in Table III.1 revealed that the PR sequences of each *Pm. italicum* subgroup were structurally similar, while distinctive differences were observed among different *Pm. italicum* subgroups (Figure III.b and c). Isolates belonging to A, B and C sub-groups shared a common organization of R elements (R10-R5-R5-R4-Rt2-R11-R12-R8-B2-B3) in their PR region, but they differ in the copy number of P elements (7, 8 or 10 copies). Similarly, isolates belonging to sub-groups D and E had the same organization of R elements (R10-R5-R8-R5-R4-Rt2-R11-R12-R8-B2-B3), but they vary in P repeat copies (6 or 7 copies). In contrast, isolates within sub-group F were the most polymorphic exhibiting uncommon copy numbers of the P repeat (2 copies) and the R elements structure (R10-R5-R8-R4-Rt2-R11-R8t-B2-B3) (Figure III.b and c).

We found that polymorphism and size variation observed among all IGS sequences occurred as a result of copy number variations of the short repeat elements P and R and their positions within the polymorphic region PR, also the presence of indels of varying sizes in the latter region.

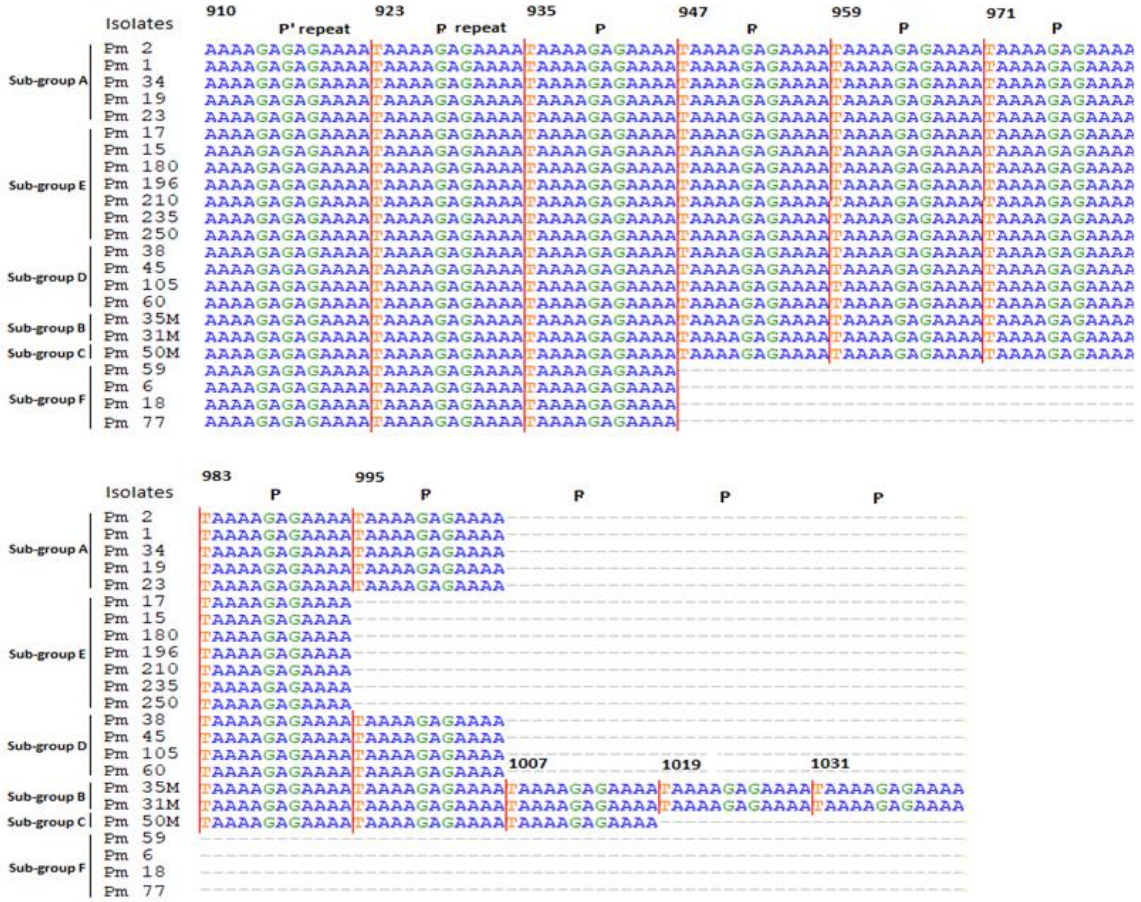

Figure III.5. Alignment of the repeat elements P in the polymorphic region IGS of *Pm. italicum* differentiating isolates based on the copy number variations of P elements. Lines demarcate the 12 nt P repeats and numbers indicate their position within IGS sequences.

III.3.3 Structural analysis of the IGS region of *Pm. scolyti and Pm. minimum*

The IGS sequences of *Pm. scolyti* and *Pm. minimum* were also analyzed and grouped to subgroups based on their length heterogeneity and polymorphism at the intraspecies level. Four representative isolates were identified for *Pm. scolyti* (Pm 51M, Pm 73M, Pm 5 and Pm 92A) but also for *Pm. minimum* (Pm 67, Pm 41, Pm 109 and Pm 68), in order to outline the structural organization of the IGS region in these species (Figure III.6 and III.7). Similar to *Pm. italicum* and based on the distribution of polymorphisms along the multiple sequence alignment, the spacer is divided into three regions: a polymorphic region PR (nucleotide positions 236–2086), and two conserved regions CR1 (nucleotides 1–235) and CR2 (nucleotides 2087–2634), as shown in Figures (III.6.a) and (III.7.a).

The CR1 region in both species, adjacent to the 28S rRNA gene, revealed 100% sequence conservation (pairwise identities). Region CR2, adjacent to the 18S rRNA gene, showed high conservation of about 99.8% and 100% pairwise identities in *Pm. scolyti* and *Pm. minimum* respectively. However, the polymorphic region (PR) was less conserved among isolates, with percentages of pairwise identities of about 90%.

The structural analysis of IGS sequences of the four representative isolates in *Pm. scolyti* revealed the presence of three short repeat elements in the polymorphic region PR: Repeat elements (distinguished as R, RS and RSt), elements B and I (Figure III.6.b and c). Regarding the IGS structure of *Pm. minimum*, the analysis of the four representative isolates, revealed the presence of short repeat elements distinguished here as (R, M and t) in the polymorphic region PR (Figure III.7.b and c). In fact, the imperfect repeat elements of 15-bp identified in *Pm. scolyti* and *Pm. minimum* as elements R, were found previously in *Pm. italicum* IGS sequences and are encountered in all isolates studied here (Figures III.4, III.8 and III.9).

Characteristic differences were found between the different IGS sequences of *Pm. scolyti* and *Pm. minimum,* mainly due to the presence or absence of some repeat elements in the PR region and the presence of indels of varying sizes as well as point mutations.

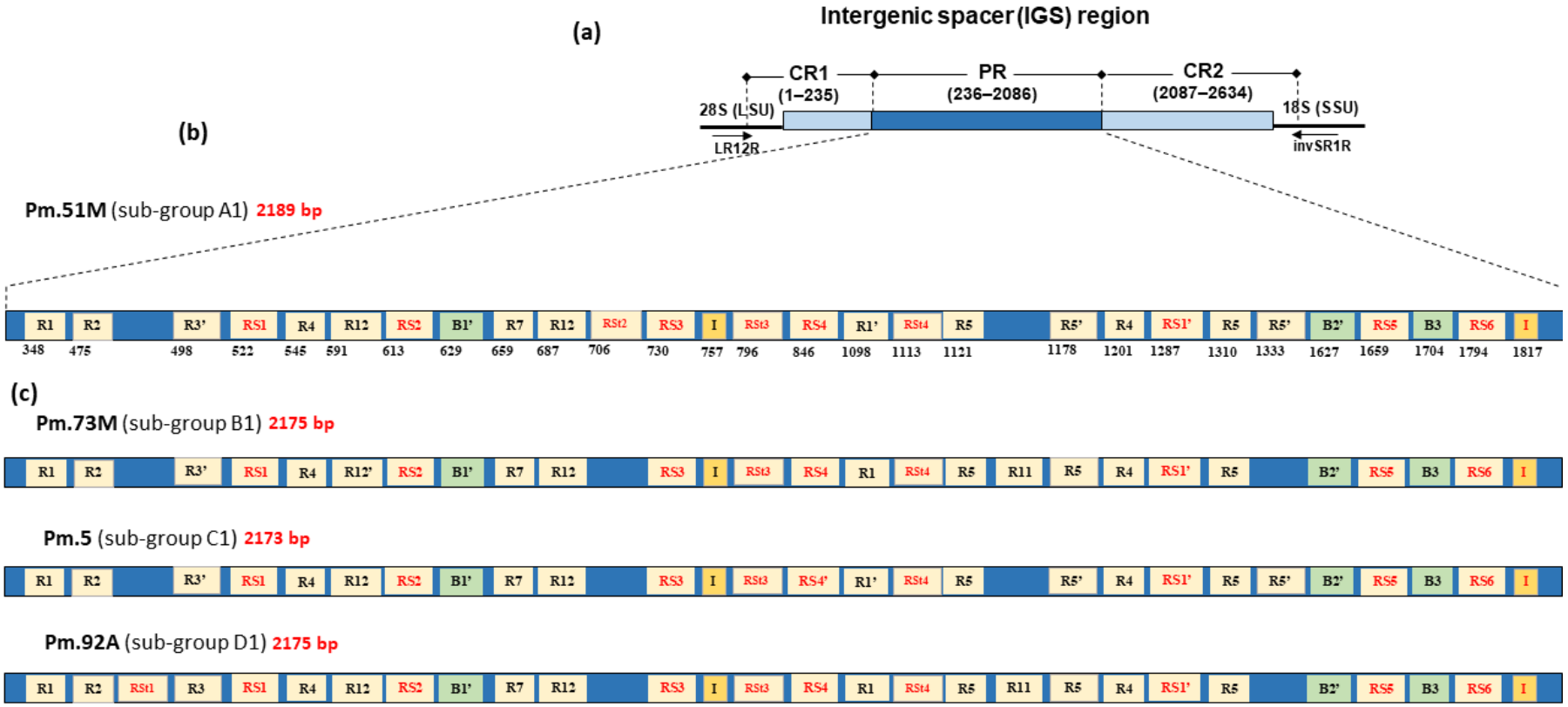

Figure III.6. (a) Organization of the nuclear rDNA IGS region of *Phaeoacremonium scolyti* isolate Pm 51M divided into regions CR1, PR, and CR2, with corresponding nucleotide positions indicated in parentheses. The arrows below the bar indicate the annealing positions of PCR universal primers LR12R and invSR1R, within the extremities of the 28S and 18S rRNA genes. **(b)** Structural organization of repeat elements R, B and I in the IGS region of *Pm. scolyti* Pm 51M. Nucleotide start positions of R, B, and I copies is provided below the bar. The number next to the designations of R (R, RS and RSt) and B elements indicates sequence variants of them; the corresponding sequences are shown in Figure.III.8. **(c)** Organization of region PR sequences of different representative *Pm. scolyti* isolates. Areas CR1 and CR2 are not shown because they have the same structural organization in all isolates. The numbers in red next to each sub group indicate the sequence length.

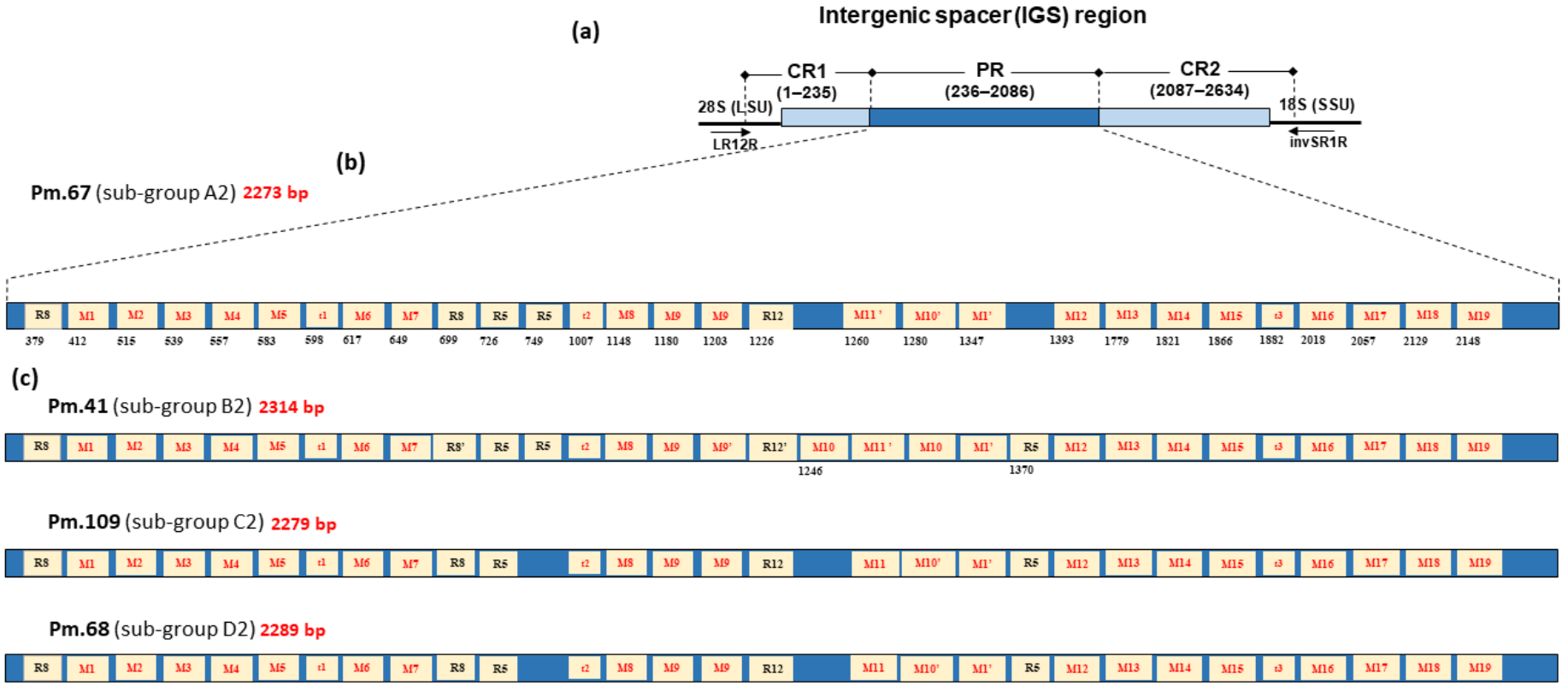

Figure III.7. (a) Organization of the nuclear rDNA IGS region of *Phaeoacremonium minimum* isolate Pm 67 divided into regions CR1, PR, and CR2, with corresponding nucleotide positions indicated in parentheses. The arrows below the bar indicate the annealing positions of PCR universal primers LR12R and invSR1R, within the extremities of the 28S and 18S rRNA genes. **(b)** Structural organization of repeat elements (R, M and t) in the IGS region of *Pm. minimum* Pm 67. Nucleotide start positions of Repeat elements is provided below the bar. The number next to the designations of (R, M and t) indicates sequence variants of them; the corresponding sequences are shown in Figure.III.9. **(c)** Organization of region PR sequences of different representative *Pm. minimum* isolates. Areas CR1 and CR2 are not shown because they have the same structural organization in all isolates. The numbers in red next to each sub group indicate the sequence length.

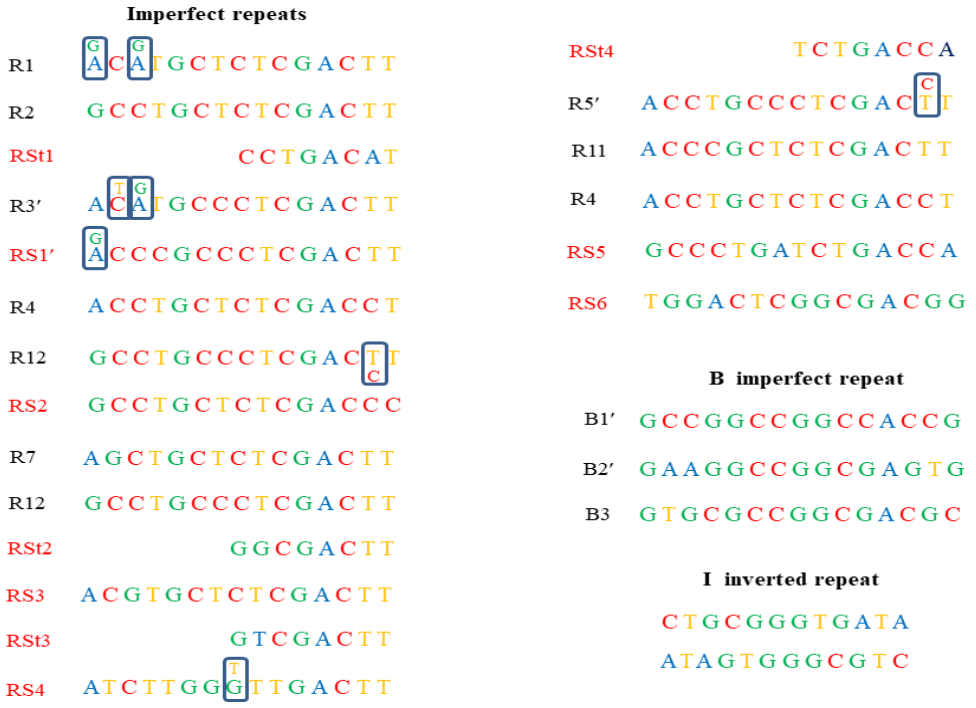

Figure III.8. DNA short repeat elements (R, RS, RSt), B and I elements present in *Pm. scolyti* isolates. For each element, the sequences identified in the four representative isolates shown in Figure III.6 are provided. Polymorphic bases in the repeat elements are indicated with boxes.

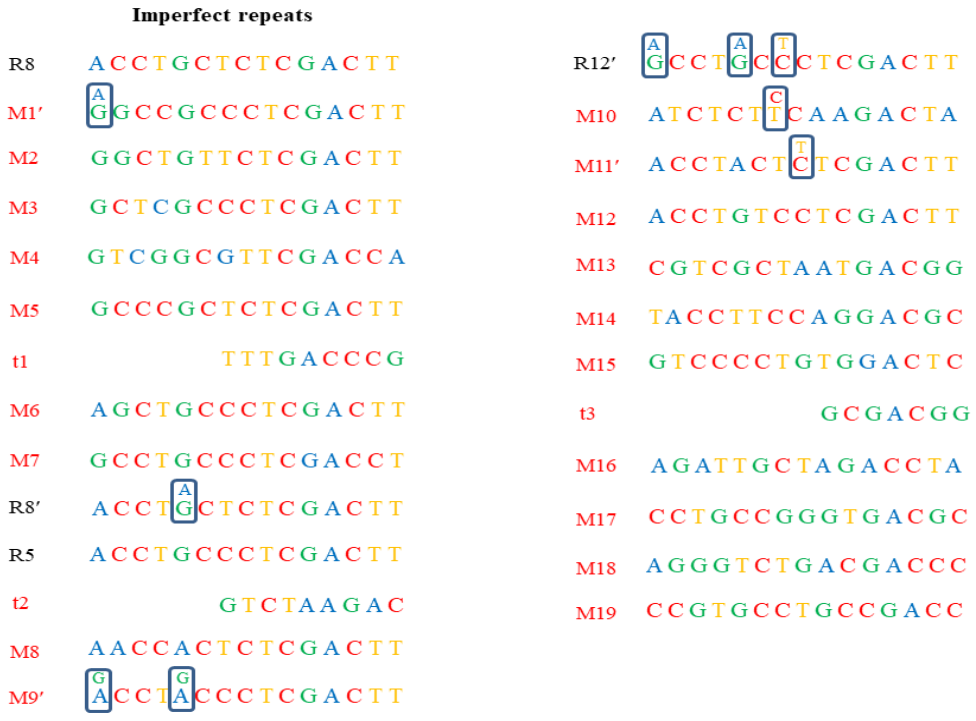

Figure III.9. DNA short repeat elements (R, RS, RSt) present in *Pm. minimum* isolates. For each element, the sequences identified in the four representative isolates shown in Figure III.7 are provided. Polymorphic bases in the repeat elements are indicated with boxes.

III.4 Discussion

This study described the first genetic analysis of the intergenic spacer (IGS) region of rDNA of *Pm. italicum,* in addition to *Pm. scolyti* and *Pm. minimum*, using a set of strains that we isolated from olive trees in Salento, including also strains from grapevine and almond plants. The entire IGS region of *Phaeoacremonim* isolates was successfully amplified in all of the samples, yielding a single DNA product. Indeed, the standard primers used in our study, annealing to sites located in the conserved 28S and 18S rDNA gene coding regions flanking the IGS, have been successfully used to amplify this region in various fungi and oomycetes (James *et al*. 2001; Nigro *et al.* 2005; Mahmoud Mohamed Ahmed, 2013; Durkin *et al.* 2015). As in this study, the 5S rDNA gene was not possibly identified within the IGS sequences. It could consequently be spread throughout the genome. This is supported by the fact that most filamentous ascomycetes have a single uninterrupted IGS region (between the end of the LSU and start of the next SSU sequence) and the 5S genes are dispersed throughout the genome (Bartnik *et al.* 1986, Garber *et al.* 1988; Walker *et al.* 2011).

Structural analysis of the nuclear rDNA IGS region of *Pm. italicum, Pm. scolyti* and *Pm. minimum* isolates permitted the identification of three different regions based on polymorphism distribution within IGS, namely: a polymorphic region (PR), flanked by two conserved regions (CR1 and CR2). The overall organization proposed here matches with the IGS structure described by Papaioannou *et al.* (2013) for *Verticillium dahliae.* The IGS structure defined in our results agrees with the distinct functioning of these regions. The polymorphic region PR could be responsible for the promotion of unequal crossing-over events and the maintenance of homogeneity within rDNA units, whereas the conserved regions CR1 and CR2 are likely associated with functions related to rRNA production and processing (Pramateftaki *et al.* 2000; Ganley and Kobayashi, 2011; Papaioannou *et al.* 2013; Huang *et al.* 2017).

Intraspecific polymorphism was found in terms of difference in IGS length among isolates, observing IGS sizes ranging between 2.1 kb and 2.3 kb. Indeed, intraspecific length variation in the intergenic spacer (IGS) region has been reported in various fungi (Buchko *et al.* 1990; Albee *et al.* 1996; White *et al.* 1996; Pramateftaki *et al.* 2000; kim *et al.* 2001; Roose-Amsaleg *et al.* 2002; Pantou *et al.* 2003; Hong *et al*. 2005; Durkin *et al*. 2015).

Furthermore, the IGS region is considered the most variable part of the rDNA unit. It varies greatly in length among different fungal species, ranging from about 1 to over 4 kb (Martin *et al.* 1999). The IGS has faster mutation rates than the other rDNA areas, resulting in molecular variation (Moss and Stefanovsky, 1995; Martin *et al.* 1999; Ciarmela *et al.* 2001; Schmidt and Moreth, 2008).

It is well known that IGS region contains several repeat elements, indels, and variable regions with nucleotide substitutions. In fact, the length differences in the IGS reported in many studies is attributed to insertions or deletions in the arrays of subrepeats in such a large non-conserved region and this elucidate the polymorphisms of this region (Albee *et al.* 1996; White *et al.* 1996; James *et al.* 2001). Similarly, in this study, we identified various short repeat sequences within IGS of *Pm. italicum* (Repeats P, R, A and B). Our sequence analysis revealed that length variation occurs due to the fact of variation in the copy numbers of these repeat elements (P) and (R). The incidence of commonly occurring TAAAAGAGAAAA modules are examples of repeats that contributed to the presence of length polymorphisms. Also, occurrence of point mutations and short indel areas of varying size, unrelated to repeat elements are responsible for the different size variation seen within isolates. The indels sequences were restricted to polymorphic regions, suggesting that these elements are well involved in the length variation observed.

It is to be mentioned that the degree of sequence similarities among isolate*s* was considerably very high in CR1 and CR2 regions, indicating that they are more conservative and, therefore, can accommodate more functions related to rRNA production and processing (Hancock and Dover, 1990; Diaz *et al*. 2005). The polymorphism of the IGS within rDNA units, can be attributed to unequal crossing over between repeats elements in the polymorphic region (Pramateftaki *et al.* 2000; Papaioannou *et al.* 2013).

III.5 References

Altschul, S. F., Madden, T. L., Schäffer, A. A., Zhang, J., Zhang, Z., Miller, W., & Lipman, D. J. (1997). Gapped BLAST and PSI-BLAST: a new generation of protein database search programs. *Nucleic acids research*, *25*(17), 3389-3402.

Albee, S. R., Mueller, G. M., & Kropp, B. R. (1996). Polymorphisms in the large intergenic spacer of the nuclear ribosomal repeat identify Laccaria proxima strains. *Mycologia*, 970-976.

Bartnik, E., Bartoszewski, S., Borsuk, P., & Empel, J. (1986). Aspergillus nidulans 5S rRNA genes and pseudogenes. *Current genetics*, *10*(6), 453-457.

Buchko, J., & Klassen, G. R. (1990). Detection of length heterogeneity in the ribosomal DNA of Pythium ultimum by PCR amplification of the intergenic region. *Current genetics*, *18*(3), 203-205.

Carlucci, A., Lops, F., Cibelli, F., & Raimondo, M. L. (2015). *Phaeoacremonium* species associated with olive wilt and decline in southern Italy. *European Journal of Plant Pathology*, *141*(4), 717-729.

Carlucci A., Raimondo M. L., Cibelli F., Phillips A. J. and F. Lops. (2013). *Pleurostomophora richardsiae, Neofusicoccum parvum* and *Phaeoacremonium aleophilum* associated with a decline of olives in southern Italy. *Phytopathologia Mediterranea,* 52(3),517-527.

Ciarmela, P., Potenza, L., Cucchiarini, L., Zeppa, S., & Stocchi, V. (2002). PCR amplification and polymorphism analysis of the intergenic spacer region of ribosomal DNA in Tuber borchii. *Microbiological research*, *157*(1), 69-74.

Diaz, M. R., Boekhout, T., Kiesling, T., & Fell, J. W. (2005). Comparative analysis of the intergenic spacer regions and population structure of the species complex of the pathogenic yeast Cryptococcus neoformans. *FEMS yeast research*, *5*(12), 1129-1140.

Durkin, J., Bissett, J., Pahlavani, M., Mooney, B., & Buchwaldt, L. (2015). IGS minisatellites useful for race differentiation in Colletotrichum lentis and a likely site of small RNA synthesis affecting pathogenicity. *PloS one*, *10*(9), e0137398.

Ganley, A. R., & Kobayashi, T. (2011). Monitoring the rate and dynamics of concerted evolution in the ribosomal DNA repeats of Saccharomyces cerevisiae using experimental evolution. *Molecular biology and evolution*, *28*(10), 2883-2891.

Garber, R. C., Turgeon, B. G., Selker, E. U., & Yoder, O. C. (1988). Organization of ribosomal RNA genes in the fungus Cochliobolus heterostrophus. *Current Genetics*, *14*(6), 573-582.

Hall, T. A. (1999). BioEdit: a user-friendly biological sequence alignment editor and analysis program for Windows 95/98/NT. In *Nucleic acids symposium series*, 41, 95-98.

Hancock, J. M., & Dover, G. A. (1990). 'Compensatory slippage'in the evolution of ribosomal RNA genes. *Nucleic acids research*, *18*(20), 5949-5954.

Hong, S. G., Derong, L. I. U., & Pryor, B. M. (2005). Restriction mapping of the IGS region in Alternaria spp. reveals variable and conserved domains. *Mycological research*, *109*(1), 87-95.

Huang, Y., Yu, F., Li, X., Luo, L., Wu, J., Yang, Y., ... & Zhang, M. (2017). Comparative genetic analysis of the 45S rDNA intergenic spacers from three Saccharum species. *PloS one*, *12*(8), e0183447.

James, T. Y., Moncalvo, J. M., Li, S., & Vilgalys, R. (2001). Polymorphism at the ribosomal DNA spacers and its relation to breeding structure of the widespread mushroom Schizophyllum commune. *Genetics*, *157*(1), 149-161.

Kim, H. J., Choi, Y. K., & Min, B. R. (2001). Variation of the Intergenic Spacer (IGS) region of ribosomal DNA among Fusarium oxysporum formae speciales. *JOURNAL OF MICROBIOLOGY-SEOUL*, *39*(4), 265-272.

Mahmoud Mohamed Ahmed, Y. (2013). Studies on mango soilborne diseases with special reference to Phytophtora root rot.

Martin, F., Selosse, M. A., & Le Tacon, F. (1999). The nuclear rDNA intergenic spacer of the ectomycorrhizal basidiomycete Laccaria bicolor: structural analysis and allelic polymorphism. *Microbiology*, *145*(7), 1605-1611.

Moss, T., & Stefanovsky, V. Y. (1995). Promotion and Regulation of Ribosomal Transcription in Eukaryotes by RNA Polymerase1. In *Progress in nucleic acid research and molecular biology* (Vol. 50, pp. 25-66). Academic Press.

Mostert, L., Groenewald, J. Z., Summerbell, R. C., Gams, W., & Crous, P. W. (2006). Taxonomy and pathology of Togninia (Diaporthales) and its Phaeoacremonium anamorphs. *Studies in Mycology*, *54*, 1-113.

Nigro, F., Boscia, D., Antelmi, I., & Ippolito, A. (2013). Fungal species associated with a severe decline of olive in southern Italy. *Journal of plant pathology*, *95*(3).

Nigro, F., Yaseen, T., Schena, L., Ippolito, A., & Cooke, D. E. L. (2005). Specific PCR detection of Phytophthora megasperma using the intergenic spacer region of ribosomal DNA. *Journal of Plant Pathology*, *87*(4), 300.

Pantou, M. P., Mavridou, A., & Typas, M. A. (2003). IGS sequence variation, group-I introns and the complete nuclear ribosomal DNA of the entomopathogenic fungus Metarhizium: excellent tools for isolate detection and phylogenetic analysis. *Fungal Genetics and Biology*, *38*(2), 159-174.

Papaioannou, I. A., Dimopoulou, C. D., & Typas, M. A. (2013). Structural and phylogenetic analysis of the rDNA intergenic spacer region of Verticillium dahliae. *FEMS microbiology letters*, *347*(1), 23-32.

Pramateftaki, P. V., Antoniou, P. P., & Typas, M. A. (2000). The complete DNA sequence of the nuclear ribosomal RNA gene complex of Verticillium dahliae: intraspecific heterogeneity within the intergenic spacer region. *Fungal Genetics and Biology*, *29*(1), 19-27.

Roose-Amsaleg, C., BRYGOO, Y., & LEVIS, C. (2002). Characterisation of a length polymorphism in the two intergenic spacers of ribosomal RNA in Puccinia striiformis f. sp. tritici, the causal agent of wheat yellow rust. *Mycological Research*, *106*(8), 918-924.

Raimondo, M. L., Lops, F., & Carlucci, A. (2014). *Phaeoacremonium italicum* sp. nov., associated with esca of grapevine in southern Italy. *Mycologia*, *106*(6), 1119-1126.

Sambrook, J., Fritsch, E. F., & Maniatis, T. (1989). Molecular Cloning Cold Spring Harbor Laboratory Press, New York. *Molecular cloning: Cold spring harbor laboratory press New York*.

Schmidt, O., & Moreth, U. (2008). Ribosomal DNA intergenic spacer of indoor wood-decay fungi. *Holzforschung*, *62*(6), 759-764.

Thompson, J. D., Gibson, T. J., Plewniak, F., Jeanmougin, F., & Higgins, D. G. (1997). The CLUSTAL_X windows interface: flexible strategies for multiple sequence alignment aided by quality analysis tools. *Nucleic acids research*, *25*(24), 4876-4882.

Vilgalys, R., & Gonzalez, D. (1990). Organization of ribosomal DNA in the basidiomycete Thanatephorus praticola. *Current genetics*, *18*(3), 277-280.

Walker, A. S., Bouguennec, A., Confais, J., Morgant, G., & Leroux, P. (2011). Evidence of host-range expansion from new powdery mildew (Blumeria graminis) infections of triticale (× Triticosecale) in France. *Plant pathology*, *60*(2), 207-220.

White, E. E., Foord, B. M., & Kinloch Jr, B. B. (1996). Genetics of Cronartium ribicola. II. Variation in the ribosomal gene cluster. *Canadian journal of botany*, *74*(3), 461-468.

Yaseen, T., Nigro, F., Schena, L., & Ippolito, A. (unpublished data). The Complete Sequence of intergenic spacer region (IGS) of nuclear rDNA and specific PCR based detection of *Phytophthora megasperm*. Submitted to *European Journal of Plant Pathology*.

IV. THE RIBOSOMAL DNA INTERGENIC SPACER (IGS) REGION AS A TARGET FOR DEVELOPING PCR-BASED DETECTION OF *PHAEOACREMONIUM ITALICUM* GROUP - A STUDY MODEL

IV.1 Introduction

The genus *Phaeoacremonium* introduced by Crous *et al.* (1996), and currently accommodated in the monogeneric family *Togniniaceae,* is composed of 65 *Phaeoacremonium* species (Huang *et al.* 2018; Spies *et al.* 2018). These species are well-known vascular plant pathogens causing wilt and dieback of various woody plants. They have a global distribution, with species being reported from Europe, Africa, South, Central and North America, Scandinavia, Ukraine, the Middle East and Oceania (Gramaje *et al.* 2015). Several recent studies have reported the importance of *Phaeoacremonium* species in causing brown wood streaking of *Olea europaea* (Nigro *et al.* 2013; Carlucci *et al.* 2015).

An accurate detection and identification of these fungi in olive trees and many other host plants are crucial in disease management. Identification of *Phaeoacremonium* species based on morphological and cultural characters has been proven to be difficult because the cultural and microscopic distinguishing characteristics are relatively minor. Subsequently, molecular techniques have been developed to confirm species identifications in infected plants, using internal transcribed spacer (ITS) regions, the actin and b-tubulin gene sequences (Groenewald *et al.* 2001; Dupont *et al.* 2002; Mostert *et al.* 2006).

Moreover, a number of detection methods have been developed for the detection of several *Phaeoacremonium* spp. Most of the detection techniques described so far are based on the internal transcribed spacer (ITS) regions (Overton *et al*. 2004; Aroca and Raposo, 2007), and the β-tubulin gene sequences (Aroca *et al*. 2008; Martın *et al.* 2012; Pouzoulet *et al.* 2013; Urbez-Torres *et al.* 2015). These molecular markers provided attractive targets to design specific primers since they are highly stable, can be amplified and sequenced with universal primers, and possess conserved as well as variable sequences (White *et al.*,1990; Glass and Donaldson, 1995). However, the identification and detection of *Phaeoacremonium* species remain a challenge considering the increasing recognition of novel

species of *Phaeoacremonium*, consequently the ITS and β-tubulin sequences seem to be not sufficiently variable, making the design of primers to identify and detect closely related species very difficult.

In this context, the identification of new molecular markers to provide more accurate detection of *Phaeoacremonium* spp. is relevant. In fact, the intergenic spacer (IGS) region was shown to be polymorphic at the interspecific level for several fungi, such as *Verticillium dahliae*, *Fusarium oxysporum, Botrytis cinerea*…etc. (Pantou *et al.* 2003; Suarez *et al.* 2005; Srinivasan *et al.* 2010; Bilodeau *et al.* 2012) and was used to design species-specific primers. In contrast, this region has not previously been studied in *Phaeoacremonium* genus. To this end, the aim of the present work was to study the possibility to set up a new PCR-based approach for the specific detection of *Phaeoacremonium italicum* group, that was specifically chosen here, being commonly isolated from olive trees in previous studies (Chapter II), by designing species-specific primers targeting the rDNA intergenic spacer (IGS) region, previously studied in Chapter III for the target species.

IV.2 Materials and methods

IV.2.1 Fungal isolates

DNA of the different fungal isolates were provided from different sources listed in Table IV.3 and IV.4. Isolates of *Phaeoacremonium italicum* recovered from olive orchards in Salento, were selected for this work (See chapter II). Purified cultures were routinely grown and maintained on potato dextrose agar (PDA; 3.9 % potato dextrose agar; Oxoid Ltd., UK).

Fresh mycelium was collected from the surface of a 15-20 days old cultures of *Pm. italicum* using a sterile scalpel, and DNA was extracted using two different protocols. Manual extractions were performed according to a protocol provided by Carlucci *et al.* (2013) vs. an extraction kit E.Z.N.A.® Plant DNA Kit-short protocol (Omega Bio-tek, Georgia, USA) following the manufacturer's instructions. DNA of the different fungal isolates and of *Pm. italicum* was quantified using a NanoDrop 2000 spectrophotometer (Thermo Fisher Scientific, Waltham, MA, USA) and kept at -20 ºC until use in the sensitivity and specificity tests.

IV.2.2 Design of IGS primers and PCR amplification

Sequences of the IGS region of *Pm. italicum* isolates and other sequences of *Phaeoacremonium* spp., that were amplified in other studies (Chapter III and V), were aligned using the MAFFT program v.7 (Kato and Standley, 2013) and were visually checked for regions having homologies among *Pm. italicum* isolates but not among other species belonging to the genus *Phaeoacremonium*.

The IGS regions conserved among *Pm. italicum* isolates and specific for this group, were selected to design possible species-specific oligonucleotides. Since the isolates belonging to *Pm. italicum* group showed polymorphisms within the IGS (as described in chapter III), one pair of primer was manually designed on conservative portions of IGS region in order to amplify all isolates belonging to this group. The forward primer was designed at the start of the PR region, while the reverse primer was designed at the end of the PR region (Figure IV.1).

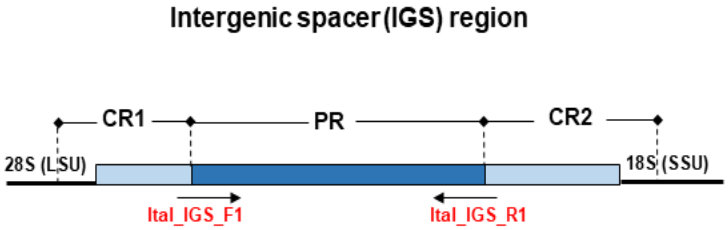

Figure IV.1. Schematic representation of the rDNA intergenic spacer region and the location of the IGS specific primers designed. IGS region included CR1, PR, and CR2 regions. The arrows below the bar indicate the annealing positions of IGS PCR specific primers ITAL_IGS_F1 and ITAL_IGS_R1.

The primer pair was analyzed with OligoAnalyzer 3.1 software (Integrated DNA Technologies Inc., Coralville, IA) for melting temperature, GC content %, hetero-dimer and hairpin structure formation and synthesized by Eurofins Genomics (Ebersberg, Germany).

Genomic DNA aliquots from diferent representative *Pm. italicum* isolates were used to assess and optimize amplification from the primer pair designed. The PCRs were performed in a 25 µl final volume with a C-1000 Touch™ Thermal Cycler (Bio Rad, USA) and annealing temperature gradient (±8°C) PCRs were run for the primer pair. Each reaction mixture contained 1× Canvax™ reaction buffer, 3mM $MgCl_2$ (Canvax), 200 µM

deoxynucleoside triphosphates, 0.4 µM forward and reverse primers, 1 U of Taq DNA Polymerase (Horse-Power™), and 30ng template DNA. Optimized PCR amplifications involved an initial denaturation step of 3 min at 94°C; 35 cycles of amplification consisting of denaturation (30 s at 94°C), primer annealing (30 s at 55°C), and primer extension (1 min at 72°C); and a final extension step of 5 min at 72°C. Amplified DNA fragments were analyzed by electrophoresis in a 1.5% (w/v) agarose gel, stained with ethidium bromide and visualized in a Gel Doc EZ system under UV light (Biorad).

IV.2.3 Design of β-tubulin primers and PCR amplification

A pair of primer targeting β-tubulin gene was designed in order to evaluate the IGS primers designed here. An alignment of 196 β-tubulin gene sequences of different *Phaeoacremonium* spp., that were downloaded from NCBI's GenBank database, was checked to find regions having homologies among *Pm. italicum* isolates but not among other species belonging to the genus *Phaeoacremonium*. Based on alignment, a primer pair specific to *Pm. italicum* was manually designed and analyzed as described above.

The β-tubulin PCR assays were carried out in a final volume of 25 µl, following a modified protocol (Raimondo *et al*. 2014). Each reaction contained 2.5 µl of Bovine Serum Albumin (BSA), 1× Canvax™ reaction buffer, 3mM MgCl2 (Canvax), 200 µM deoxynucleoside triphosphates, 0.2 µM forward and reverse primers, 1.25 U of Taq DNA Polymerase (Horse-Power™), and 30ng/µl template DNA. Optimized PCR amplifications were performed at an initial denaturation step of 3 min at 94°C; 35 cycles of amplification consisting of: denaturation (40 s at 94°C), primer annealing (30 s at 52°C), and primer extension (1.30 min at 72°C); and a final extension step of 10 min at 72°C. Amplified products were separated on 1.5% agarose gel, stained with ethidium bromide and visualized under UV light.

IV.2.4 Specificity of the PCR assays

The specificity of both PCR assays was evaluated using several isolates of *Phaeoacremonium* species (Table VI.3 and VI.4) and one no-template control consisting of nuclease-free water. DNA templates of the different isolates were diluted to 30 ng/µl before use.

IV.2.5 Sensitivity of the PCR assays

The detection limit of IGS specific primer pair was evaluated using serial dilutions of *Pm. italicum* DNA, that was isolated using two different extraction protocols as mentioned above, in order to compare the sensitivity of detection. Stock DNA normalized to 100ng/µl was serially diluted 10-fold in TE buffer pH.8, to reach DNA concentrations ranging from 10 ng/µl to 1 fg/µl.

In addition, the sensitivity of β-tubulin primers (both specific and universal; T1/Bt-2b; Glass and Donaldson, 1995) was also evaluated. All PCR reactions were repeated twice using the conditions above mentioned.

IV.3 Results

IV.3.1 PCR amplification with designed primers

The PCR cycling conditions were optimized for both PCR assays. The primers which gave PCR species-specific amplified products are listed in Table IV.1. The primer pairs amplified a single band with the genomic DNA from representative *Pm. italicum* isolates. No amplification was obtained with the negative control. In addition, reproducibility of PCR results was demonstrated since the same results were obtained in at least 3 independent PCR assays for each primer set tested.

Table IV.1 Specific PCR primers designed in this study for *Pm. italicum* detection

Target	Primer name	Primer sequence (5′->3′)	Length (bp)	Direction
IGS	ITAL_IGS_F1	5`- GTTTGTTTAGTGTCGAGG -3`	18	Forwad
	ITAL_IGS_R1	5`- TTGCGCACACCATATAAG -3`	18	Reverse
β-tubulin	ITAL_BT_F	5`- GACATACGACTGACGATT -3`	18	Forwad
	ITAL_BT_R	5`- CATAWCAAATATCACGAACTG -3`	21	Reverse

The IGS primer designed for *Pm. italicum* group, ITAL_IGS_F1/ITAL_IGS_R1, gave a PCR product, which varied in length between 512 and 621 bp among isolates. Fragments length of the representative isolates are indicated at table IV.2, as shown in Figure IV.2.

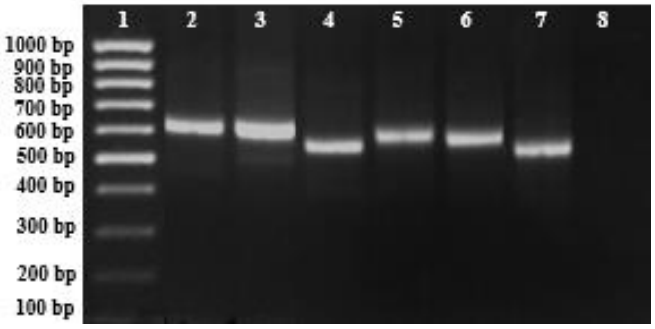

Figure IV.2 IGS PCR products for detecting *Pm. italicum* group using ITAL_IGS_F1/ITAL_IGS_R1 primer set. Different representative isolates were used. Lane 1: 100 bp DNA marker; Lane 2: isolate Pm 31M; Lane 3: isolate Pm 45; Lane 4: isolate Pm 2; Lane 5: isolate Pm 17; Lane 6: isolate Pm 50M; Lane 7: isolate Pm 59; Lane 8: negative control.

Table IV.2 Size of IGS fragments obtained in representative *Phaeoacremonium italicum* isolates using primer set ITAL_IGS_F1/ITAL_IGS_R1

Target	Isolate code	Length (bp)
IGS	Pm 31M	621
	Pm 45	618
	Pm 2	585
	Pm 17	606
	Pm 50M	597
	Pm 59	512

The PCR amplification using β-tubulin primers ITAL_BT_F/ ITAL_BT_R resulted in a single product, 336 bp in size from *Pm. italicum* isolates (Figure IV.3).

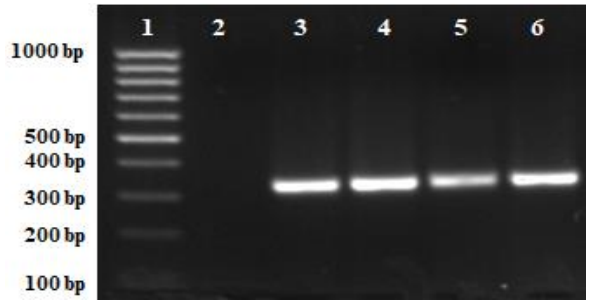

Figure IV.3 PCR products for detecting *Pm. italicum* using β-tubulin primer set. Lane 1: size marker; Lane 2: negative control; Lane 3,4,5 and 6: *Pm. italicum* isolates.

IV.3.2 Specificity of IGS and β-tubulin PCR assays

The designed primers were assessed for specificity against several isolates of *Phaeoacremonium* species. The results showed that all designed primers amplified products of the expected size from all tested isolates of *Pm. italicum*, whereas no cross-reaction occurred with the other tested *Phaeoacremonium* species (see Table IV. 3 and IV.4).

Table IV.3 Isolates of *Phaeoacremonium* species used for specificity tests of the IGS assay. The PCR specificity test results are indicated as amplified (+) and not-amplified (-)

Species	Isolate Code	Host species	Country	Origin	IGS PCR reaction
Pm. italicum	Pm 1	*Olea europaea*	Italy	Salento, Apulia	+
Pm. italicum	Pm 2	*Olea europaea*	Italy	Salento, Apulia	+
Pm. italicum	Pm 15	*Olea europaea*	Italy	Salento, Apulia	+
Pm. italicum	Pm 17	*Olea europaea*	Italy	Salento, Apulia	+
Pm. italicum	Pm 23	*Olea europaea*	Italy	Cerignola (Fg), Apulia	+
Pm. italicum	Pm 31M	*Olea europaea*	Italy	San Giovanni Rotondo, (Fg), Apulia	+
Pm. italicum	Pm 35M	*Olea europaea*	Italy	Salento, Apulia	+
Pm. italicum	Pm 45	*Olea europaea*	Italy	Salento, Apulia	+
Pm. italicum	Pm 50M	*Olea europaea*	Italy	Salento, Apulia	+
Pm. italicum	Pm 59	*Olea europaea*	Italy	Salento, Apulia	+
Pm. minimum	L-288	*Vitis vinifera*	Spain	Requena, Valencia	-
Pm. minimum	15	*Vitis vinifera*	Spain	Socuéllamos, Ciudad Real	-
Pm. minimum	34	*Vitis vinifera*	Spain	Argamasilla de Alba, Ciudad Real	-
Pm. minimum	57	*Vitis vinifera*	Spain	Ocaña, Toledo	-
Pm. minimum	73	*Vitis vinifera*	Spain	Aielo de Malferit, Valencia	-
Pm. minimum	89	*Vitis vinifera*	Spain	Aielo de Malferit, Valencia	-
Pm. minimum	90	*Vitis vinifera*	Spain	Aielo de Malferit, Valencia	-
Pm. minimum	104	*Vitis vinifera*	Spain	Ciudad Real	-
Pm. minimum	113	*Vitis vinifera*	Spain	Aielo de Malferit, Valencia	-
Pm. minimum	127	*Vitis vinifera*	Spain	Aielo de Malferit, Valencia	-
Pm. minimum	Bv 77	*Vitis vinifera*	Spain	La Rioja Comunidad	-
Pm. minimum	Bv 78	*Vitis vinifera*	Spain	La Rioja Comunidad	-
Pm. minimum	Bv 100	*Vitis vinifera*	Spain	La Rioja Comunidad	-
Pm. minimum	Pm 67	*Vitis vinifera*	Italy	Barletta (Bat), Apulia	-
Pm. minimum	Pm 68	*Vitis vinifera*	Italy	Barletta (Bat), Apulia	-
Pm. parasiticum	Pm 88	*Olea europaea*	Italy	Stornara, Foggia, Apulia	-
Pm. parasiticum	L-145	*Vitis vinifera*	Spain	Onteniente, Valencia	-
Pm. parasiticum	L-287	*Vitis vinifera*	Spain	Requena, Valencia	-
Pm. parasiticum	Bv 68	*Vitis vinifera*	Spain	La Rioja Comunidad	-
Pm. parasiticum	Ppa 5	*Vitis vinifera*	Spain	Badajoz, Spain	-
Pm. parasiticum	Ppa 6	*Vitis vinifera*	Spain	Aielo de Malferit, Valencia	-
Pm. parasiticum	Ppa 7	*Vitis vinifera*	Spain	Aielo de Malferit, Valencia	-
Pm. parasiticum	Ppa 8	*Vitis vinifera*	Spain	Aielo de Malferit, Valencia	-

Table IV.3 Continued

Species	Code	Host species	Country	Origin	IGS reaction
Pm. parasiticum	Ppa 9	*Vitis vinifera*	Spain	Aielo de Malferit, Valencia	-
Pm. parasiticum	Ppa 14	*Vitis vinifera*	Spain	Ugijar, Granada	-
Pm. parasiticum	Ppa 15	*Vitis vinifera*	Spain	Laujar, Almería	-
Pm. parasiticum	Ppa 16	*Vitis vinifera*	Spain	Cártama, Granada	-
Pm. parasiticum	Ppa 1	*Vitis vinifera*	Spain	La Communidad Valenciana	-
Pm. parasiticum	137	*Vitis vinifera*	Spain	Cártama, Granada	-
Pm. hispanicum	Pmr 1	*Vitis vinifera*	Spain	Requena, Valencia	-
Pm. hispanicum	Pmr 5	*Vitis vinifera*	Spain	Onteniente, Valencia	-
Pm. hispanicum	Phi 1	*Vitis vinifera*	Spain	La Communidad Valenciana	-
Pm. iranianum	Pmr 7	*Vitis vinifera*	Spain	Onteniente, Valencia	-
Pm. iranianum	L-289	*Vitis vinifera*	Spain	Requena, Valencia	-
Pm. iranianum	L-271	*Vitis vinifera*	Spain	Campo Arcís, Valencia	-
Pm. iranianum	Pm 121	*Vitis vinifera*	Italy	Campomarino (CB)	-
Pm. iranianum	Pir 3	*Vitis vinifera*	Spain	La Communidad Valenciana	-
Pm. sicilianum	L-176	*Vitis vinifera*	Spain	Onteniente, Valencia	-
Pm. sicilianum	Pm 65	*Olea europaea*	Italy	Cerignola, Foggia, Apulia	-
Pm. sicilianum	Bv 297	*Vitis vinifera*	Spain	La Rioja Comunidad	-
Pm. sicilianum	Bv 298	*Vitis vinifera*	Spain	La Rioja Comunidad	-
Pm. sicilianum	Bv 299	*Vitis vinifera*	Spain	La Rioja Comunidad	-
Pm. sicilianum	Bv 300	*Vitis vinifera*	Spain	La Rioja Comunidad	-
Pm. sicilianum	Bv 41-1	*Vitis vinifera*	Spain	La Rioja Comunidad	-
Pm. sicilianum	Bv 41	*Vitis vinifera*	Spain	La Rioja Comunidad	-
Pm. sicilianum	Pmr 10	*Vitis vinifera*	Spain	Onteniente, Valencia	-
Pm. sicilianum	Pmr 16	*Vitis vinifera*	Spain	Benitatxell, Valencia	-
Pm. scolyti	Psco 1	*Vitis vinifera*	Spain	La Comunidad Valenciana	-
Pm. scolyti	Pm 92A	*Prunus avium*	Italy	Foggia, Apulia	-
Pm. scolyti	Pm 25	*Olea europaea*	Italy	Cerignola, Foggia, Apulia	-
Pm. krajdenii	Bv 387	*Vitis vinifera*	Spain	La Rioja Comunidad	-
Pm. krajdenii	Bv 390	*Vitis vinifera*	Spain	La Rioja Comunidad	-
Pm. krajdenii	Bv 581	*Vitis vinifera*	Spain	La Rioja Comunidad	-
Pm. krajdenii	Bv 583	*Vitis vinifera*	Spain	La Rioja Comunidad	-
Pm. krajdenii	Bv 585	*Vitis vinifera*	Spain	La Rioja Comunidad	-
Pm. kradjenii	Bv 588	*Vitis vinifera*	Spain	La Rioja Comunidad	-
Pm. amygdalinum	Pam 1	*Prunus dulcis*	Spain	La Comunidad Valenciana	-
Pm. mortoniae	Bv 95	*Vitis vinifera*	Spain	La Rioja Comunidad	-
Pm. mortoniae	Pmo 1	*Vitis vinifera*	Spain	La Comunidad Valenciana	-
Pm. mortoniae	Pmo 2	*Vitis vinifera*	Spain	Valencia	-
Pm. croatiense	Pm 120	*Vitis vinifera*	Italy	Campomarino (CB)	-
Pm. inflatipes	Pmr 31	*Vitis vinifera*	Spain	Valencia	-
Pm. cinereum	Pci 2	*Vitis vinifera*	Spain	La Comunidad Valenciana	-
Pm. cinereum	Pci 7	*Vitis vinifera*	Spain	La Comunidad Valenciana	-
Pm. viticola	Vic 29	*Vitis vinifera*	Spain	Valencia	-
Pm. viticola	Vic 34	*Vitis vinifera*	Spain	Valencia	-
Pm. viticola	Pm 34	*Olea europaea*	Italy	Vieste, Apulia	-
Pm. oleae	Pm 14	*Olea europaea*	Italy	Carpino (Fg), Apulia	-

Table IV.4 Isolates of *Phaeoacremonium* species used for specificity tests of the β-tubulin PCR assay. The PCR specificity results are indicated as amplified (+) and not-amplified (-)

Species	Isolate Code	Host species	Country	Origin	β-tubulin PCR reaction
Pm. italicum	Pm 1	*Olea europaea*	Italy	Salento, Apulia	+
Pm. italicum	Pm 2	*Olea europaea*	Italy	Salento, Apulia	+
Pm. italicum	Pm 15	*Olea europaea*	Italy	Salento, Apulia	+
Pm. italicum	Pm 17	*Olea europaea*	Italy	Salento, Apulia	+
Pm. italicum	Pm 23	*Olea europaea*	Italy	Cerignola (Fg), Apulia	+
Pm. italicum	Pm 35M	*Olea europaea*	Italy	Salento, Apulia	+
Pm. italicum	Pm 45	*Olea europaea*	Italy	Salento, Apulia	+
Pm. italicum	Pm 50M	*Olea europaea*	Italy	Salento, Apulia	+
Pm. italicum	Pm 59	*Olea europaea*	Italy	Salento, Apulia	+
Pm. minimum	Bv 100	*Vitis vinifera*	Spain	La Rioja Comunidad	-
Pm. minimum	Pm 67	*Vitis vinifera*	Italy	Barletta (Bat), Apulia	-
Pm. minimum	Pm 68	*Vitis vinifera*	Italy	Barletta (Bat), Apulia	-
Pm. parasiticum	Pm 88	*Olea europaea*	Italy	Stornara, Foggia, Apulia	-
Pm. parasiticum	Ppa 1	*Vitis vinifera*	Spain	La Communidad Valenciana	-
Pm. hispanicum	Phi 1	*Vitis vinifera*	Spain	La Communidad Valenciana	-
Pm. iranianum	Pm 121	*Vitis vinifera*	Italy	Campomarino (CB)	-
Pm. iranianum	Pir 3	*Vitis vinifera*	Spain	La Communidad Valenciana	-
Pm. sicilianum	Pm 65	*Olea europaea*	Italy	Cerignola, Foggia, Apulia	-
Pm. scolyti	Psco 1	*Vitis vinifera*	Spain	La Comunidad Valenciana	-
Pm. scolyti	Pm 92A	*Prunus avium*	Italy	Foggia, Apulia	-
Pm. scolyti	Pm 25	*Olea europaea*	Italy	Cerignola, Foggia, Apulia	-
Pm. amygdalinum	Pam 1	*Prunus dulcis*	Spain	La Comunidad Valenciana	-
Pm. croatiense	Pm 120	*Vitis vinifera*	Italy	Campomarino (CB)	-
Pm. mortoniae	Pmo 1	*Vitis vinifera*	Spain	La Comunidad Valenciana	-
Pm. mortoniae	Pmo 2	*Vitis vinifera*	Spain	Valencia	-
Pm. cinereum	Pci 2	*Vitis vinifera*	Spain	La Comunidad Valenciana	-
Pm. cinereum	Pci 7	*Vitis vinifera*	Spain	La Comunidad Valenciana	-
Pm. viticola	Pm 34	*Olea europaea*	Italy	Vieste, Apulia	-
Pm. oleae	Pm 14	*Olea europaea*	Italy	Carpino (Fg), Apulia	-

IV.3.3 Sensitivity of PCR assays

The sensitivity of PCR assays was determined by using *Pm. italicum* DNA serial dilutions ranging from 10 ng/µl to 1 fg/µl. IGS primer pair tested, generated the expected PCR products up to 10^{-4} dilution allowing the detection of 1 pg/µl, using the DNA extracted with the E.Z.N.A kit (Figure IV.4.b). However, the PCR detection limit was 10 pg/µl of DNA obtained at 10^{-3} dilution, using DNA isolated with the classic protocol (Figure IV.4.a).

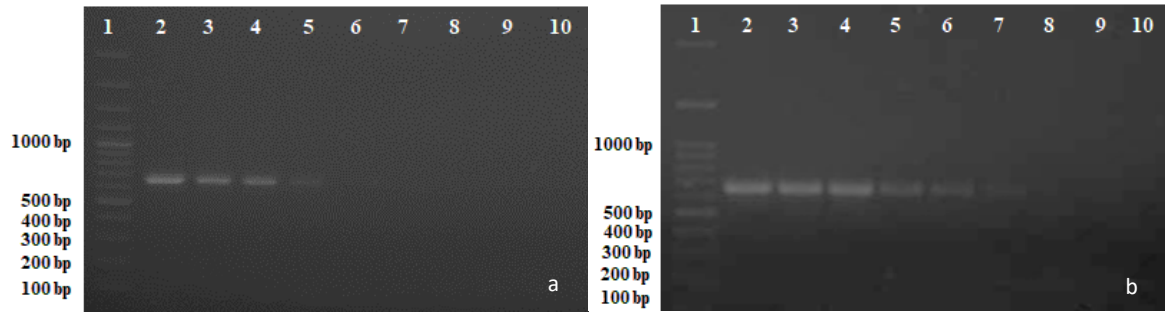

Figure IV.4. Sensitivity of IGS PCR using primer pair ITAL_IGS_F1/ ITAL_IGS_R1. (a) DNA extracted using classic protocol (b) DNA extracted using E.Z.N.A.® Plant DNA Kit. Lane 1: 100 bp DNA ladder; Lane 2: stock DNA (100 ng/µl); Lane 3-9: 10^{-1} to 10^{-7} dilutions of genomic DNA of *Pm. italicum;* Lane 10: negative control.

With respect to the β-tubulin primer pair ITAL_BT_F/ITAL_BT_R, a fragment of the expected size was amplified (336 bp), and the lowest amount of DNA that could generate a visible band was found to be 10 pg/µl, obtained at 10^{-3} dilution (Figure IV.5.a). Same detection limit was obtained with the beta-tubulin universal primers T1/Bt-2b (Figure IV.5.b).

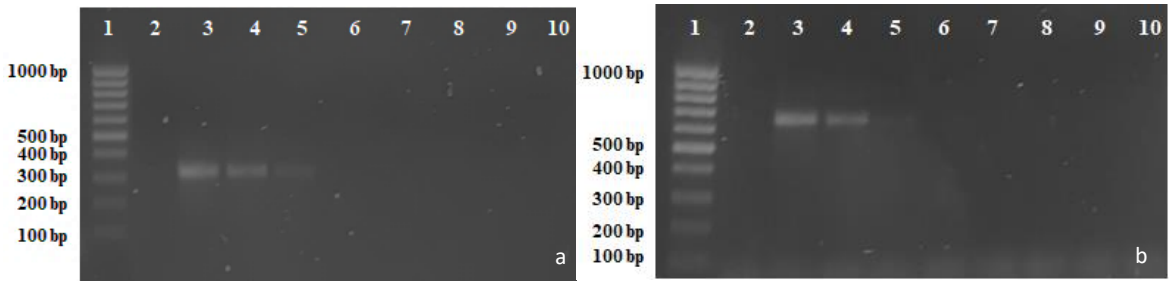

Figure IV.5. Sensitivity of β-tubulin PCR primers. (a) Specific designed primers ITAL_BT_F/ ITAL_BT_R. (b) Universal primers T1/Bt-2b. DNA serial dilutions ranging from 10ng/ul to 1fg/ul. Lane 1: 100 bp DNA ladder; Lane 2: stock DNA; Lane 3-9: 10^{-1} to 10^{-7} dilutions of genomic DNA of *Pm. italicum;* Lane 10: negative control.

IV.4 Discussion

In this study, the possibility to set up a new PCR-based approach, providing a specific detection of *Pm. italicum* group was demonstrated. *Pm. italicum* was chosen as a study model being commonly isolated from olive trees in Salento, as reported in chapter II. Specific PCR primer pair was successfully developed, based on the rDNA intergenic spacer (IGS) of *Pm. italicum*. PCR products obtained from the new primer pair showed the expected size

according to their priming size on the sequences. Moreover, their specificity was checked and confirmed, using 10 isolates of *Pm. italicum* and other 68 non target *Phaeoacremonium* isolates.

Until now, a number of studies on detection methods are available for some *Phaeoacremonium* spp., even though *Phaeoacremonium* are known to have a global distribution and are associated with wood diseases of various host plants (Gramaje *et al.* 2015). All techniques previously developed were focused on the detection of particular species and therefore are not enough to assess which *Phaeoacremonium* species might be present in mixed natural ecosystem samples. Moreover, all detection methods described so far are based mainly on internal transcribed spacer (ITS) regions and β-tubulin gene. Effectively, the internal transcribed spacer (ITS) region has been used to design primers for detection of some *Phaeoacremonium* species on grapevine, namely, *Pm. minimum*; *Pm. parasiticum; Pm. inflatipes; Pm. mortoniae; Pm. angustius; Pm. viticola; Pm. scolyti; Pm. krajdenii* and *Pm. venezuelense* (Overton *et al*. 2004; Aroca and Raposo, 2007 & Aroca *et al*. 2008). However, the ITS sequences are short and not sufficiently variable, making the design of primers to identify and detect closely related species very difficult or impossible.

Nowadays, the β-tubulin gene is commonly used in phylogenetic analyses for molecular characterization of *Phaeoacremonium* species (Mostert *et al.* 2006). Likewise, it has been used for development of Real-time PCRs to detect *Pm. minimum* and *Pm. parasiticum* from isolated fungi and in inoculated grapevine-wood samples and young vines from nurseries (Dupont *et al.* 2002; Martın *et al.* 2012; Pouzoulet *et al.* 2013). Urbez-Torres *et al.* (2015) developed probes for a DNA macroarray, for detection of young vine decline fungi and allowed the discrimination of 29 *Phaeoacremonium* species. The use of this target gene is favored by the availability of universal primers designed in conserved coding regions (exons) (Glass and Donaldson, 1995), but also in variable regions (introns) that could differentiate closely related taxa (Aroca *et al.* 2008). However, considering the increasing recognition of novel species of *Phaeoacremonium*, and the short length of β-tubulin amplified fragments, therefore not variable enough to be used for primers designing toward the specific detection of closely related species.

In fact, the β-tubulin primer designed in the present study seems to be specific and allowed detection of *Pm. italicum*, however, its specificity was not assessed on all *Phaeoacremonium* spp. and in particular closely related species, such as *Pm. alvesii* and *Pm. rubrigerum.* Moreover, when the β-tubulin sequences were aligned for primers design, the nucleotide sequence dissimilarities appeared to be more dispersed along the β-tubulin gene fragments than being accumulated in short spots. Barely, few exceptions were found, in which the β-tubulin gene enabled to develop one PCR primer pair for *Pm. italicum*.

Based on previous findings, the present study aimed to explore for the first time the usefulness of the intergenic spacer (IGS) to design species-specific primers for the detection of *Pm. italicum* group. Indeed, it has been reported that the IGS can be used to detect or distinguish closely related species such as, *Phytophthora medicaginis; Phytophtora megasperma, Botrytis cinerea, Verticillium dahliae* complex, *Fusarium oxysporum formae speciales*, since it evolves faster and more sequence polymorphisms are present (Liew *et al.* 1989; Nigro *et al.* 2005; Suarez *et al.* 2005; Srinivasan *et al.* 2010; Bilodeau *et al.* 2012).

When the IGS sequences were first analyzed in the present study for primers design, inter-specific variation of IGS region among *Phaeoacremonium* species was observed, allowing the identification of suitable regions for primers design. This is confirmed by the fact that IGS has faster mutation rates than the other rDNA regions, resulting in molecular variation among species (Moss and Stefanovsky, 1995; Martin *et al.* 1999; Ciarmela *et al.* 2001; Schmidt and Moreth, 2008).

In addition to the nucleotide sequence differences among the isolates of *Phaeoacremonium* species examined here, length polymorphism of IGS amplified PCR products was also detected in *Pm. italicum* isolates. This finding can be explained by the variation in copy numbers of the short repeat elements (R, A, B and P) present within IGS, as well occurrence of point mutations and short indels of varying size within *Pm. italicum* isolates, as reported in chapter III. In this regard, length differences in the IGS reported in many studies were attributed to insertions or deletions in the arrays of subrepeats (Albee *et al.* 1996; White *et al.* 1996; James *et al.* 2001). For this reason, particular attention is needed when identifying areas within IGS sequences for primers design.

Chapter IV. IGS as a target for developing PCR-based detection of *Pm. italicum*

The PCR detection limit is an important parameter for evaluation the feasibility of the PCR assay. It could depend mainly on the copy number of the targeted DNA marker and the PCR amplification efficiency related to amplicons length (Fan *et al.* 2015). The PCR detection limit determined here for the IGS assay, up to 1 pg/µl, appeared higher than in the B-tubulin assay. This is supported by the fact that IGS region is known to be in high copy number, thus improving the sensitivity of detection. Furthermore, the sensitivity of IGS PCR assay determined using *Pm. italicum* DNA, extracted with the E.Z.N.A kit generated the expected PCR products up to 10^{-4} dilution, while using DNA isolated with classic extraction protocol, the PCR produced bands up 10^{-3} dilution. The decreased sensitivity might be due to the presence of some inhibitors in the DNA extract, which can reduce the reproducibility of the PCR.

The intergenic spacer (IGS) region of rDNA has not previously been studied in *Phaeoacremonium* species, although it might provide specific molecular tool to facilitate the detection of these fungi. In this study, a variability was identified in IGS region between *Pm. italicum* and the other *Phaeoacremonium* species analysed here. This variability allowed the specific detection of *Pm. italicum* group by designing species-specific primers binding at the most conservative areas in PR region identified within *Pm. italicum* IGS.

III.5 References

Albee, S. R., Mueller, G. M., & Kropp, B. R. (1996). Polymorphisms in the large intergenic spacer of the nuclear ribosomal repeat identify Laccaria proxima strains. *Mycologia*, 970-976.

Aroca A. and Raposo R. (2007). PCR-based strategy to detect and identify species of *Phaeoacremonium* causing grapevine diseases. *Applied and Environmental Microbiology*, 73(9),2911-2918.

Aroca, A., Raposo, R., & Lunello, P. (2008). A biomarker for the identification of four *Phaeoacremonium* species using the β-tubulin gene as the target sequence. *Applied microbiology and biotechnology*, 80(6),1131-1140.

Bilodeau, G. J., Koike, S. T., Uribe, P., & Martin, F. N. (2012). Development of an assay for rapid detection and quantification of Verticillium dahliae in soil. *Phytopathology*, *102*(3), 331-343.

Ciarmela, P., Potenza, L., Cucchiarini, L., Zeppa, S., & Stocchi, V. (2002). PCR amplification and polymorphism analysis of the intergenic spacer region of ribosomal DNA in Tuber borchii. *Microbiological research*, *157*(1), 69-74.

Suarez, M. B., Walsh, K., Boonham, N., O'Neill, T., Pearson, S., & Barker, I. (2005). Development of real-time PCR (TaqMan®) assays for the detection and quantification of Botrytis cinerea in planta. *Plant Physiology and Biochemistry*, *43*(9), 890-899.

Carlucci A., Raimondo M. L., Cibelli F., Phillips A. J. and F. Lops. (2013). *Pleurostomophora richardsiae, Neofusicoccum parvum* and *Phaeoacremonium aleophilum* associated with a decline of olives in southern Italy. *Phytopathologia Mediterranea*, 52(3),517-527.

Carlucci, A., Lops, F., Cibelli, F., & Raimondo, M. L. (2015). *Phaeoacremonium* species associated with olive wilt and decline in southern Italy. *European Journal of Plant Pathology*, 141(4),717-729.

Crous, P. W., Gams, W., Wingfield, M. J., & Van Wyk, P. S. (1996). Phaeoacremonium gen. nov. associated with wilt and decline diseases of woody hosts and human infections. *Mycologia*, *88*(5), 786-796.

Dupont, J., Magnin, S., Cesari, C., & Gatica, M. (2002). ITS and β-tubulin markers help delineate *Phaeoacremonium* species, and the occurrence of *P. parasiticum* in grapevine disease in Argentina. *Mycological Research*, 106(10),1143-1150.

Fan, X., Zhang, J., Yang, L., Wu, M., Chen, W., & Li, G. (2015). Development of PCR-based assays for detecting and differentiating three species of Botrytis infecting broad bean. *Plant disease*, *99*(5), 691-698.

Glass, N. L., & Donaldson, G. C. (1995). Development of primer sets designed for use with the PCR to amplify conserved genes from filamentous ascomycetes. *Applied and Environmental Microbiology*, *61*(4), 1323-1330.

Groenewald, M., Ji-Chuan, K. A. N. G., Crous, P. W., & Walter, G. A. M. S. (2001). ITS and β-tubulin phylogeny of Phaeoacremonium and Phaeomoniella species. *Mycological Research*, *105*(6), 651-657.

Gramaje, D., Mostert, L., Groenewald, J. Z., & Crous, P. W. (2015). Phaeoacremonium: from esca disease to phaeohyphomycosis. *Fungal biology*, *119*(9), 759-783.

Huang, S. K., Jeewon, R., Hyde, K. D., Bhat, D. J., Chomnunti, P., & Wen, T. C. (2018). Beta-tubulin and Actin gene phylogeny supports *Phaeoacremonium ovale as* a new species from freshwater habitats in China. *MycoKeys*, (41), 1.

James, T. Y., Moncalvo, J. M., Li, S., & Vilgalys, R. (2001). Polymorphism at the ribosomal DNA spacers and its relation to breeding structure of the widespread mushroom Schizophyllum commune. *Genetics*, *157*(1), 149-161.

Katoh, K., & Standley, D. M. (2013). MAFFT multiple sequence alignment software version 7: improvements in performance and usability. *Molecular biology and evolution*, *30*(4), 772-780.

Kumar, P., Gupta, V. K., Tiwari, A. K., & Kamle, M. (Eds.). (2016). *Current Trends in Plant Disease Diagnostics and Management Practices*. Springer.

Liew, E. C. Y., Maclean, D. J., & Irwin, J. A. G. (1998). Specific PCR based detection of Phytophthora medicaginis using the intergenic spacer region of the ribosomal DNA. *Mycological Research*, *102*(1), 73-80.

Martín, M. T., Cobos, R., Martín, L., & López-Enríquez, L. (2012). Real-time PCR detection of *Phaeomoniella chlamydospora* and *Phaeoacremonium aleophilum*. *Applied and environmental microbiology*, AEM-07360.

Martin, F., Selosse, M. A., & Le Tacon, F. (1999). The nuclear rDNA intergenic spacer of the ectomycorrhizal basidiomycete Laccaria bicolor: structural analysis and allelic polymorphism. *Microbiology*, *145*(7), 1605-1611.

Moss, T., & Stefanovsky, V. Y. (1995). Promotion and Regulation of Ribosomal Transcription in Eukaryotes by RNA Polymerase1. In *Progress in nucleic acid research and molecular biology* (Vol. 50, pp. 25-66). Academic Press.

Mostert, L., Groenewald, J. Z., Summerbell, R. C., Gams, W., & Crous, P. W. (2006). Taxonomy and pathology of Togninia (Diaporthales) and its Phaeoacremonium anamorphs. *Studies in Mycology*, *54*, 1-113.

Nigro, F., Boscia, D., Antelmi, I., & Ippolito, A. (2013). Fungal species associated with a severe decline of olive in southern Italy. *Journal of plant pathology*, 95(3).

Overton, B. E., Stewart, E. L., Qu, X., Wenner, N. G., & Christ, B. J. (2004). Qualitative real-time PCR SYBR® Green detection of Petri disease fungi. *Phytopathologia Mediterranea*, *43*(3), 403-410.

Pantou, M. P., Mavridou, A., & Typas, M. A. (2003). IGS sequence variation, group-I introns and the complete nuclear ribosomal DNA of the entomopathogenic fungus Metarhizium: excellent tools for isolate detection and phylogenetic analysis. *Fungal Genetics and Biology*, *38*(2), 159-174.

Pouzoulet, J., Mailhac, N., Couderc, C., Besson, X., Daydé, J., Lummerzheim, M., & Jacques, A. (2013). A method to detect and quantify *Phaeomoniella chlamydospora* and *Phaeoacremonium* aleophilum DNA in grapevine-wood samples. *Applied microbiology and biotechnology*, 97(23),10163-10175.

Raimondo M. L., Lops F. and Carlucci A. (2014). *Phaeoacremonium italicum* sp. nov., associated with esca of grapevine in southern Italy. *Mycologia,* 106(6),1119-1126.

Schena, L., Li Destri Nicosia, M. G., Sanzani, S. M., Faedda, R., Ippolito, A., & Cacciola, S. O. (2013). Development of quantitative PCR detection methods for phytopathogenic fungi and oomycetes. *Journal of Plant Pathology*, 7-24.

Schmidt, O., & Moreth, U. (2008). Ribosomal DNA intergenic spacer of indoor wood-decay fungi. *Holzforschung*, *62*(6), 759-764.

Sicoli, G., Fatehi, J., & Stenlid, J. (2003). Development of species-specific PCR primers on rDNA for the identification of European Armillaria species. *Forest Pathology*, *33*(5), 287-297.

Spies, C. F. J., Moyo, P., Halleen, F., & Mostert, L. (2018). *Phaeoacremonium* species diversity on woody hosts in the Western Cape Province of South Africa. *Persoonia*, 40,26-62.

Suarez, M. B., Walsh, K., Boonham, N., O'Neill, T., Pearson, S., & Barker, I. (2005). Development of real-time PCR (TaqMan®) assays for the detection and quantification of Botrytis cinerea in planta. *Plant Physiology and Biochemistry*, *43*(9), 890-899.

Srinivasan, K., Gilardi, G., Spadaro, D., Gullino, M. L., & Garibaldi, A. (2010). Molecular characterization through IGS sequencing of formae speciales of Fusarium oxysporum pathogenic on lamb's lettuce. *Phytopathologia Mediterranea*, *49*(3), 309-320.

Úrbez-Torres, J. R., Haag, P., Bowen, P., Lowery, T., & O'Gorman, D. T. (2015). Development of a DNA macroarray for the detection and identification of fungal pathogens causing decline of young grapevines. *Phytopatholog*y, 105(10),1373-1388.

White, T. J., Bruns, T., Lee, S. J. W. T., & Taylor, J. L. (1990). Amplification and direct sequencing of fungal ribosomal RNA genes for phylogenetics. *PCR protocols: a guide to methods and applications*, *18*(1), 315-322.

White, E. E., Foord, B. M., & Kinloch Jr, B. B. (1996). Genetics of Cronartium ribicola. II. Variation in the ribosomal gene cluster. *Canadian journal of botany*, *74*(3), 461-468.

V. PHYLOGENETIC ANALYSES OF THE RIBOSOMAL DNA INTERGENIC SPACER (IGS) REGION, β-TUBULIN AND ACTIN GENES SEQUENCES OF *PHAEOACREMONIUM* SPECIES

V.1 Introduction

The genus *Phaeoacremonium* (Togniniales, Togniniaceae) was originally described 23 years ago (Crous *et al.* 1996), during a re-evaluation of isolates similar to what was considered to be *Phialophora parasitica*. To date, 65 *Phaeoacremonium* species have been described in this genus (Mostert *et al.* 2006; Gramaje *et al.* 2015; Spies *et al.* 2018). Most species of the *Togniniaceae* are associated with wood diseases of various plants such as, *Vitis vinefera*, *Oleae* spp. and *Prunus* spp., and have been reported to colonise substrates in different types of habitats. More recent studies have reported the importance of *Phaeoacremonium* species in causing brown wood streaking of *Oleae* spp. (Nigro *et al.* 2013; Carlucci *et al.* 2013).

The characterization of *Phaeoacremonium* species proved to be difficult based on morphological characteristics alone. Subsequently, molecular techniques played an increasingly important role in their identification, including phylogenetic analyses of the genus *Phaeoacremonium*. Indeed, detailed taxonomic treatment including phylogenetic analyses of this genus by Mostert *et al.* (2006), provided a solid basis for the identification and description of new species within the genus. The actin and beta-tubulin gene sequences have been widely used for the discrimination of *Phaeoacremonium* spp. over the last decade, nevertheless, the increasing number of species within the genus and the reports of new species assoacietd with many other wood host plants could lead to misidentifications. The identification of phylogenetic markers to improve phylogenetic resolution of species is of importance. Hence, other markers that could be considered is the ribosomal DNA intergenic spacer (IGS). This region has been used in phylogenetic analyses of various fungi (Morton *et al.* 1995; Pramateftaki *et al.* 2000; Pantou *et al.* 2003; Mbofung *et al.* 2007). It has not yet been sequenced for any *Phaeoacremonium* species. In this context and in an attempt to establish a more robust resolution in the *Phaeoacremonium* phylogeny, the aim of this study was to amplify and sequence for the first time, the IGS region of *Phaeoacremonium* spp., and phylogenetically

analyze these sequences individually and in combination with β-tubulin and actin gene sequences, to assess whether this region could be used in combined phylogenetic analyses to improve phylogenetic resolution, among *Phaeoacremonium* species.

V.2 Materials and methods

V.2.1 Fungal isolates and culture conditions

A total of 58 isolates of *Phaeoacremonium* spp. and *Pleurostoma richardsiae* were employed in this study. Thirty-three representative isolates including *Phaeoacremonium italicum, Pm. minimum and Pm. scolyti*, recovered from olive orchards in Salento were selected for this work (See chapter. II). In addition, other isolates of *Phaeoacremonium* spp., collected from different hosts and localities, obtained from the culture collection of Department of Science of Agriculture, Food and Environment (SAFE), University of Foggia, Italy, were also used. *Phaeoacremonium amygdalinum* and *Pm. hispanicum* were obtained from Instituto de Ciencias de la Vid y del Vino (ICVV), Logroño; Spain (Table V.1).

Single spore cultures were made from each isolate by dilution plating onto water agar plates. After 1–2 days incubation, single germinating spores were collected under a light microscope and transferred to fresh plates of potato dextrose agar (PDA; 3.9 % potato dextrose agar; Oxoid Ltd., UK).

V.2.2 DNA extraction and PCR amplification

Genomic DNA of all of the fungal isolates was extracted from fresh fungal mycelia grown on PDA plates at 25 °C for 2–3 weeks, following the same extraction protocol previously described in Chapter III (Carlucci *et al.* 2013). The DNA was quantified by spectrophotometry at 260 and 280 nm, diluted to 30 ng/µl and stored at -20°C until needed for PCR assays.

Table V.1 Fungal isolates used for PCR amplifications. Isolates collected from Salento are highlighted in bold.

Species name	Isolate code	Host	Origin	Source
Pm. italicum	**Pm 1**	Olive	Salento, Apulia, Italy	Dept. SAFE
	Pm 2	Olive	Salento, Apulia, Italy	Dept. SAFE
	Pm 6	Olive	Salento, Apulia, Italy	Dept. SAFE
	Pm 15	Olive	Salento, Apulia, Italy	Dept. SAFE
	Pm 17	Olive	Salento, Apulia, Italy	Dept. SAFE
	Pm 18	Olive	Salento, Apulia, Italy	Dept. SAFE
	Pm 19 CBS 137763	Grapevine	San Severo, (Fg), Apulia, Italy Raimondo *et al.* 2014	Dept. SAFE
	Pm 23	Grapevine	Cerignola (Fg), Apulia, Italy	Dept. SAFE
	Pm 31M	Almond	San Giovanni Rotondo, (Fg), Apulia, IT	Dept. SAFE
	Pm 34	Olive	Salento, Apulia, Italy	Dept. SAFE
	Pm 35M	Olive	Salento, Apulia, Italy	Dept. SAFE
	Pm 38	Olive	Salento, Apulia, Italy	Dept. SAFE
	Pm 45	Olive	Salento, Apulia, Italy	Dept. SAFE
	Pm 50M	Olive	Salento, Apulia, Italy	Dept. SAFE
	Pm 59	Olive	Salento, Apulia, Italy	Dept. SAFE
	Pm 60	Olive	Salento, Apulia, Italy	Dept. SAFE
	Pm 77	Olive	Salento, Apulia, Italy	Dept. SAFE
	Pm 105	Olive	Salento, Apulia, Italy	Dept. SAFE
	Pm 180	Olive	Salento, Apulia, Italy	Dept. SAFE
	Pm 196	Olive	Salento, Apulia, Italy	Dept. SAFE
	Pm 210	Olive	Salento, Apulia, Italy	Dept. SAFE
	Pm 235	Olive	Salento, Apulia, Italy	Dept. SAFE
	Pm 250	Olive	Salento, Apulia, Italy	Dept. SAFE
Pm. scolyti	**Pm 1M**	Olive	Salento, Apulia, Italy	Dept. SAFE
	Pm 5	Cherry	Foggia, Apulia, Italy	Dept. SAFE
	Pm 10M	Olive	Salento, Apulia, Italy	Dept. SAFE
	Pm 44M	Olive	Salento, Apulia, Italy	Dept. SAFE
	Pm 51M	Olive	Salento, Apulia, Italy	Dept. SAFE
	Pm 73M	Olive	Salento, Apulia, Italy	Dept. SAFE

Table V.1 Continued

Species name	Isolate code	Host	Origin	Source
Pm. scolyti	**Pm 81M**	Olive	Salento, Apulia, Italy	Dept. SAFE
	Pm 90	Cherry	Foggia, Apulia, Italy	Dept. SAFE
	Pm 92A	Cherry	Foggia, Apulia, Italy	Dept. SAFE
	Pm 155	Olive	Foggia, Apulia, Italy	Dept. SAFE
	Pm 223	Cherry	Foggia, Apulia, Italy	Dept. SAFE
Pm. minimum	Pm 7	Grapevine	Cerignola, Apulia, Italy	Dept. SAFE
	Pm 35	Olive	Salento, Apulia, Italy	Dept. SAFE
	Pm 39	Olive	Salento, Apulia, Italy	Dept. SAFE
	Pm 41	Olive	Salento, Apulia, Italy	Dept. SAFE
	Pm 67	Olive	Cerignola, Apulia, Italy	Dept. SAFE
	Pm 68	Grapevine	Barletta (Bat), Apulia, Italy	Dept. SAFE
	Pm 90	Grapevine	Barletta (Bat), Apulia, Italy	Dept. SAFE
	Pm 109	Olive	Salento, Apulia, Italy	Dept. SAFE
	Pm 302	Olive	Salento, Apulia, Italy	Dept. SAFE
	Pm 351	Grapevine	Barletta (Bat), Apulia, Italy	Dept. SAFE
	Pm 369	Grapevine	Barletta (Bat), Apulia, Italy	Dept. SAFE
	Pm 400	Olive	Salento, Apulia, Italy	Dept. SAFE
Pm. parasiticum	Pm 88	Olive	Stornara (Fg), Apulia, Italy	Dept. SAFE
Pm. oleae	Pm 14	Olive	Carpino (Fg), Italy	Dept. SAFE
	Pm 46	Olive	Carpino (Fg), Italy	Dept. SAFE
Pm. croatiense	Pm 120	Grapevine	Campomarino (CB), Italy	Dept. SAFE
Pm. iranianum	Pm 50B	Grapevine	Torremaggiore (Fg), Italy	Dept. SAFE
	Pm 121	Grapevine	Campomarino (CB), Italy	Dept. SAFE
	Pm 122	Grapevine	Campomarino (CB), Italy	Dept. SAFE
Pm. sicilianum	Pm 65	Olive	Cerignola A, Italy	Dept. SAFE
Pm. amygdalinum	Pam 1	Almond	Valencia, Spain	(ICVV) Logroño
Pm. hispanicum	Phi 1	Grapevine	Valencia, Spain	(ICVV) Logroño
Pl. richardsiae	Pl 4	Olive	Salento, Apulia, Italy	Dept. SAFE
	Pl 31	Olive	Salento, Apulia, Italy	Dept. SAFE

V.2.2.1 Amplification of IGS

The IGS rDNA of each isolate was amplified with PCR using the universal primers LR12R (5`-GAACGCCTCTAAGTCAGAATCC-3`) and invSR1R (5`-ACTGGCAGAATCAACCAGGTA -3`) that amplify the region from the ends of the 28S and 18S genes (Vilgalys' laboratory). We selected this pair of primers for amplification because they amplified efficiently all *Pm. italicum* isolates in Chapter III.

The PCR assays were set up in a 25 µl mixture final volume with a C-1000 Touch™ Thermal Cycler (Bio Rad, USA). The primers pair was used in four sets of PCRs, as follows. The first set of PCRs was standardized to amplify IGS region of *Pm. italicum, Pm. sicilianum* and *Pm. scolyti*. The reaction mixture contained 30 ng of genomic DNA, 1x PCR buffer (TaKaRa), 3 mM MgCl2 (TaKaRa), 200 µM deoxynucleotide triphosphates (TaKaRa), 0.2 µM forward and reverse primers and 1.25 unit of Taq DNA Polymerase (TaKaRa LA Taq®). The amplification conditions were: 95°C denaturation for 10 min, followed by 25 cycles in series of denaturation at 95°C for 1 min, annealing at 55°C for 1 min, and extension at 72°C for 150 s, with a final extension at 72°C for 10 min. The second set of PCRs was done to amplify IGS region of *Pm. parasiticum* and *Pl. richardsiae.* The reaction mixture and conditions were the same as those used for the first set of PCRs, with two exceptions the number of amplification cycles was 30 and the annealing temperature was 58°C. The third set of PCRs was performed to amplify the IGS of *Pm. minimum, Pm. iranianum, Pm. oleae, Pm. hispanicum* and *Pm. amygdalinum*. The reaction mixture and conditions were the same as described above, with the exception that the annealing temperature was fixed to 55°C. The fourth set of PCRs was done to amplify the IGS of *Pm. croatiense*. The mixture and conditions were the same as above, with the exception that the annealing temperature was 62°C. For all the PCR sets, a reaction mixture without sample DNA was used as a negative control to ensure that there was no contaminating DNA in the solution.

The amplicons were separated by electrophoresis at 100 volts, on 1.2 % (w/v) agarose gels in 1× TAE buffer (40 mM Tris, 40 mM acetate, 2 mM EDTA, pH 8.0) (Sambrook *et al.*, 1989). The gels were stained with ethidium bromide and visualized in a Gel Doc™ EZ System under UV light (Biorad). The size of IGS fragments was estimated using the DNA ladder 500pb -10kb (Canvax™).

V.2.2.2 Amplification of β-tubulin and actin genes

Fragments of the β-tubulin (TUB) and actin (ACT) genes were isolated from the genomic DNA of each isolate using the primer sets T1 (O'Donnell and Cigelnik, 1997) and Bt-2b (Glass and Donaldson, 1995), and ACT-512F and ACT-783R (Carbone and Kohn 1999), respectively. The PCR amplification reactions contained 1x PCR buffer, 2.5 mM $MgCl_2$, 200 mM deoxynucleotide triphosphates, 2.5 pmol each primer, 0.5 U Taq polymerase and 30ng fungal DNA template, taken to a total volume of 50 µl with sterile ultrapure water. The PCR conditions for β-tubulin gene were: initial denaturation at 94 °C for 3 min, followed by 36 cycles of denaturation at 94 °C for 40 secs, annealing at 58 °C for 30 secs, then 72 °C for 90 secs, and final extension step at 72 °C for 10 mins. The cycling conditions for actin gene were: initial denaturation at 94 °C for 2 min, followed by 36 cycles of denaturation at 94 °C for 30 secs, annealing at 55 °C for 30 secs, then 72 °C for 90 secs, and final extension step at 72 °C for 10 mins. Negative control reaction was used to detect contamination in the samples.

The PCR amplicons were separated on 1.5% (w/v) agarose gels in 1x TAE buffer with electrophoresis conditions of 100 V, for 30 min and stained with ethidium bromide. The gels were visualized under UV in a Gel Doc™ EZ System (Biorad). The DNA Ladder 100-1000pb (Canvax™) was used as a molecular size marker.

V.2.3 Sequencing and phylogenetic analyses

All PCR products were purified before sequencing using the NucleoSpin® Plasmid kit (NoLid) (Machery-Nagel, Düren, Germany) according to the manufacturer instructions. The two strands of the PCR products were sequenced by Eurofins Genomics (Ebersbeg, Germany). For IGS sequences, internal primers were designed based on the initial sequences for further sequencing and assembly of the complete IGS regions (Table V.2).

Table V.2 Internal sequencing primers designed for IGS

Primer name	Sequence (5′->3′)	Direction
Ital_INT_R	5`- ATATAATGTCGCAGGGTC -3`	Reverse
Paras_INT_F	5`- TAGTCGGATCTATAGTTAG -3`	Forward
Scol_INT_F	5`- TGATATCCTTCGCGCTGG -3`	Forward
Croa_INT_ F	5`- GTAGCTGCTCTCGACTTT -3`	Forward
Oleae_INT_R	5`- GCCTCTTAGGTATCCTACCT -3`	Reverse
Minim_ INT_R1	5`- GCCTCTTAGGTATCATAC -3`	Reverse
Minim_INT_R2	5`- GGCTATATCCTTATCCTACC -3`	Reverse
Iran_INT _F	5`- GCAACCTGCTCTCGACTT-3`	Forward
Iran_INT_R	5`- GCACCTTAGGGTCTAACG -3`	Reverse
Hispan_INT_F	5`- GCTCTCGACCTTCTTCCA-3`	Forward
Hispan_INT_R	5`- GCTAGACCTACGCACTGA -3`	Reverse
Amygd_INT_F	5`- GCAACCTGCTCTCGACT-3`	Forward
Amygd_INT_R	5`- GACCCTAAGGTGCCACCTAT-3`	Reverse
Pleuro_INT_F	5`- TTTCACTTACCCTACACC -3`	Forward
Pleuro_INT_F	5`- CTGTGATACGATGCCGGA-3`	Forward

The complete sequences were assembled for each isolate into a contiguous (contig) sequences using BioEdit v7.2.6 (Hall, 1999). Sequence homology searches were performed with Basic Local Alignment Search Tool (BLAST 2.7.1+; Altschul *et al.,* 1997).

De novo generated sequences of the IGS, β-tubulin and Actin genes were aligned separately using ClustalX version 1.83 (Thompson *et al.,* 1997), visually inspected for alignment errors, then concatenated and aligned again to make it possible to perform multigenic analysis.

Maximum parsimony analyses were performed on the individual gene alignments, and on the concatenated alignment using PAUP version 4.0b10 (Swofford, 2003). Alignment gaps were treated as missing data for β-tubulin and Actin genes alignments, and were treated as fifth character for IGS individual and concatenated alignments. All of the characters were unordered and of equal weight. Maximum parsimony analyses were performed with PAUP version 4.0b10, using the heuristic search option with 100 random taxa additions and tree

bisection and reconstruction as the branch swapping algorithm. Branches of zero length were collapsed and all multiple, equally parsimonious trees were saved. Bootstrap support values were calculated from 100 heuristic search replicates and 10 random taxon additions. The trees length (TL), consistency index (CI), retention index (RI), homoplasy index (HI), and rescaled consistency index (RC) were calculated and the resulting trees were visualized with TreeView version. 2.0.8 (Page, 1996). *Pleurostoma richardsiae* was used as outgroup in all phylogenetic analyses. Submission of newly generated sequences to GenBank database (NCBI) is going on in order to obtain the accession numbers and trees in TreeBase (www.treebase.org).

V.2.4 Morphological characterization

Based on *Pm. italicum* IGS structure studied in Chapter III, and on phylogenetic analyses performed here, five isolates (Pm 31M, Pm 50M, Pm 45, Pm 17, and Pm 59) representatives of sub-groups B, C, D, E and F respectively, were examined afterward for morphological study. A list of these strains with host and origin information is given in Table V.1.

The *Phaeoacremonium* isolates were morphologically characterized on malt extract agar (MEA; 2% malt extract, Oxoid Ltd., UK; 2% agar, Difco, USA), on PDA, and on oatmeal agar (OA; 30 g oats; 8 g Oxoid agar; 1000 mL water), after 2–3 weeks of incubation at 23 ± 2 °C in the dark. Colony colours were evaluated using the color charts of Rayner (1970). Radial growth was measured after 8 and 16 days at 25 °C.

Slide cultures for micromorphologcial characterization were prepared following a similar protocol as Carlucci *et al.* (2012). Small agar blocks (about 2 mm^3) from actively growing fungal colonies were placed on sterile microscope slides in sterile Petri plates containing autoclaved discs of filter paper that has been moistened with sterile water. After 7–10 days of incubation at 25 °C in the dark, agar blocks were removed and sterile cover slips were placed on colonized parts of the microscope slides with 100 % lactic acid. Slides were pressed under stacks of books for hours, and sealed with nail polish.

Images of phialides (types I, II and III), conidiophores, collarettes, hyphal coils, bundles, and conidia were captured at (1000×) using a Leica DFC420 digital camera on a Leica DMR microscope fitted with Nomarski differential interference contrast optics. Thirty individual

structures of each type were viewed and measured using a Leica DM5500 measurement module (Leica Microsystems GmbH, Wetzlar, Germany).

V.3 Results

V.3.1 PCR amplification and sequencing of IGS region, β-tubulin and actin genes

The PCR amplification for all isolates using targeted IGS primers was successfully carried out. Agarose gel electrophoresis of the PCR products of *Phaeoacremonium* spp. and *Pleurostoma richardsiae* showed that IGS, amplified by the generic primers showed length polymorphism among the fungi tested, thereby indicating that IGS is more variable region in the 28S and 18S rRNA genes (Figure V.1).

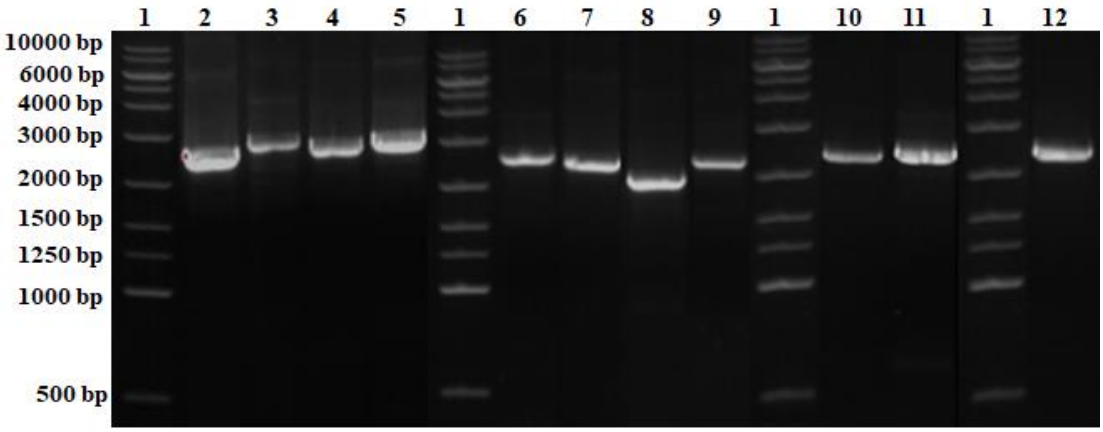

Figure V.1. Agarose gel electrophoresis of the IGS-PCR amplification products of *Phaeoacremonium* spp. and *Pleurostoma richardsiae*. Lane 1: 10-kb DNA ladder; Lane 2: *Pm. scolyti*; Lane 3: *Pm. parasiticum*; Lane 4: *Pm. italicum*; Lane 5: *Pm. sicilianum*; Lane 6: *Pm. iranianum*; Lane 7: *Pm. minimum*; Lane 8: *Pm. oleae*; Lane 9: *Pm. croatiense;* Lane 10: *Pm. hispanicum*; Lane 11: *Pm. amygdalinum;* Lane 12: *Pl. richardsiae.*

The amplified IGS fragments consisted of a partial region of LSU-rRNA gene followed by complete sequences of IGS and a partial region of SSU-rRNA gene with fragments size ranging from 2163 to 2314 bp nucleotides long. Substantial full-length sequences of the IGS gene was obtained for the isolates of *Phaeoacremonium* spp. and *Pleurostoma richardsiae.*

Similarly, β-tubulin and Actin genes were amplified for all isolates, with the expected fragments size of about 700 bp and 300 bp respectively, using the T1-Bt2b and ACT512F-

ACT783R primer sets (Figures not shown). Full-length sequences of the TUB and actin genes were obtained.

V.3.2 Phylogenetic analyses

Five dendrograms were constructed based on the β-tubulin gene, actin gene, combined TUB2-ACT, IGS region and combined IGS- TUB2-ACT. Individual and combined maximum parsimony (MP) analyses yielded trees, which were topologically congruent in terms of species groupings (Figures V.2, V.3, V.4, V.5 and V.7). *Phaeoacremonium* isolates obtained during the field survey in Salento (see Table. V.1) clustered with previously published species. Within clade I, twenty isolates of *Pm. italicum* recovered from the field clustered with the type strain of *Pm. italicum* (CBS 137763). Similarly, six isolates of *Pm. scolyti* and seven of *Pm. minimum* clustered in Clades II and III respectively, with reference species, thus, ascertaining the identity of our field isolates.

The actin (ACT) maximum parsimony (MP) analysis was conducted using 58 isolates, from which two sequences were retrieved from GenBank. The dataset consisted of 58 taxa, including the outgroup taxa (*Pleurostoma richardsiae*). After alignment, the final dataset consisted of 266 characters with gaps treated as missing, of which 135 were constant and 13 were variable and parsimony uninformative. Maximum parsimony analysis of the remaining 118 parsimony-informative characters yielded eight most-parsimonious trees with the same overall topology differing mainly in the order of the taxa at the terminal nodes (TL = 297; CI = 0.717; RI = 0.938; RC = 0.673; HI = 0.283) (TreeBASE---). The actin phylogenetic tree shown below indicates that all *Pm. italicum* isolates clustered together in one clade, named here clade I, with high support (100% bootstrap value) without distinction among isolates. Similarly, *Pm. scolyti* and *Pm. minimum* isolates clustered together into clades II and III respectively (100% bootstrap support) (Figure V.2).

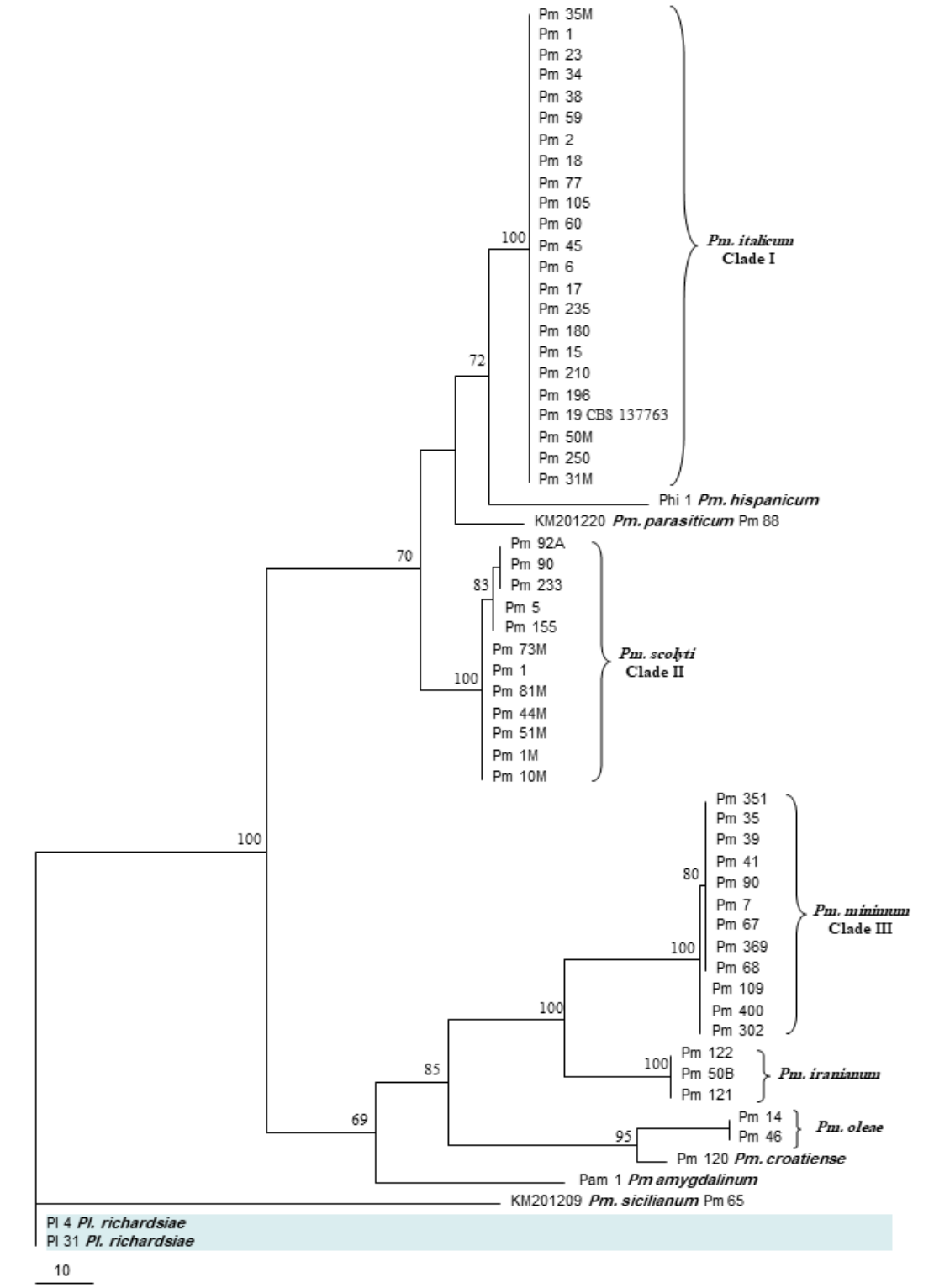

Figure V.2 One of the eight parsimonious trees obtained from actin sequence data with bootstrap support values from Maximum Parsimony. Gaps were treated as missing data. Number of each node indicates bootstrap value. *Pleurostoma richardsiae* was included as outgroup.

The β-tubulin maximum parsimony (MP) analysis included 58 isolates, from which two sequences were retrieved from GenBank, including the outgroup taxa (*Pleurostoma richardsiae*). After alignment, the final dataset consisted of 586 characters excluding the gaps, of which 280 were constant and 56 were variable and parsimony uninformative. Maximum parsimony analysis of the remaining 250 parsimony-informative characters yielded one parsimonious tree (TL = 668; CI = 0.714; RI = 0.935; RC = 0.668; HI = 0.286) (TreeBASE--). The β-tubulin phylogenetic tree shows that *Pm. italicum* isolates sort out three sub-clades (1), (2) and (3), although supported by low bootstrap values (60% and 76%) and short branch lengths. Similarly, *Pm. scolyti* isolates sort out two sub-clades (A) and (B) with 70% and 100% bootstrap values respectively, while *Pm. minimum* isolates were grouped all in one clade III (Figure V.3).

The combined TUB2-ACT phylogenetic sequence dataset comprised 58 taxa, including the outgroup taxon (*Pleurostoma richardsiae*). After alignment and exclusion of incomplete portions at either end, the dataset consisted of 855 characters excluding the gaps. Of these characters, 417 were constant, while 71 were variable and parsimony uninformative. Maximum parsimony analysis of the remaining 367 parsimony-informative characters resulted in ten most-parsimonious trees (TL = 979; CI = 0.708; RI = 0.935; RC = 0.662; HI = 0.292) (TreeBASE-). The maximum parsimony analysis of the combined TUB2-ACT genes yielded a tree that is topologically similar to the individual β-tubulin tree, in terms of isolates groupings (refer to Figures V.3 and V.4), although it suggested changes in the placement of sub-clades (A) and (B) within *Pm. scolyti* group (Figure V.4, Clade II).

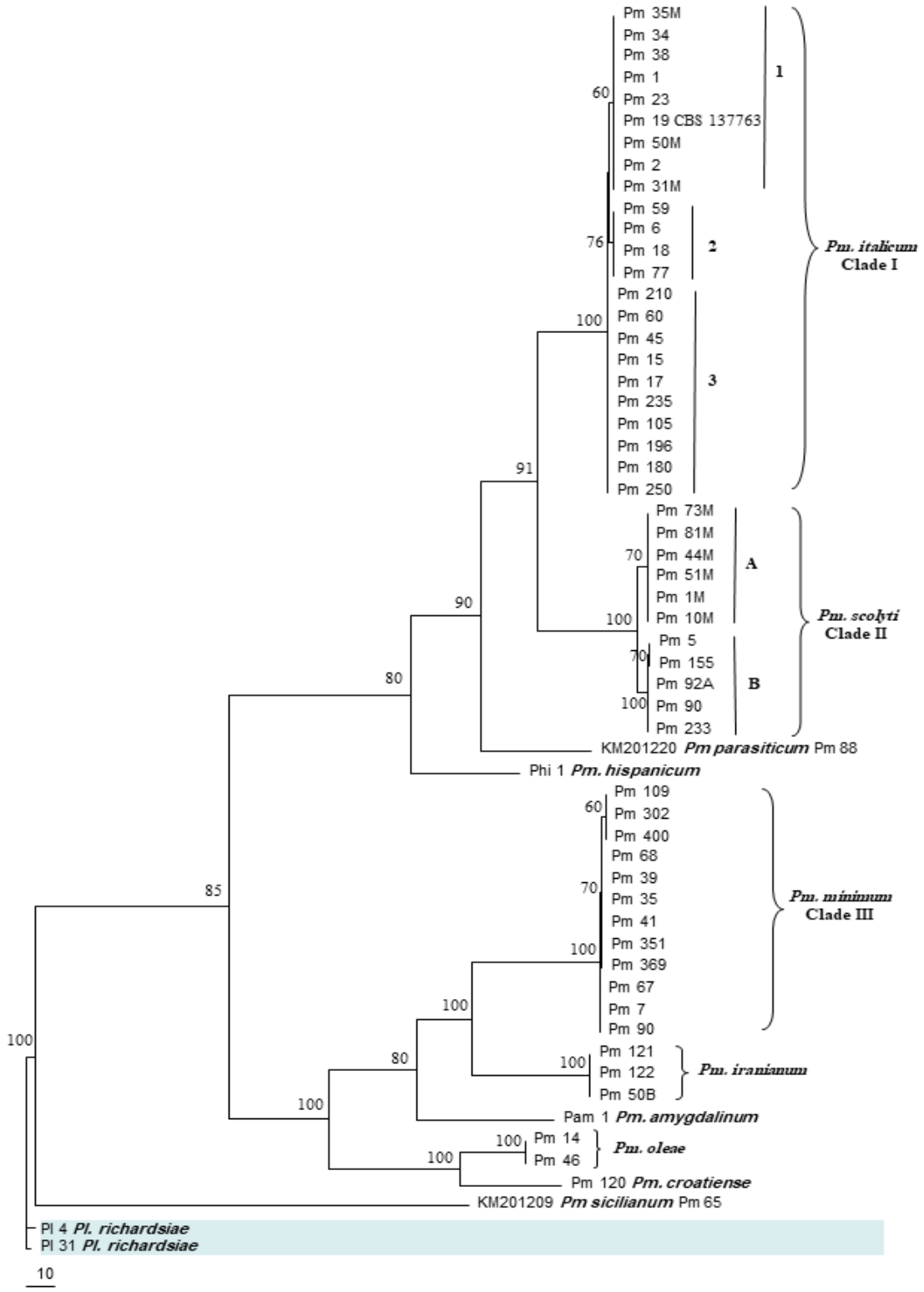

Figure V.3 Parsimonious tree obtained from β-tubulin sequence data with bootstrap support values from Maximum Parsimony. Gaps are treated as missing data. Number of each node indicates bootstrap value. *Pleurostoma richardsiae* was included as outgroup.

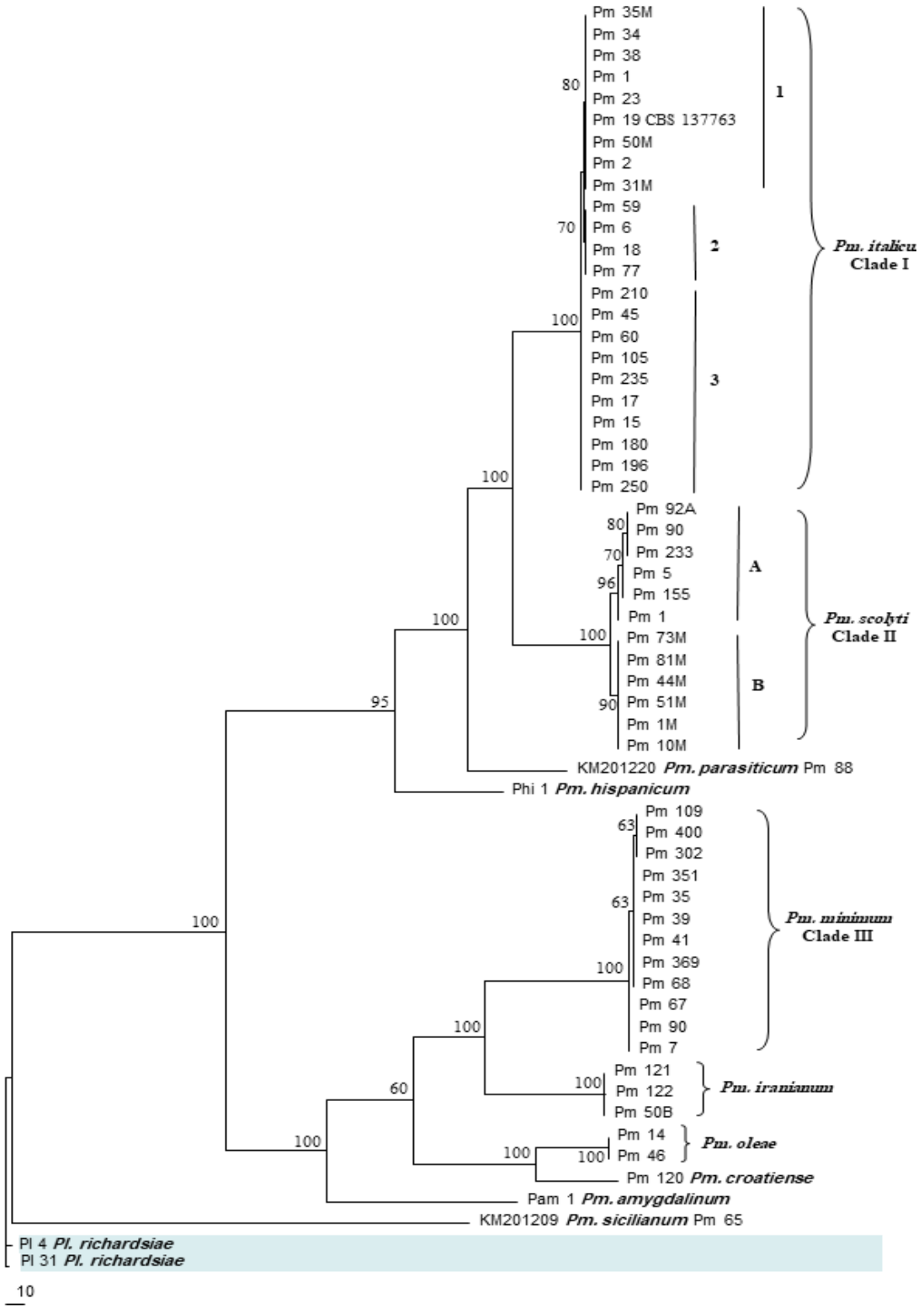

Figure V.4 One of the ten parsimonious trees obtained from combined TUB2-ACT sequence data with bootstrap support values from Maximum Parsimony. Gaps are treated as missing data. Number of each node indicates bootstrap value. *Pleurostoma richardsiae* was included as outgroup.

The IGS maximum parsimony (MP) analysis comprised 58 taxa, which included the outgroup taxon *Pleurostoma richarsiae*. The dataset consisted of 3711 characters (including alignment gaps). Of these characters, 628 were constant, while 328 were variable and parsimony uninformative. Maximum parsimony analysis of the remaining 2755 parsimony-informative characters resulted in four most-parsimonious trees (TL = 7825; CI = 0.692; RI = 0.925; RC = 0.640; HI = 0.308) (TreeBASE---).

In the IGS phylogenetic tree, *Pm. italicum* forms a well-supported two major independent clades (100% bootstrap). The latter consisting of isolates from the clade I.a and clade I.b (Figure V.5). Clade (I.a) was further subdivided into three subclades, one of them encompassing isolates containing the ex-type strain which has been designated the sensu stricto (1) subclade, distinctly from Pm 45, Pm 105 and Pm 60 (grouped in the subclade 2) and from Pm 15, Pm 17, Pm 180, Pm 196, Pm 210, Pm 235 and Pm 250 (grouped in the subclade 3), while clade (I.b) includes separately isolates Pm 59, Pm 6, Pm 18 and Pm 77 (grouped in the subclade 4). Similarly, *Pm. scolyti* isolates clustered into four subclades (II.a), (II.b), (II.c) and (II.d) with 100 % bootstrap support. *Pm. minimum* isolates clustered in their subclades namely, (III.a), (III.b) and (III.c) with high bootstrap support (Figure V.5).

Considering *Pm. italicum*, the IGS phylogeny obtained from IGS region sequences was generally consistent with the fungus IGS structure studied in Chapter III. Two main intraspecific clades were distinguished (clades I.a and I.b) with excellent phylogenetic support (100 % bootstrap. Clade (I.a) was subdivided into three subclades, one of them (subclade 1 containing the ex-type isolate), in addition to subclades (2) and (3), clustering all *Pm. italicum* isolates (of representative subgroups A, B, C, D and E, refer to IGS structure in Figure V.6). However, clade (I.b) clustered distinctly isolates of subgroup F (grouped in the subclade 4). This distinction was supported by their IGS polymorphic region structure (see subgroup F in Figure V.6).

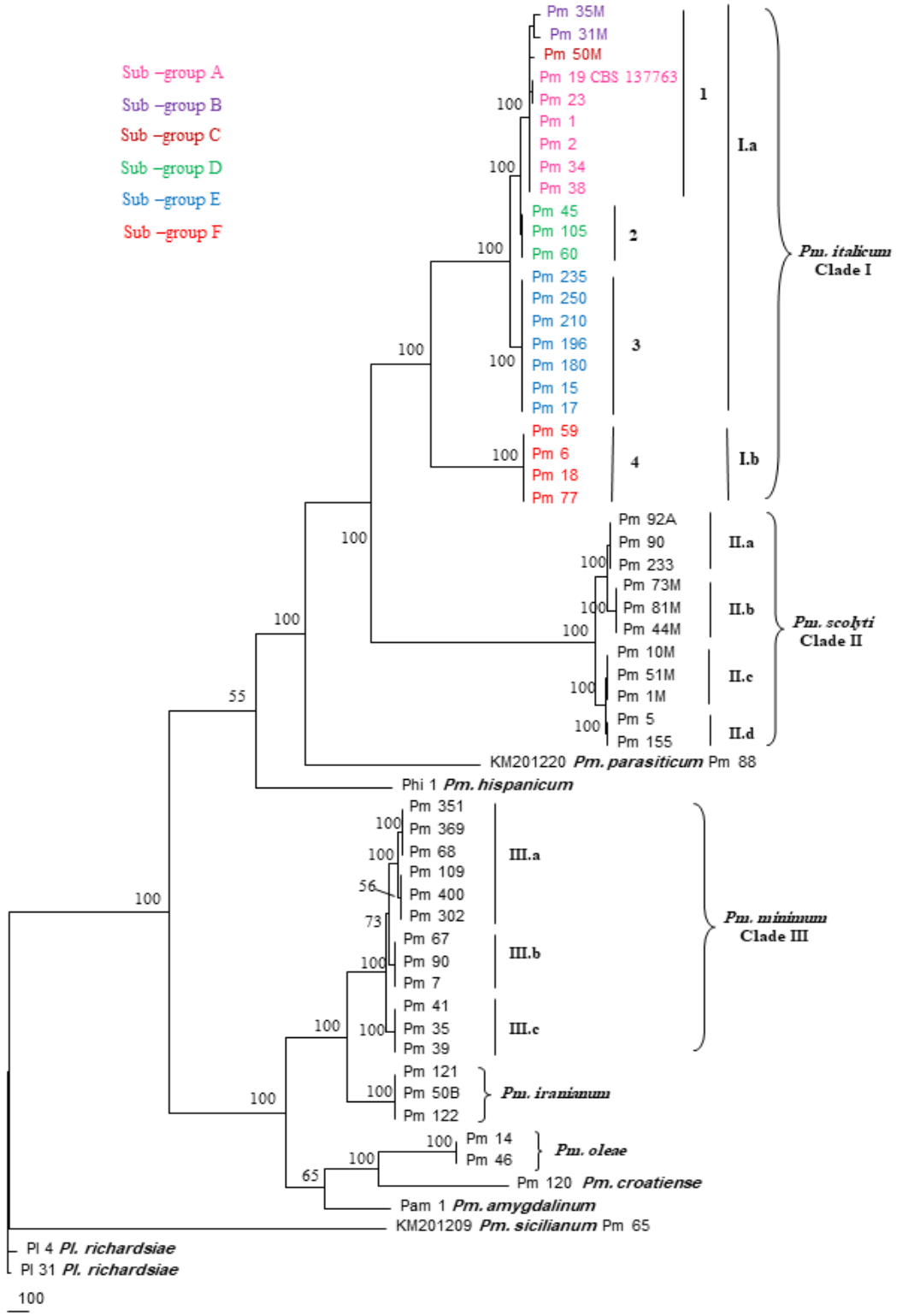

Figure V.5 One of the four parsimonious trees obtained from IGS sequence data with bootstrap support values from Maximum Parsimony. Gaps are treated as a fifth character. Number of each node indicates bootstrap value. *Pleurostoma richardsiae* was included as outgroup.

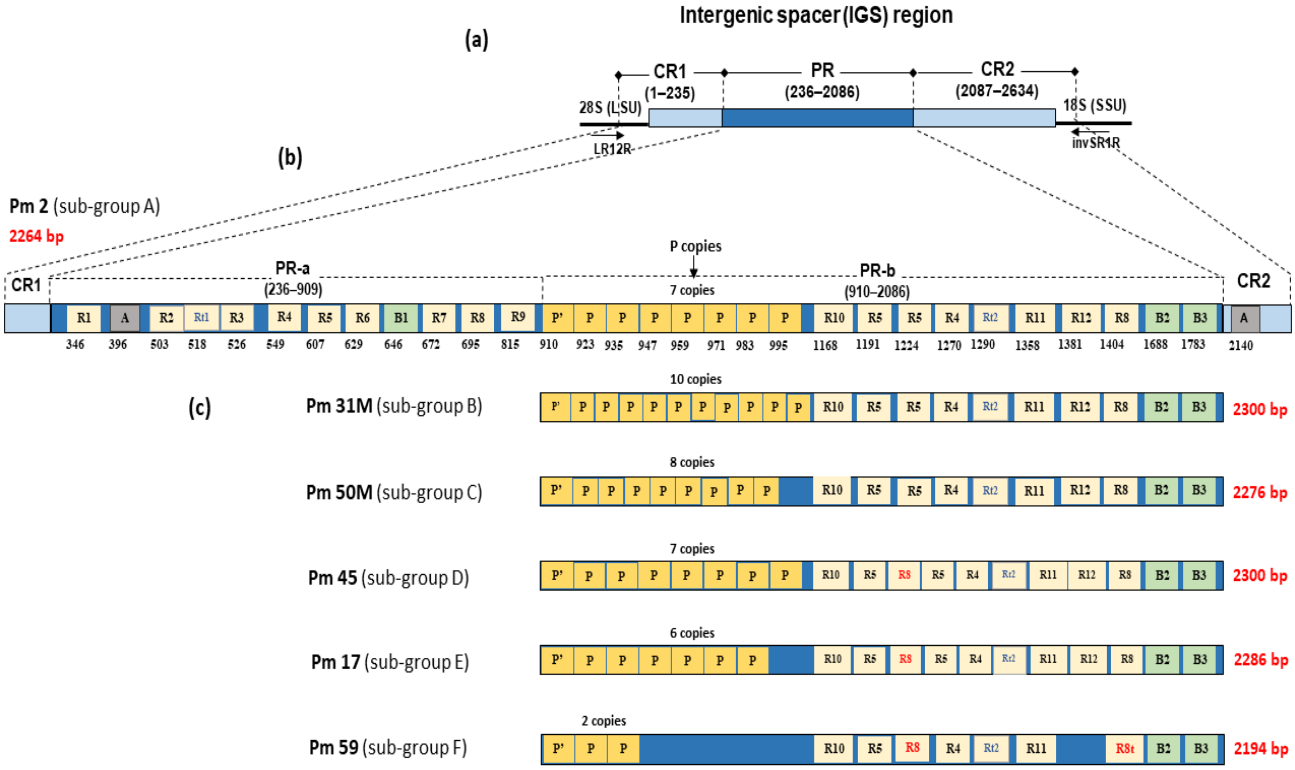

Figure V.6. Structural organization of the nuclear rDNA IGS region in *Pm. italicum* representative isolates.

The combined IGS-TUB2-ACT phylogenetic sequence dataset comprised 58 taxa, including the outgroup taxon (*Pleurostoma richarsiae*). The final dataset consisted of 4289 characters (including alignment gaps). Of these characters, 1020 were constant, while 463 were variable and parsimony uninformative. Maximum parsimony analysis of the remaining 2806 parsimony-informative characters resulted in two most-parsimonious trees (TL = 8452; CI = 0.689; RI = 0.923; RC = 0636; HI = 0.311) (TreeBASE---).

The maximum parsimony analysis of the combined IGS-TUB2-ACT regions yielded a phylogeny with high bootstrap support (from 80 % to 100 % bootstraps) for all species-level clades (Figure V.7), as well, a tree that is topologically similar to the individual IGS phylogeny, in terms of species groupings (refer to Figures V.5 and V.7). The combined MP phylogeny produced here, resolved identical sub-clades within *Pm. italicum*, *Pm. scolyti*, and *Pm. minimum*, comparing with the individual IGS phylogeny, and well supported by high bootstrap values (Figures V.5 and V.7).

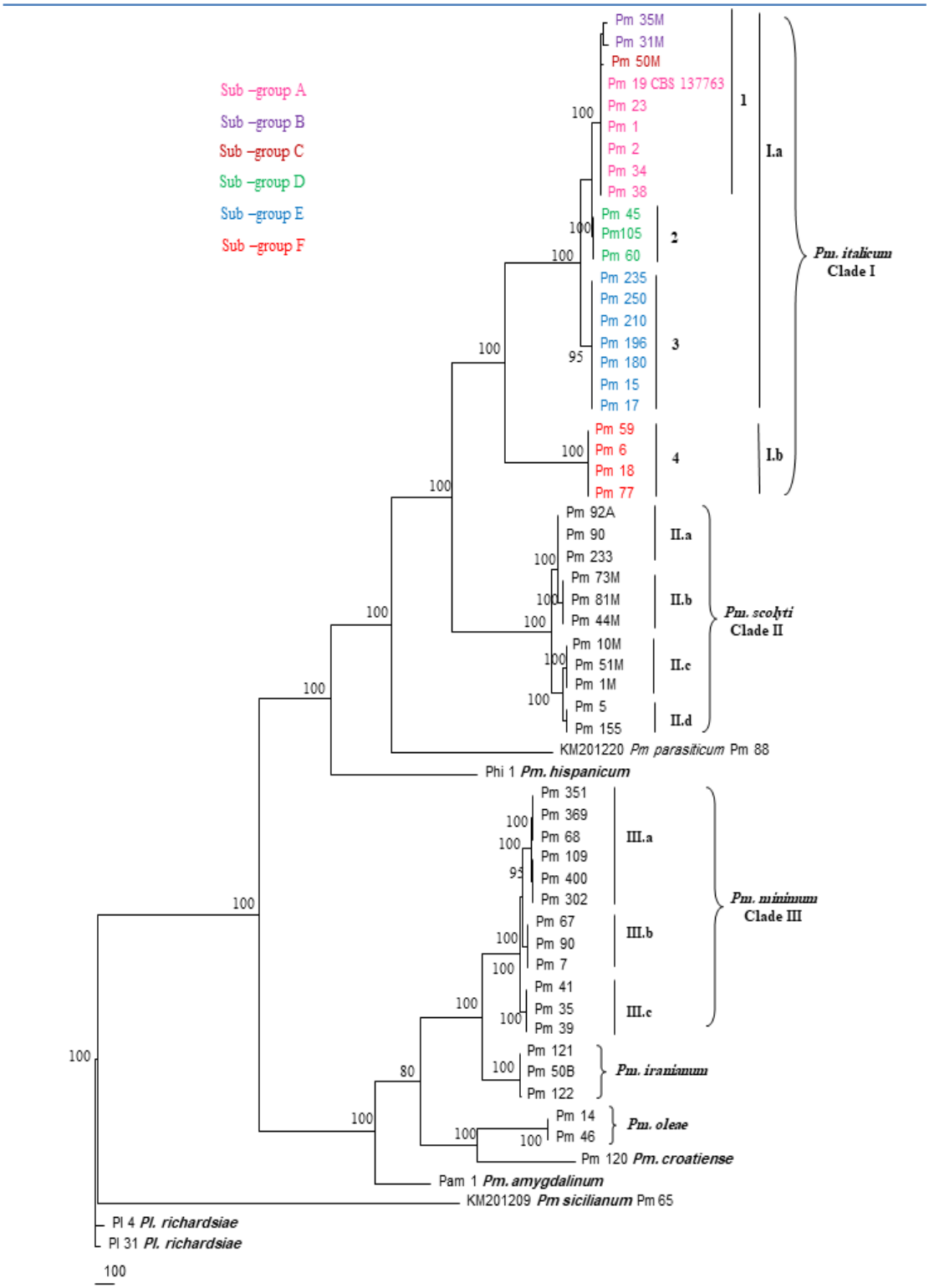

Figure V.7 One of the two parsimonious trees obtained from combined IGS-TUB2-ACT sequence data with bootstrap support values from Maximum Parsimony. Gaps are treated as a fifth character. Number of each node indicates bootstrap value. *Pleurostoma richardsiae* was included as outgroup

V.3.3 Morphological Characterization

Morphological and cultural characteristics of the representative isolates of sub-groups (B, C, D, E and F) illustrated previously in Chapter III, are explained as follows:

Sub-group B; Figure V.8

Material examined: Isolate Pm 31M; Italy, Foggia, San Giovanni Rotondo, from internal necrotic wood of almond (*Prunus dulcis*).

Colony morphology — Colonies reaching a radius of 14–20 mm in 8 d and 29–37 mm in 16 d at 25 °C. Colonies on MEA vinaceous buff to fawn aerial mycelia spread on the entire colony, with entire edge; after 16 d light Vinaceous-Buff (15'"d) to white at margin and Umber (13m) to Fawn (13'") at the center. Colonies on PDA flat, with white aerial mycelia in the center, entire edge; after 16 d Vinaceous-Buff (17 '"d) at margin to Bay (5k) becoming Fawn (13'") at the center. Colonies on OA vinaceous buff to fawn aerial mycelia spread on the entire colony, with entire edge; after 16 d Vinaceous-Buff (17'"d) to Vinaceous purple (65'"b) with Brown-Vinaceous (5'"m) at the center. No yellow pigment production was observed.

Slide culture micromorphology — Mycelia septate, hyaline to pale brown, smooth to verruculose, 0.8–1.2 µm wide, that occur singly or in bundles of up to 4 strands. Conidiophores mostly short and unbranched, short conidiophores with up to 2 septa, the long ones with up to 4 septa, ending in a single terminal phialide, and sometimes two terminal phialides, (11.8–) 16–21 (–38.4) (av. 18.5) µm long and (0.3) 1.2–1.4 (–1.8) (av. 1.3) µm wide; conidiophores sometimes bearing next to the terminal phialide 1 to 2-3 lateral ones but mostly one lateral phialide, (1.4–) 19.2–27.5 (–52.6) (av. 23.3) µm long and (0.9) 1.3–1.6 (–2.5) (av. 1.5) µm wide; hyaline to pale brown; smooth to verruculose; percurrent rejuvenation observed. Branched conidiophores are frequent, (16.1–) 25.9–32.1 (–47.3) × (1.0–) 1.3–1.5 (–1.9) (av. 29 × 1.4) µm. Hyphal coils observed. Phialides terminal or lateral, mostly monophialidic, predominantly type II, smooth to verruculose, hyaline to pale brown; collarettes 0.1–1.2 µm long, 0.2–1.3 µm wide, polyphialides rarely observed; Type I phialides subcylindrical to elongate-ampulliform and attenuated at the base, rarely widened at the base, sometimes long, (1.6–) 3.7–4.9 (–7.9) × (0.5) 0.9–1.0 (–1.4) (av. 4.3 × 0.9) µm; type II phialides elongate ampulliform and attenuated at the

base, sometimes navicular, elongate-ampulliform and constricted at the base or subcylindrical, (6.0–) 7.9–9.0 (–11.1) × (0.3–) 1.2–1.4 (–1.7) (av. 8.4 × 1.3) µm; type III subcylindrical to elongate-ampulliform and attenuated at the base, (7.5–) 9.4–10.6 (–13.7) × (0.7–) 1.0–1.1 (–1.4) (av. 10 × 1.1) µm. Conidia oblong-ellipsoidal, sometimes allantoid, (1.5–) 2.1–2.6 (–4.3) × (0.6–) 0.9–1.1 (–1.5) (av. 2.4 × 1.0) µm.

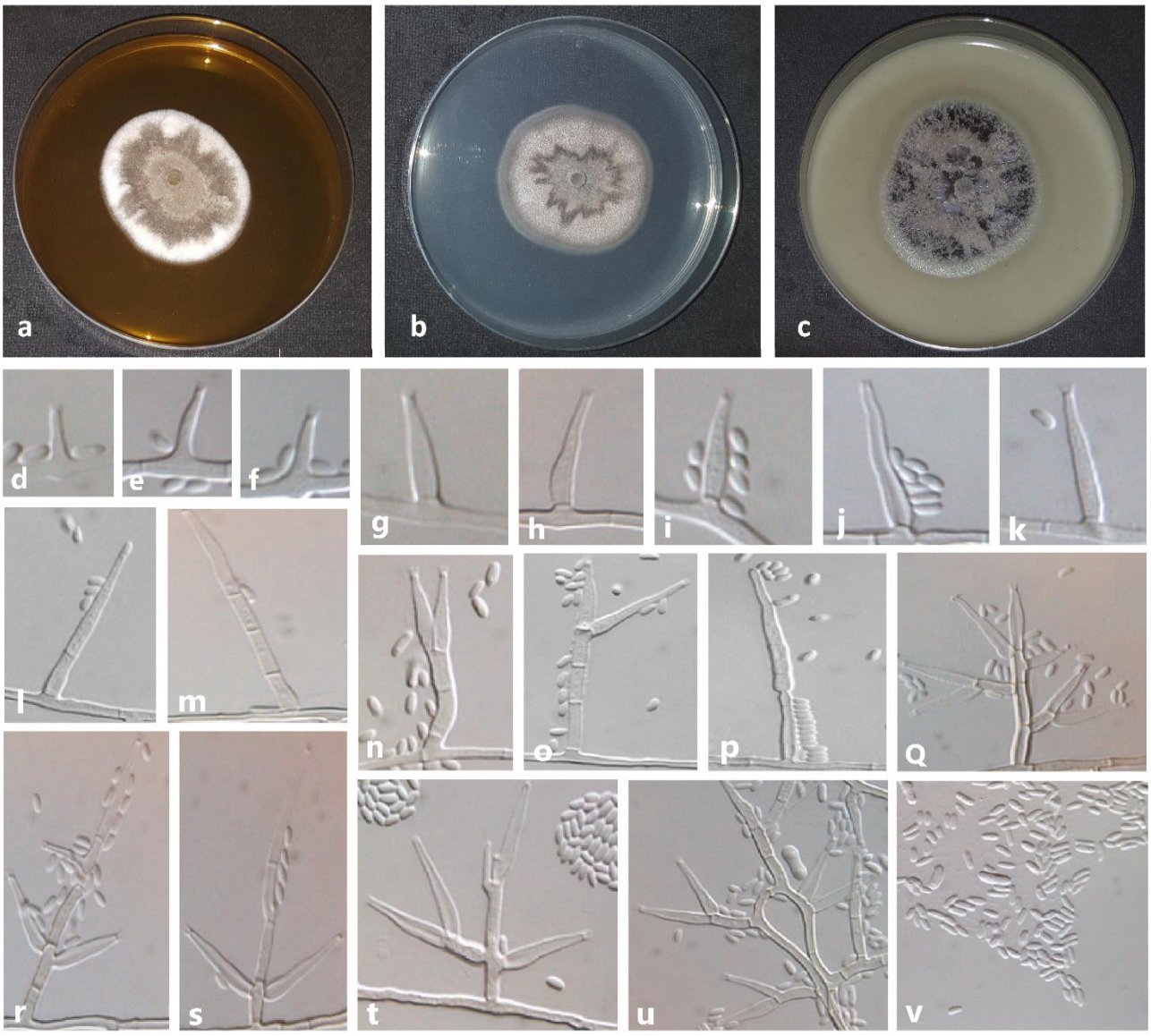

Figure V.8 *Phaeoacremonium* isolate Pm 31M. a-c. Sixteen-day-old colonies incubated at 25 °C on MEA (a), PDA (b) and OA (c); d-f. type I phialides; g-i. type II phialides; j-k. type III phialides; l-o. unbranched conidiophores with one or two terminal phialides or lateral one; p. conidiophore showing percurrent rejuvenation; q-t. branched conidiophores; u. hyphal coils with unbranched or branched conidiophores; v. Conidia. Scale bar: d = 10 µm.

Sub-group C; Figure V.9

Material examined: Isolate Pm 50M; Italy, Apulia, Salento, from internal wood necrosis of olive (*Olea europaea*).

Colony morphology — Colonies reaching a radius of 13–18 mm in 8 d and 29–39 mm in 16 d at 25 °C. Colonies on MEA felty-like mycelia, with entire edge; after 16 d Cream-Buff (19"d) at margin to light Hazel (17'"i) becoming Vinaceous-Buff (17'"d) at the center. Colonies on PDA felty-like grey aerial mycelia, with entire edge; after 16 d Cream-Buff (19"d) at margin to Livid Vinaceous (1'") with Hazel to Fawn (13'") at the center. Colonies on OA with aerial mycelia, entire edge; after 16 d Cream-Buff (19"d) becoming chestnut (7'm) towards the center. No yellow pigment production was observed.

Slide culture micromorphology —Mycelia septate, hyaline to pale brown, smooth to verruculose, 0.7–1.3 µm wide. Conidiophores mostly short and unbranched, short conidiophores with up to 2 septa, the long ones with up to 4 septa, ending in a single terminal phialide, (10–) 14.9–18.8 (–35.4) (av. 16.9) µm long and (1.0) 1.2–1.3 (–1.6) (av. 1.2) µm wide; frequently bearing next to the terminal phialide a lateral one, (1.3–) 19–26.9 (–48.9) (av. 22.9) µm long and (1.0) 1.2–1.3 (–1.7) (av. 1.3) µm wide; hyaline to pale brown; smooth to verruculose; percurrent rejuvenation observed. Branched conidiophores are less frequent, (14.5–) 25.1–32.2 (–48.1) × (0.8–) 1.2–1.3 (–1.5) (av. 28.7 × 1.3) µm. Hyphal coils commonly observed. Phialides terminal or lateral, mostly monophialidic, predominantly type II, smooth to verruculose, hyaline to pale brown; collarettes 0.1–1.2 µm long, 0.4–0.9 µm wide, polyphialides occasionally observed; Type I phialides subcylindrical, occasionally widened at the base, (2.1–) 4.1–5.0 (–7.1) × (0.6–) 0.8–0.9 (–1.2) (av. 4.6 × 0.9) µm; type II phialides elongate-ampulliform and attenuated at the base, sometimes navicular or subulate, (2.9–) 7.4–8.8 (–13.7) × (0.6–) 1.1–1.2 (–1.4) (av. 8.1 × 1.2) µm; type III elongate-ampulliform and attenuated at the base, sometimes subulate or subcylindrical, (8.8–) 10.8–11.9 (–14.1) × (0.8–) 1.1–1.2 (–1.4) (av. 11.4 × 1.1) µm. Conidia oblong, reniform, sometimes allantoid, bigutulate, (2.0–) 2.5–2.7 (–3.5) × (0.6–) 0.8–0.9 (–1.1) (av. 2.6 × 0.9) µm.

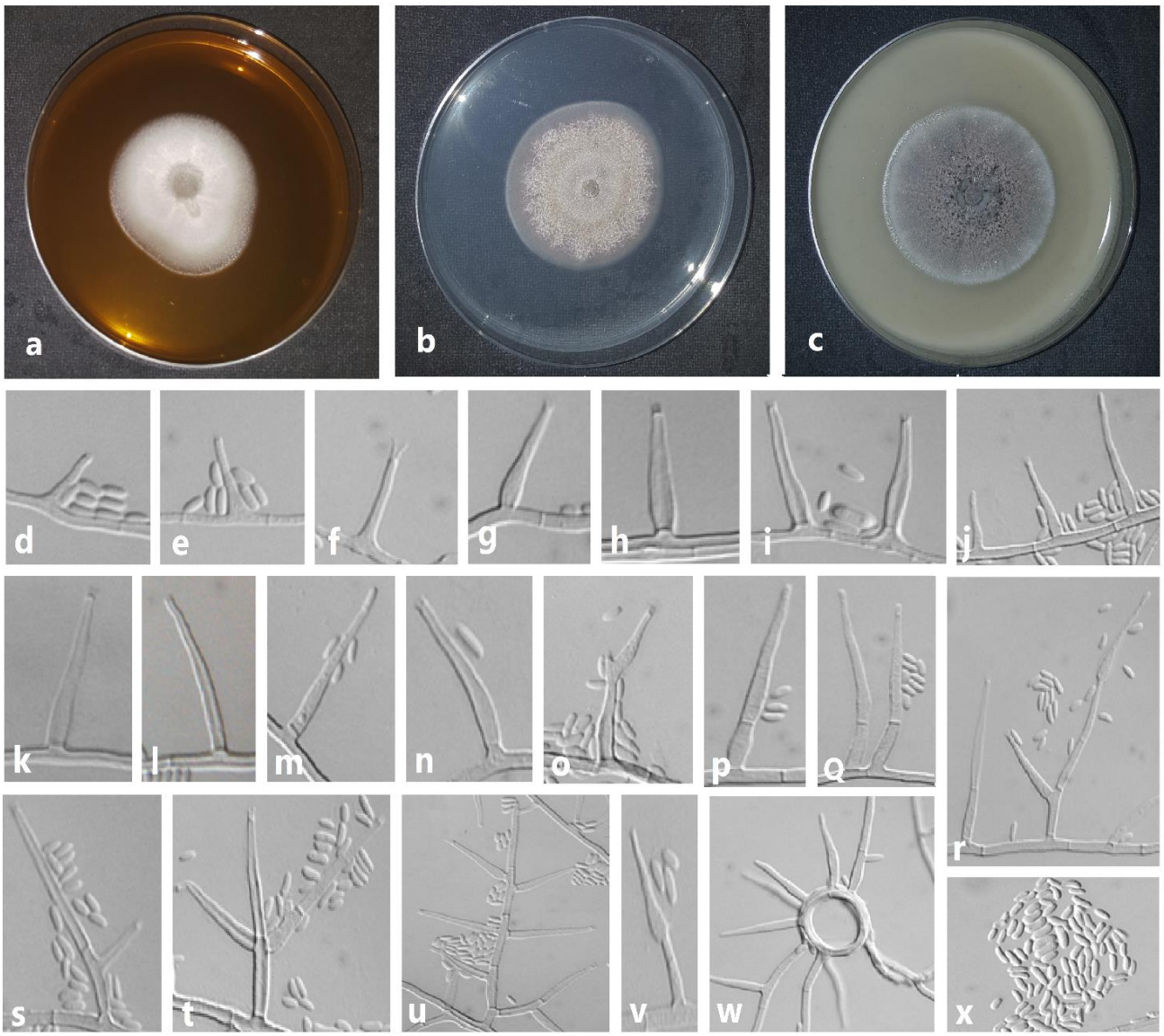

Figure V.9 *Phaeoacremonium* isolate Pm 50M. a-c. Sixteen-day-old colonies incubated at 25 °C on MEA (a), PDA (b) and OA (c); d-f. type I phialides; g-i. type II phialides; j. phialides type I, II and III; k-n. type III phialides; o. conidiophore with polyphialide; p-s. unbranched conidiophores with terminal or lateral phialide; t-u. branched conidiophores; v. conidiophore showing percurrent rejuvenation; w. hyphal coils with conidiophores and phialides; x. Conidia. Scale bar: d = 10 µm.

Sub-group D; Figure V.10

Material examined: Isolate Pm 45; Italy, Apulia, Salento, from internal wood necrosis of olive (*Olea europaea*).

Colony morphology — Colonies reaching a radius of 15–18 mm in 8 d and 31–40 mm in 16 d at 25 °C. Colonies on MEA felty mycelia, with entire edge; after 16 d Vinaceous Buff (17'"d) at margin to Fawn (13'") with Fawn and areas of Dark Brick (7"k) at the center. Colonies on PDA felt-like, with white mycelia covering the center of colony, entire edge; after 16 d Cream-Buff (19"d) at margin to Livid Vinaceous (1'") becoming Dark Vinaceous (71"k) toward the center and Vinaceous-Buff (17'"d) at the center. Colonies on OA flat, with fluffy aerial mycelia at the center, entire edge; after 16 d Buff (19") above and reverse with Dark Purple (65m) at the center. Yellow pigment production on OA.

Slide culture micromorphology — Mycelia septate, hyaline to pale brown, smooth to verruculose, 0.8–1.5 µm wide, that occur singly or in bundles of up to 6 strands. Conidiophores mostly short and unbranched, short conidiophores with up to 2 septa, the long ones with up to 5 septa, ending in a single terminal phialide, (10.3–) 14.1–17.4 (–28.9) (av. 15.8) µm long and (0.8) 1.2–1.3 (–1.6) (av. 1.3) µm wide; frequently bearing next to the terminal phialide a lateral one, and occasionally 2-3 lateral ones, (12.1–) 18.6–21.9 (–31.2) (av. 20.3) µm long and (0.8) 1.1–1.3 (–1.6) (av. 1.2) µm wide; hyaline to pale brown; smooth to verruculose; percurrent rejuvenation commonly observed. Branched conidiophores are occasionally observed, (12.6–) 21.8–28.4 (–47.8) × (0.8–) 1.2–1.3 (–1.7) (av. 25.1 × 1.2) µm. Hyphal coils occasionally observed. Phialides terminal or lateral, mostly monophialidic, predominantly type II, smooth to verruculose, hyaline to pale brown; collarettes 0.2–1.4 µm long, 0.1–1.0 µm wide, polyphialides sometimes observed; Type I phialides short, subcylindrical to navicular, sometimes long, subcylindrical and widened at the base, (1.1–) 2.7–3.6 (–5.7) × (0.3–) 0.7–1.0 (–1.7) (av. 0.9 × 3.2) µm; type II phialides elongate-ampulliform and attenuated at the base, sometimes subcylindrical or navicular, (4.2) 6.0–7.2 (–11.3) × (0.1–) 1.2–1.5 (–2.5) (av. 6.6 × 1.4) µm; type III subcylindrical, (5.2–) 7.1–8.3 (–10.4) × (0.6–) 1.0–1.2 (–1.7) (av. 7.7 × 1.1) µm. Conidia oblong-ellipsoidal, sometimes allantoid, (1.4–) 2.4–2.9 (–4.3) × (0.7–) 0.9–1.1 (–1.5) (av. 2.7 × 1.0) µm.

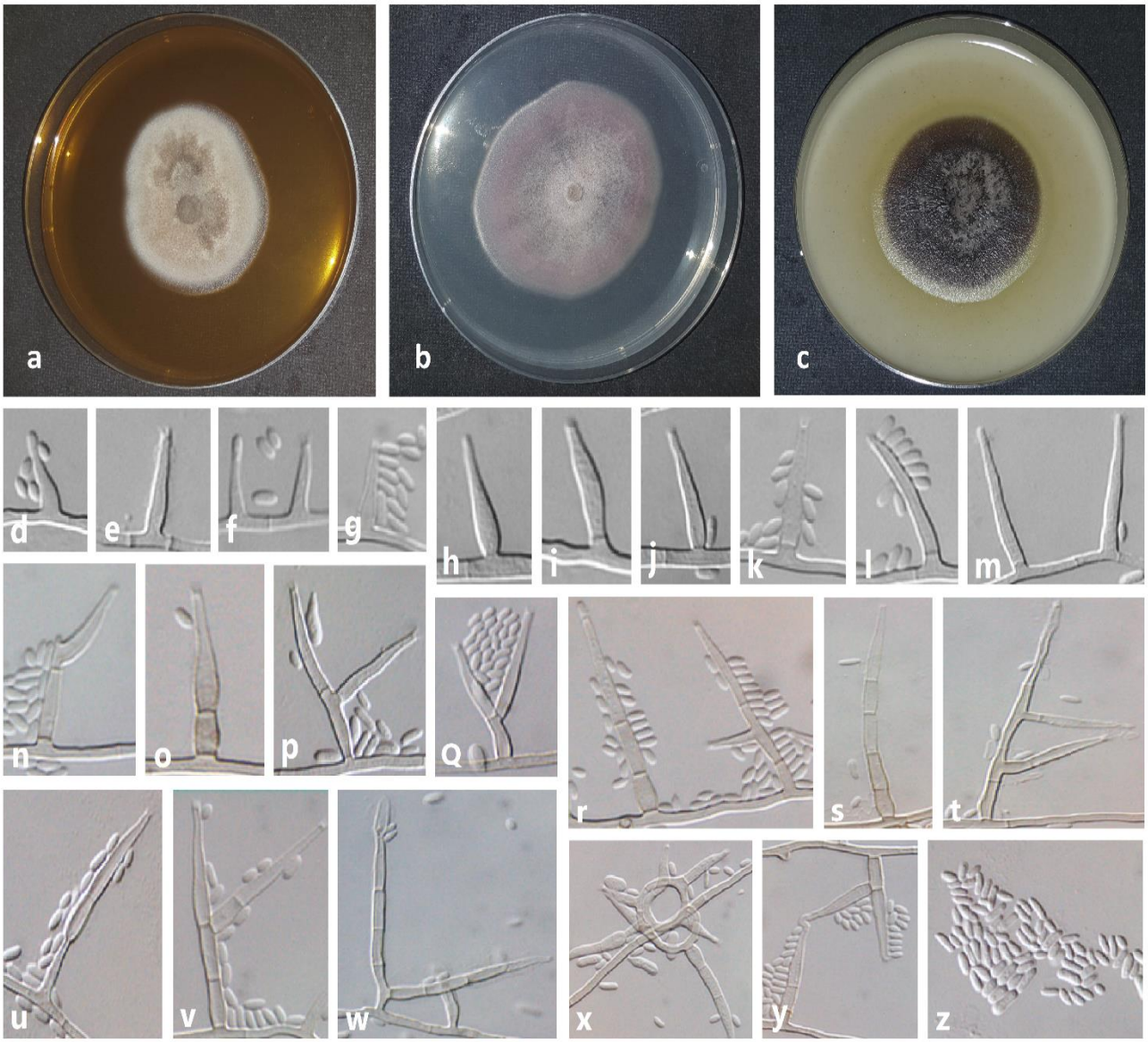

Figure V.10 *Phaeoacremonium* isolate Pm 45. a-c. Sixteen-day-old colonies incubated at 25 °C on MEA (a), PDA (b) and OA (c); d-g. type I phialides; h-k. type II phialides; l.m type III phialides; n. conidiophore with polyphialide; o-t. unbranched conidiophores with terminal or lateral phialide; u. conidiophore showing percurrent rejuvenation; v-w. branched conidiophores; x. hyphal coils with phialides and conidiophores; y. short unbranched conidiophores showing terminal and lateral vegetative proliferation. z. Conidia. Scale bar: d = 10 μm.

Sub-group E; Figure V.11

Material examined: Isolate Pm 17; Italy, Apulia, Salento, from internal wood necrosis of olive (*Olea europaea*).

Colony morphology — Colonies reaching a radius of 16–21 mm in 8 d and 32–42 mm in 16 d in the dark at 25 °C. Colonies on MEA flat, felt-like in the center, with entire edge; after 16 d Vinaceous-Buff (17 '"d) to Fawn (13'") in the center. Colonies on PDA flat, felt-like, with entire edge; after 16 d Hazel ring (17'"i) at margin to Vinaceous-Buff (17'"d) becoming Livid Vinaceous (1'") to Livid purple (71") in the center. Colonies on OA flat with aerial mycelia in the center, entire edge; after 16 d Buff (19") at margin to Sepia ring (13") with Buff ring (19") to Sepia (13") in the center. Yellow pigment production on OA.

Slide culture micromorphology — Mycelia septate, hyaline to pale brown, smooth to verruculose, 0.8–1.2 µm wide. Conidiophores mostly short and unbranched, short conidiophores with up to 3 septa, the long ones with up to 7 septa, usually ending in a solitary terminal phialide, rarely bearing next to the terminal phialide one or two lateral phialides; hyaline to pale brown; smooth to verruculose; percurrent rejuvenation occasionally occurring; (8.6–) 14.4–21.1 (–43.7) (av. 17.8) µm long and (1.0) 1.3–1.4 (–1.7) (av. 1.4) µm wide. Branched conidiophores (11.6–) 20.4–27.5 (–47.8) × (0.9–) 1.1–1.3 (–1.7) (av. 24 × 1.2) µm. Hyphal coils observed. Phialides terminal or lateral, mostly monophialidic, predominantly type II, smooth to verruculose, hyaline to pale brown; collarettes 0.3–1.2 µm long, 0.2–0.9 µm wide, polyphialides occasionally observed; Type I phialides subcylindrical often widened at the base, (1.6–) 3.3–4.2 (–6.5) × (0.6–) 0.9–1.0 (–1.4) (av. 3.7 × 0.9) µm; type II phialides navicular to elongate-ampulliform and attenuated at the base, (4.3–) 6.3–7.2 (–9.4) × (0.7–) 1.2–1.4 (–1.8) (av. 6.7 × 1.3) µm; type III subcylindrical to elongate-ampulliform and attenuated at the base, (6.6–) 9.0–11.9 (–28.5) × (0.7–) 1.0–1.2 (–1.6) (av. 10.5 × 1.1) µm. Conidia small, allantoid or oblong-ellipsoidal, gutulate, (1.4–) 1.8–2.1 (–2.9) × (0.6–) 0.7–0.8 (–1.0) (av. 1.9 × 0.8) µm.

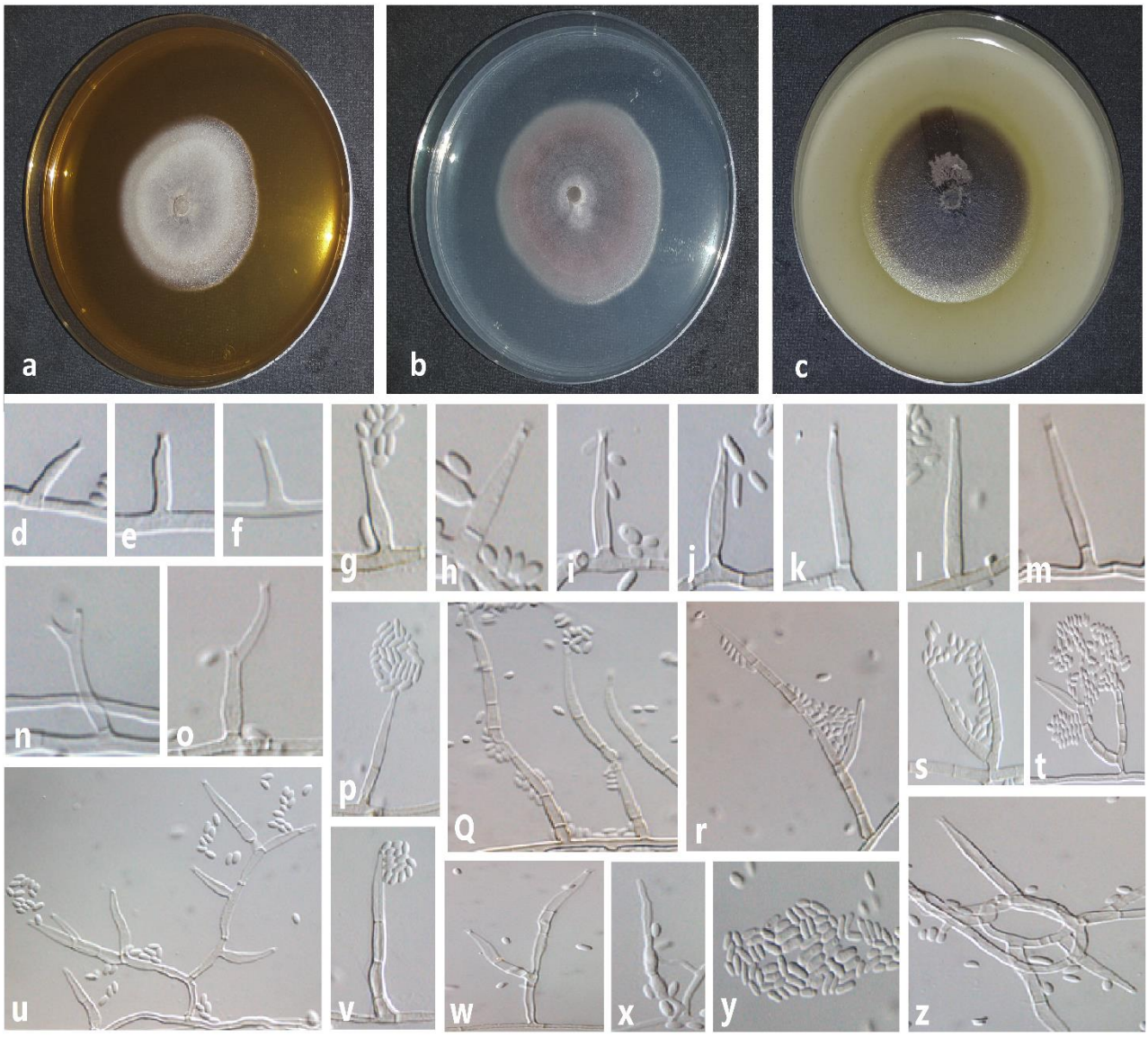

Figure V.11 *Phaeoacremonium* isolate Pm 17. a-c. Sixteen-day-old colonies incubated at 25 °C on MEA (a), PDA (b) and OA (c); d-f. type I phialides; g-j. type II phialides; k.m type III phialides; n-o. conidiophores with polyphialide; p-q. unbranched conidiophores with terminal phialides; r. long 7-septate unbranched condiophore with latetal phialide; s-u. branched conidiophores; v. unbranched conidiophore with head of conidia; w. short unbranched conidiophore with lateral phialide; x. conidiophore with inflated segments; y. Conidia; z. hyphal coils with short conidiophores. Scale bar: d = 10 µm.

Sub-group F; Figure V.12

Material examined: Isolate Pm 59; Italy, Apulia, Salento, from internal wood necrosis of olive (Olea europaea).

Colony morphology — Colonies reaching a radius of 15–20 mm in 8 d and 33–44 mm in 16 d at 25 °C. Colonies on MEA flat, with two sectors of aerial mycelia Buff to Fawn, entire edge; after 16 d Buff (19"f) at margin to Fawn (13"') with Dark Vinaceous (71"k) at the center. Colonies on PDA felty-like mycelia, with entire edge; after 16 d Cream-Buff at margin (19"d) to Hazel ring (17"'i) becoming Lilac (67'd) to Hazel at the center. Colonies on OA flat, with one sector of aerial mycelia, entire edge; after 16 d Cream-Buff (19"d) at margin with Umber (13m) to chestnut (7'm) at the center. No yellow pigment production was observed.

Slide culture micromorphology — Mycelia septate, hyaline to pale brown, smooth to verruculose, 0.7–1.3 µm wide, that occur singly or in bundles of up to 3 strands. Conidiophores mostly short and unbranched, short conidiophores with up to 3 septa, the long ones with up to 5 septa, ending in a single terminal phialide, (9.1–) 15–18.7 (–26.6) (av. 16.8) µm long and (0.8) 1.1–1.2 (–1.5) (av. 1.2) µm wide; sometimes bearing next to the terminal phialide lateral ones, (12.9–) 24–32.5 (–61.9) (av. 28.2) µm long and (0.9) 1.2–1.3 (–1.6) (av. 1.2) µm wide; hyaline to pale brown; smooth to verruculose; percurrent rejuvenation and lateral proliferation observed occasionally. Branched conidiophores are long, (18.7–) 32.2–40.7 (–65.1) × (0.7–) 1.2–1.3 (–2.0) (av. 36.4 × 1.3) µm. Hyphal coils observed. Phialides terminal or lateral, mostly monophialidic, predominantly type III, smooth to verruculose, hyaline to pale brown; collarettes 0.2–1.0 µm long, 0.4–0.9 µm wide, polyphialides occasionally observed; Type I phialides long, subcylindrical, with long collarettes, sometimes widened at the base, (0.2–) 3.4–4.5 (–7.5) × (0.5–) 0.9–1.0 (–1.5) (av. 0.9 × 4.0) µm; type II phialides, navicular, sometimes elongate-ampulliform and attenuated at the base, (1.8–) 6.9–8.2 (–10.4) × (0.8–) 1.2–1.3 (–1.7) (av. 7.6 × 1.3) µm; type III subcylindrical to elongate-ampulliform and attenuated at the base, sometimes subulate, (7.7–) 9.9–11 (–13.4) × (0.9–) 1.0–1.1 (–1.3) (av. 10.5 × 1.1) µm. Conidia allantoid and more regular, reniform, bigutulate, (1.4–) 2.3–2.8 (–4.4) × (0.6–) 0.8–0.9 (–1.5) (av. 2.5 × 0.8) µm.

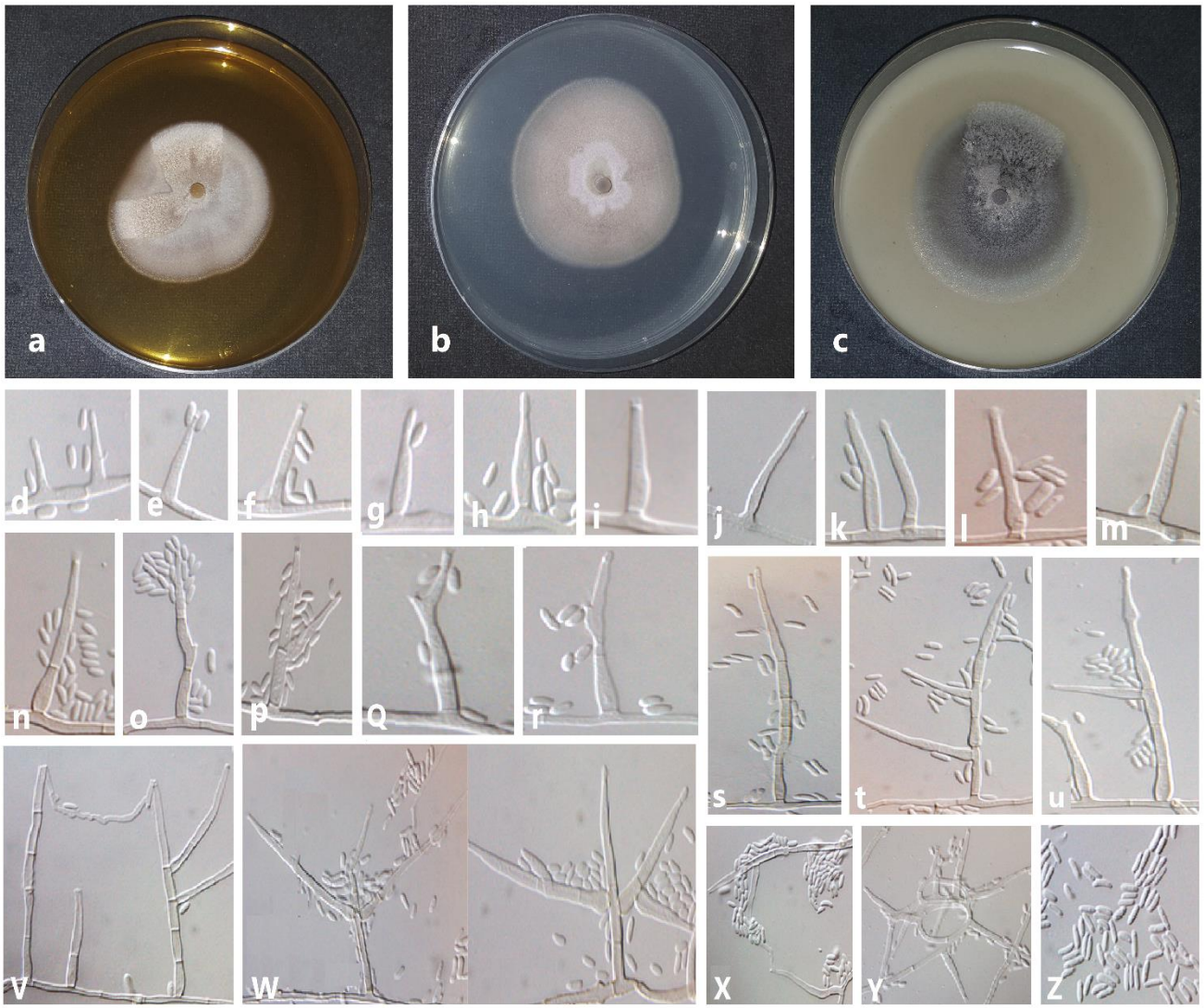

Figure V.12 *Phaeoacremonium* isolate Pm 59. a-c. Sixteen-day-old colonies incubated at 25 °C on MEA (a), PDA (b) and OA (c); d-f. type I phialides; g-i. type II phialides; j.m type III phialides; n-o short unbranched conidiophores; p. short conidiophore with lateral phialide; q-r. conidiophore with polyphialide; s-t. long 5-septate conidiophores with terminal or lateral phialides; u. conidiophore showing percurrent rejuvenation; v. long conidiophores showing vegetative terminal proliferation; w. branched conidiophores; x. type III phialides showing terminal vegetative proliferation; y. hyphal coils with phialides and unbranched condiophores; z. Conidia. Scale bar: d = 10 μm.

V.4 Discussion

The present study aimed at individual and combined phylogenetic analyses of the rDNA intergenic spacer (IGS), β-tubulin and actin genes sequences of *Phaeoacremonium* spp. isolated from olive trees and other host plants, in order to assess whether the intergenic spacer (IGS) region could be used to improve phylogenetic resolution of *Phaeoacremonium* species.

The intergenic spacer IGS, a highly variable region, has been exploited since many years, for phylogenetic analyses of various fungi such as *Verticillium dahliae* group complex, *Fusarium oxysporum* formae speciales, *Metarhizium…ect.* (Morton *et al.* 1995; Pramateftaki *et al.* 2000; Pantou *et al.* 2003; Mbofung *et al.* 2007; Papaioannou *et al.* 2013). This study considered for the first time, the IGS region as genetic marker for phylogenetic analyses among *Phaeoacremonium* species. The entire IGS regions of *Phaeoacremonium* spp. studied here were successfully amplified and sequenced in all of the samples. Indeed, the universal primers used in this study, annealing to the extremities of the 28S and 18S rRNA genes, have been successfully used to amplify the IGS in various fungi and oomycetes (James *et al*. 2001; Nigro *et al.* 2005; Mahmoud Mohamed Ahmed, 2013; Durkin *et al.* 2015).

Individual gene trees were produced based on the IGS region, the β-tubulin and actin genes sequences. In general, single phylogenetic trees were topologically similar and recover the same species-level clades, however, the analyses also reveal conflicts that are related to the grouping of isolates within *Pm. italicum, Pm. scolyti* and *Pm. minimum* clades. Indeed, phylogeny of the actin gene sequences showed that isolates within *Pm. italicum* are grouped all together in one clade, while that of the β-tubulin and in particular the IGS region sequences revealed a clear division of *Pm. italicum* into two main intraspecific clades, with clade (I.a) enclosing isolates from representative subclades (1), (2) and (3), whereas clade (I.b) included isolates of subclade (4).

In fact, considering *Pm. italicum*, the IGS phylogeny obtained from IGS region sequences is generally consistent with the structural organization of the fungus IGS region studied in Chapter III. Two main intraspecific clades were distinguished (clades I.a and I.b) with excellent phylogenetic support (100 % bootstrap). Clade (I.a) was subdivided into three subclades, one of them (subclade 1 containing the ex-type isolate), in addition to subclades (2) and (3),

clustering all *Pm. italicum* isolates (of representative subgroups A, B, C, D and E, refer to IGS structure in Figure V.6). However, clade (I.b) clustered distinctly isolates of subgroup F (grouped in the subclade 4). This distinction was supported by their IGS polymorphic region structure (see subgroup F in Figure V.6).

In view of differences between individual phylogenies in the grouping of isolates within species clades, including *Pm. italicum, Pm. scolyti and Pm. minimum,* a combined IGS-TUB2-ACT phylogenetic tree was produced here, to compare the results. Clearly, it was noted that the grouping of *Pm. italicum* isolates in the combined phylogeny was essentially the same as that produced in IGS phylogeny. Same findings were noted for *Pm. scolyti and Pm. minimum* clades, where the isolates were grouped into distinct subclades as in the IGS phylogeny. Thus, it was ascertained that, the IGS region method tested here, produces a congruent phylogenetic profile with that combined IGS-TUB2-ACT phylogeny. Hence, IGS could be exploited to illustrate and improve phylogenetic studies among *Phaeoacremonium* spp. Furthermore, on the grounds that comparative analysis between the entire IGS and the polymorphic region PR of *Phaeoacremonium* isolates resulted in identical phylogeny (data not shown), sequencing of only the polymorphic region PR could significantly reduce the amount of sequencing needed for an extended fungal genus and thus, can be suitable tool for phylogenetic studies.

Considering cultural and morphological differences of *Pm. italicum* representative isolates of sub-groups (B, C, D, E and F) reported here, it is unlikely that these latter are the same as *Pm. italicum* ex-type reported in Raimondo *et al.* (2014). Selected strains showed different-looking colonies and some morphological differences, e.g., differences in the number of septa in conidiophores, the number of hyphae in bundles and the predominant phialide types. Indeed, isolates Pm 31M, Pm 50M, Pm 45 and Pm 17 present predominant phialides of type II, while isolate Pm 59 differs from them as it predominantly presents phialides of type III. In addition, isolates Pm 17 and Pm 45 produced yellow pigment on OA, while Pm 31M, Pm 50M and Pm 59 did not produce yellow pigmentation.

The molecular identification of *Phaeoacremonium* spp. remains a challenge due to the increasing number of species and taxonomic reassignment (Gramaje *et al.* 2015; Spies *et al.* 2018). The internal transcribed spacer (ITS) region that has been used in *Phaeoacremonium* phylogenies by Groenewald *et al.* (2001), has proven deficiently variable to distinguish several

Phaeoacremonium species. The β-tubulin and actin genes are nowadays widely used in phylogenetic analyses and molecular characterization of *Phaeoacremonium* species (Mostert *et al.* 2006). However, recent studies reported the lack of distinction between some closely related species of *Phaeoacremonium* using ACT-TUB2 phylogenies and morphological data (Spies *et al.* 2018). The use of new genetic markers to improve their phylogeny is to be considered. Actually, various studies have indicated that, molecular phylogenetic analysis based on IGS region might be a suitable tool to investigate intra-specific divergence and would provide significant molecular evidence for taxonomic studies. Therefore, the current study has produced encouraging results useful for better discriminating the real differences between *Phaeoacremonium* species. Further investigation is needed to verify that the genetic and morphological differences found among the different species of *Phaeoacremonium* are well supported.

V.5 References

Altschul, S. F., Madden, T. L., Schäffer, A. A., Zhang, J., Zhang, Z., Miller, W., & Lipman, D. J. (1997). Gapped BLAST and PSI-BLAST: a new generation of protein database search programs. *Nucleic acids research*, *25*(17), 3389-3402.

Carbone, I., & Kohn, L. M. (1999). A method for designing primer sets for speciation studies in filamentous ascomycetes. *Mycologia*, 553-556.

Carlucci, A., Lops, F., Cibelli, F., & Raimondo, M. L. (2015). *Phaeoacremonium* species associated with olive wilt and decline in southern Italy. *European Journal of Plant Pathology*, 141(4),717-729.

Carlucci A., Raimondo M. L., Cibelli F., Phillips A. J. and F. Lops. (2013). *Pleurostomophora richardsiae, Neofusicoccum parvum* and *Phaeoacremonium aleophilum* associated with a decline of olives in southern Italy. *Phytopathologia Mediterranea,* 52(3),517-527.

Carlucci, A., Raimondo, M. L., Santos, J., & Phillips, A. J. L. (2012). Plectosphaerella species associated with root and collar rots of horticultural crops in southern Italy. *Persoonia: Molecular Phylogeny and Evolution of Fungi*, *28*, 34.

Crous, P. W., Gams, W., Wingfield, M. J., & Van Wyk, P. S. (1996). Phaeoacremonium gen. nov. associated with wilt and decline diseases of woody hosts and human infections. *Mycologia*, *88*(5), 786-796.

Durkin, J., Bissett, J., Pahlavani, M., Mooney, B., & Buchwaldt, L. (2015). IGS minisatellites useful for race differentiation in Colletotrichum lentis and a likely site of small RNA synthesis affecting pathogenicity. *PloS one*, *10*(9), e0137398.

Glass, N. L., & Donaldson, G. C. (1995). Development of primer sets designed for use with the PCR to amplify conserved genes from filamentous ascomycetes. *Applied and Environmental Microbiology*, *61*(4), 1323-1330.

Gramaje, D., Mostert, L., Groenewald, J. Z., & Crous, P. W. (2015). Phaeoacremonium: from esca disease to phaeohyphomycosis. *Fungal biology*, *119*(9), 759-783.

Groenewald, M., Ji-Chuan, K. A. N. G., Crous, P. W., & Walter, G. A. M. S. (2001). ITS and β-tubulin phylogeny of Phaeoacremonium and Phaeomoniella species. *Mycological Research*, *105*(6), 651-657.

Hall, T. A. (1999). BioEdit: a user-friendly biological sequence alignment editor and analysis program for Windows 95/98/NT. In *Nucleic acids symposium series*, 41, 95-98.

James, T. Y., Moncalvo, J. M., Li, S., & Vilgalys, R. (2001). Polymorphism at the ribosomal DNA spacers and its relation to breeding structure of the widespread mushroom Schizophyllum commune. *Genetics*, *157*(1), 149-161.

Mahmoud Mohamed Ahmed, Y. (2013). Studies on mango soilborne diseases with special reference to Phytophtora root rot

Mbofung, G. Y., Hong, S. G., & Pryor, B. M. (2007). Phylogeny of Fusarium oxysporum f. sp. lactucae inferred from mitochondrial small subunit, elongation factor 1-α, and nuclear ribosomal intergenic spacer sequence data. *Phytopathology*, *97*(1), 87-98.

Morton, A., Tabrett, A. M., Carder, J. H., & Barbara, D. J. (1995). Sub-repeat sequences in the ribosomal RNA intergenic regions of Verticillium alboatrum and V. dahliae. *Mycological Research*, *99*(3), 257-266.

Mostert, L., Groenewald, J. Z., Summerbell, R. C., Gams, W., & Crous, P. W. (2006). Taxonomy and pathology of Togninia (Diaporthales) and its Phaeoacremonium anamorphs. *Studies in Mycology*, *54*, 1-113.

Nigro, F., Boscia, D., Antelmi, I., & Ippolito, A. (2013). Fungal species associated with a severe decline of olive in southern Italy. *Journal of plant pathology*, 95(3).

Nigro, F., Yaseen, T., Schena, L., Ippolito, A., & Cooke, D. E. L. (2005). Specific PCR detection of Phytophthora megasperma using the intergenic spacer region of ribosomal DNA. *Journal of Plant Pathology*, *87*(4), 300.

O'Donnell, K., & Cigelnik, E. (1997). Two divergent intragenomic rDNA ITS2 types within a monophyletic lineage of the fungus fusarium are nonorthologous. *Molecular phylogenetics and evolution*, *7*(1), 103-116.

Page, R.D. 1996. TreeView: an application to display phylogenetic trees on personal computers. Comput. *Appl. Biosci*, 12, 357-358.

Pantou, M. P., Mavridou, A., & Typas, M. A. (2003). IGS sequence variation, group-I introns and the complete nuclear ribosomal DNA of the entomopathogenic fungus Metarhizium: excellent tools for isolate detection and phylogenetic analysis. *Fungal Genetics and Biology*, *38*(2), 159-174.

Papaioannou, I. A., Dimopoulou, C. D., & Typas, M. A. (2013). Structural and phylogenetic analysis of the rDNA intergenic spacer region of Verticillium dahliae. *FEMS microbiology letters*, *347*(1), 23-32.

Pramateftaki, P. V., Antoniou, P. P., & Typas, M. A. (2000). The complete DNA sequence of the nuclear ribosomal RNA gene complex of Verticillium dahliae: intraspecific heterogeneity within the intergenic spacer region. *Fungal Genetics and Biology*, *29*(1), 19-27.

Raimondo, M. L., Lops, F., & Carlucci, A. (2014). *Phaeoacremonium italicum* sp. nov., associated with esca of grapevine in southern Italy. *Mycologia*, *106*(6), 1119-1126.

Rayner, R. W. (1970). A mycological colour chart. Commonwealth Mycological Institute and British Mycological Society. *Kew*.

Sambrook, J., Fritsch, E. F., & Maniatis, T. (1989). Molecular Cloning Cold Spring Harbor Laboratory Press, New York. *Molecular cloning: Cold spring harbor laboratory press New York*.

Spies, C. F. J., Moyo, P., Halleen, F., & Mostert, L. (2018). *Phaeoacremonium* species diversity on woody hosts in the Western Cape Province of South Africa. *Persoonia*, 40,26-62.

Swofford, D. L., & Sullivan, J. (2003). Phylogeny inference based on parsimony and other methods using PAUP*. *The Phylogenetic Handbook: A Practical Approach to DNA and Protein Phylogeny, cáp*, *7*, 160-206.

Thompson, J. D., Gibson, T. J., Plewniak, F., Jeanmougin, F., & Higgins, D. G. (1997). The CLUSTAL_X windows interface: flexible strategies for multiple sequence alignment aided by quality analysis tools. *Nucleic acids research*, *25*(24), 4876-4882.

VI. CONCLUSIONS

This research represents the first ever genetic analysis of the IGS region of the nuclear ribosomal DNA, in *Phaeoacremonium* spp., specifically in *Pm. italicum* group as a study model, in addition to *Pm. scolyti* and *Pm. minimum.* The structural organization of the intergenic spacer was demonstrated to be polymorphic even at the intra-specific level, and the IGS-PCR amplification for the investigated fungi, yielded variable amplicons size. It is due to the fact that this region of the rDNA has faster mutation rates than the other rDNA areas, here it exhibits a remarkable variation in the presence and copy numbers of the short repeat sequences that we identified within IGS region; notably elements (P) and (R), as well the presence of short indels, resulting all in molecular variation within and among the fungal species. Moreover, the current IGS sequence data provided in this study constitute the basis for future characterization of IGS sequences from the significant group of *Phaeoacremonium* (Chapter III).

The IGS PCR-based method presented here provides a specific detection of *Pm. italicum* group. In this going, the observed polymorphism within IGS sequences opens the opportunity for better exploitation of this region for the development of species-specific primers targeting other *Phaeoacremonium* spp., further to design Real-time PCR primers for development of a molecular diagnostic assay for *Phaeoacremonium* from olive but also grapevines, applicable for pathogen detection in plant material (Chapter IV).

The main motivation of the research was the study of the usefulness of the interegenic spacer as integrative molecular tool for identification and phylogeny of *Phaeoacremonium* species. IGS analysis has proved to be a potential candidate to improve intra- and interspecific differentiation of *Phaeoacremonium* species and would contribute for phylogenetic analyses and resolve cryptic aspects in such studies. The findings are encouraging and useful for better discriminating the real differences between *Phaeoacremonium* species. Moreover, the IGS approach undertaken here exhibits intra-specific phylogenetic variation mainly among *Pm. italicum* group isolates, possibly suggestive of new putative species within these groups. For that, future research should include a more representative set of isolates, and notably closely related species to *Pm. italicum* in the IGS phylogenetic analyses; *Pm. alvesii* and *Pm.*

rubrigerum, together combined with the morphological study that we elucidate originally here, and that in order to clarify better the genetic relationships among species and to provide evidence and well support the finding of new putative species (Chapter V).